

**EUR 3765 e**

**EUROPEAN ATOMIC ENERGY COMMUNITY - EURATOM**

**STUDIES ON FILM THICKNESS AND VELOCITY DISTRIBUTION  
OF TWO-PHASE ANNULAR FLOW**

by

**L. BIASI\*, G.C. CLERICI\*, R. SALA\*\* and A. TOZZI\***

\*ARS S.p.A. and «Istituto di Scienze Fisiche», University of Milan

\*\*ARS S.p.A.

**1968**



**EURATOM/US Agreement for Cooperation**

**EURAEC Report No. 1950 prepared by ARS S.p.A.  
Applicazioni e Ricerche Scientifiche, Milan - Italy**

**Euratom Contract No. 106-66-12 TEEI**

## LEGAL NOTICE

This document was prepared under the sponsorship of the Commission of the European Communities in pursuance of the joint programme laid down by the Agreement for Cooperation signed on 8 November 1958 between the Government of the United States of America and the European Communities.

It is specified that neither the Commission of the European Communities, nor the Government of the United States, their contractors or any person acting on their behalf :

Make any warranty or representation, express or implied, with respect to the accuracy; completeness, or usefulness of the information contained in this document, or that the use of any information, apparatus, method, or process disclosed in this document may not infringe privately owned rights; or

Assume any liability with respect to the use of, or for damages resulting from the use of any information, apparatus, method or process disclosed in this document.

This report is on sale at the addresses listed on cover page 4

at the price of FF 12.50	FB 125.—	DM 10.—	Lit. 1.560	Fl. 9.—
--------------------------	----------	---------	------------	---------

**When ordering, please quote the EUR number and the title, which are indicated on the cover of each report.**

Printed by SMEETS  
Brussels, April 1968

This document was reproduced on the basis of the best available copy.

**EUR 3765 e**

**STUDIES ON FILM THICKNESS AND VELOCITY DISTRIBUTION OF TWO-PHASE ANNULAR FLOW**

by L. BIASI\*, G.C. CLERICI\*, R. SALA\*\* and A. TOZZI\*

\*ARS S.p.A. and «Istituto di Scienze Fisiche», University of Milan

\*\*ARS S.p.A.

European Atomic Energy Community - EURATOM

EURATOM/US Agreement for Cooperation

EURAE C Report No. 1950 prepared by ARS S.p.A.

Applicazioni e Ricerche Scientifiche, Milan (Italy)

Euratom Contract No. 106-66-12 TEEI

Brussels, April 1967 - 94 Pages - 33 Figures - FB 125

This report contains a theoretical study on the fluidodynamics of a two-phase annular dispersed flow in adiabatic conditions. Assuming as

**EUR 3765 e**

**STUDIES ON FILM THICKNESS AND VELOCITY DISTRIBUTION OF TWO-PHASE ANNULAR FLOW**

by L. BIASI\*, G.C. CLERICI\*, R. SALA\*\* and A. TOZZI\*

\*ARS S.p.A. and «Istituto di Scienze Fisiche», University of Milan

\*\*ARS S.p.A.

European Atomic Energy Community - EURATOM

EURATOM/US Agreement for Cooperation

EURAE C Report No. 1950 prepared by ARS S.p.A.

Applicazioni e Ricerche Scientifiche, Milan (Italy)

Euratom Contract No. 106-66-12 TEEI

Brussels, April 1967 - 94 Pages - 33 Figures - FB 125

This report contains a theoretical study on the fluidodynamics of a two-phase annular dispersed flow in adiabatic conditions. Assuming as

**EUR 3765 e**

**STUDIES ON FILM THICKNESS AND VELOCITY DISTRIBUTION OF TWO-PHASE ANNULAR FLOW**

by L. BIASI\*, G.C. CLERICI\*, R. SALA\*\* and A. TOZZI\*

\*ARS S.p.A. and «Istituto di Scienze Fisiche», University of Milan

\*\*ARS S.p.A.

European Atomic Energy Community - EURATOM

EURATOM/US Agreement for Cooperation

EURAE C Report No. 1950 prepared by ARS S.p.A.

Applicazioni e Ricerche Scientifiche, Milan (Italy)

Euratom Contract No. 106-66-12 TEEI

Brussels, April 1967 - 94 Pages - 33 Figures - FB 125

This report contains a theoretical study on the fluidodynamics of a two-phase annular dispersed flow in adiabatic conditions. Assuming as

initial condition a situation of equilibrium, the main quantities necessary for a fully macroscopic description of the system are the total pressure drop, the gaseous and liquid phase distribution, the velocity profiles.

Other quantities which are to be determined are the film thickness and the liquid and gas film flowrate. The entrained liquid flowrate and the core gas flowrate can then be obtained from these latter by using some balance equations.

An equation relating the liquid film thickness to the physical and geometrical parameters of the system is obtained. By solving this equation the film thickness, the liquid and gas film flowrates are calculated. The results are compared with some experimental data at different conditions.

initial condition a situation of equilibrium, the main quantities necessary for a fully macroscopic description of the system are the total pressure drop, the gaseous and liquid phase distribution, the velocity profiles.

Other quantities which are to be determined are the film thickness and the liquid and gas film flowrate. The entrained liquid flowrate and the core gas flowrate can then be obtained from these latter by using some balance equations.

An equation relating the liquid film thickness to the physical and geometrical parameters of the system is obtained. By solving this equation the film thickness, the liquid and gas film flowrates are calculated. The results are compared with some experimental data at different conditions.

initial condition a situation of equilibrium, the main quantities necessary for a fully macroscopic description of the system are the total pressure drop, the gaseous and liquid phase distribution, the velocity profiles.

Other quantities which are to be determined are the film thickness and the liquid and gas film flowrate. The entrained liquid flowrate and the core gas flowrate can then be obtained from these latter by using some balance equations.

An equation relating the liquid film thickness to the physical and geometrical parameters of the system is obtained. By solving this equation the film thickness, the liquid and gas film flowrates are calculated. The results are compared with some experimental data at different conditions.

**EUR 3765 e**

**EUROPEAN ATOMIC ENERGY COMMUNITY - EURATOM**

**STUDIES ON FILM THICKNESS AND VELOCITY DISTRIBUTION  
OF TWO-PHASE ANNULAR FLOW**

by

**L. BIASI\*, G.C. CLERICI\*, R. SALA\*\* and A. TOZZI\***

**\*ARS S.p.A. and «Istituto di Scienze Fisiche», University of Milan**

**\*\*ARS S.p.A.**

**1968**



**EURATOM/US Agreement for Cooperation**

**EURAEK Report No. 1950 prepared by ARS S.p.A.  
Applicazioni e Ricerche Scientifiche, Milan - Italy**

**Euratom Contract No. 106-66-12 TEEI**

## **SUMMARY**

This report contains a theoretical study on the fluidodynamics of a two-phase annular dispersed flow in adiabatic conditions. Assuming as initial condition a situation of equilibrium, the main quantities necessary for a fully macroscopic description of the system are the total pressure drop, the gaseous and liquid phase distribution, the velocity profiles.

Other quantities which are to be determined are the film thickness and the liquid and gas film flowrate. The entrained liquid flowrate and the core gas flowrate can then be obtained from these latter by using some balance equations.

An equation relating the liquid film thickness to the physical and geometrical parameters of the system is obtained. By solving this equation the film thickness, the liquid and gas film flowrates are calculated. The results are compared with some experimental data at different conditions.

## **KEYWORDS**

FILMS  
THICKNESS  
VELOCITY  
DISTRIBUTION

TWO-PHASE FLOW  
FLUID FLOW  
PRESSURE  
DIFFERENTIAL EQUATIONS

## C O N T E N T S

Introduction	5
1 - Description of the Model	7
2 - Distribution of the Liquid and Gaseous Phase	8
3 - Film Velocity Distribution	10
4 - Average Film Velocity	15
5 - Liquid and Gas Film Flowrate	17
6 - Core Velocity Distribution	19
7 - Liquid and Gas Core Flowrates	22
8 - Film Thickness Calculation	24
9 - Model Predictions and Comparisons	25
10 - Comparison	26
11 - Comparison with Harwell Data	58
12 - A Simplified Model	60
13 - Appendix	65
14 - Tables	67
15 - Bibliography	92





STUDIES ON FILM THICKNESS AND VELOCITY  
DISTRIBUTION OF TWO-PHASE ANNULAR FLOW (+)

INTRODUCTION

This report contains a theoretical study on the fluidodynamics of a two-phase annular dispersed flow in adiabatic conditions. Assuming as initial condition a situation of equilibrium, the main quantities necessary for a fully macroscopic description of the system are the total pressure drop, the gaseous and liquid phase distribution, the velocity profiles. If the flow field is subdivided into two region "film" and "core", according to a usual representation, the other quantities which are to be determined are the film thickness and the liquid and gas film flowrate. Then the entrained liquid flowrate and the core gas flowrate can be obtained from these latter by using some balance equations. The entrainment and diffusion liquid droplet velocities are also necessary but only for the description of non equilibrium conditions.

The knowledge of the equilibrium conditions here analyzed may be a useful step for this determination.

An analytical solution of two-phase annular flow with liquid entrainment has been previously presented by S. Levy.<sup>1/</sup> By assuming the knowledge of the total pressure drop for unit length, Levy builds up a quantity  $F$  depending on the film thickness only.

The relation between the function  $F$  and the film thickness is obtained by some plots correlating experimental measurements performed at CISE. Actually a fully analytical description of this type of flow though referred to time averaged quantities is exceedingly difficult. For this reason a similar approach was followed in the present work. The basic assumption is the knowledge of the total pressure drop together with the average void fraction  $\alpha$ .

(+) Manuscript received on January 12, 1968.

They are two well-studied quantities and several empirical correlations give their value with good accuracy. Under these two assumptions, an equation relating the liquid film thickness to the physical and geometrical parameters of the system is obtained. By solving this equation the film thickness, the liquid and gas film flowrates are then calculated. The results are compared with some experimental data at different conditions.

## 1 - DESCRIPTION OF THE MODEL

The model here presented is based on a subdivision of the flow field into two regions: an annulus around the solid walls of the duct (film) and a central zone (core). Both phases are assumed to be present everywhere. The film is further subdivided into a laminar sublayer and a turbulent region. In single phase systems there exists also a buffer zone where the dynamic and eddy viscosity are comparable. On the other hand in two-phase systems the mass transfer between film and core can reduce the extension of this transition region. Therefore it can be reasonable to neglect it when the film thickness is much smaller than the duct radius. The core is assumed to be completely turbulent. It is also stated that the motion conditions in the film are mainly affected by the physical properties of the liquid phase, whilst in the core by those of the gaseous phase. Thus, instead of establishing an actual separation of the phases, a separation is postulated in the motion conditions between the two regions. The velocity distribution in the turbulent region is obtained by using Von Karman assumption on the mixing length and taking into account the actual shear stress distribution. The integration constants are calculated by matching the velocities and their derivatives at the boundary between the laminar sublayer and the turbulent region, and at the film-core interface. Prandtl's universal velocity distribution was also tested for the core region. In both cases the value of the mixing length constant was modified as suggested by the experimental results obtained at CISE. A single expression of the local void fraction  $\alpha$  as a function of the film thickness is introduced. A set of equations is then derived which leads to the determination of the film thickness and partial mass flow-rates.

2 - DISTRIBUTION OF THE LIQUID AND GASEOUS PHASE.

The experimental results show that the void fraction  $\alpha$  is a function of the distance from the duct wall. As a first approximation for the void fraction  $\alpha$  a linear trend has been assumed starting from zero at the wall up to a value  $\alpha^*$  at the film-core interface. In the core it is assumed to have a constant value equal to  $\alpha^*$ . Denoting by  $R$  the duct radius,  $\Delta$  the film thickness,  $b$  the core radius and  $y$  the spatial coordinate, it is

$$(1) \quad \alpha = \begin{cases} \alpha^* \frac{R-y}{\Delta} & b \leq y \leq R \\ \alpha^* & 0 \leq y \leq b \end{cases}$$

as shown in fig. 1

If  $\bar{\alpha}$  is the average value of  $\alpha$ , the relation between  $\alpha^*$  and  $\bar{\alpha}$  is

$$(2) \quad \pi R^2 \bar{\alpha} = \pi \int_0^b \alpha^* y dy + \pi \int_b^R \alpha^* \frac{R-y}{\Delta} y dy$$

which gives

$$(3) \quad \alpha^* = \frac{R^2 \bar{\alpha}}{b^2 + \Delta(b + \Delta/3)}$$

Thus, the film and core density  $\rho_f$  and  $\rho_c$  are given by

$$(4) \quad \rho_f = \rho_l \left( 1 - \alpha^* \frac{R-y}{\Delta} \right) + \rho_g \alpha^* \frac{R-y}{\Delta}$$

$$(5) \quad \rho_c = \rho_l (1 - \alpha^*) + \rho_g \alpha^*$$

where  $\rho_l$  and  $\rho_g$  are the liquid and gas density.

Trend of  $\alpha$  as a function of the distance from the duct wall.

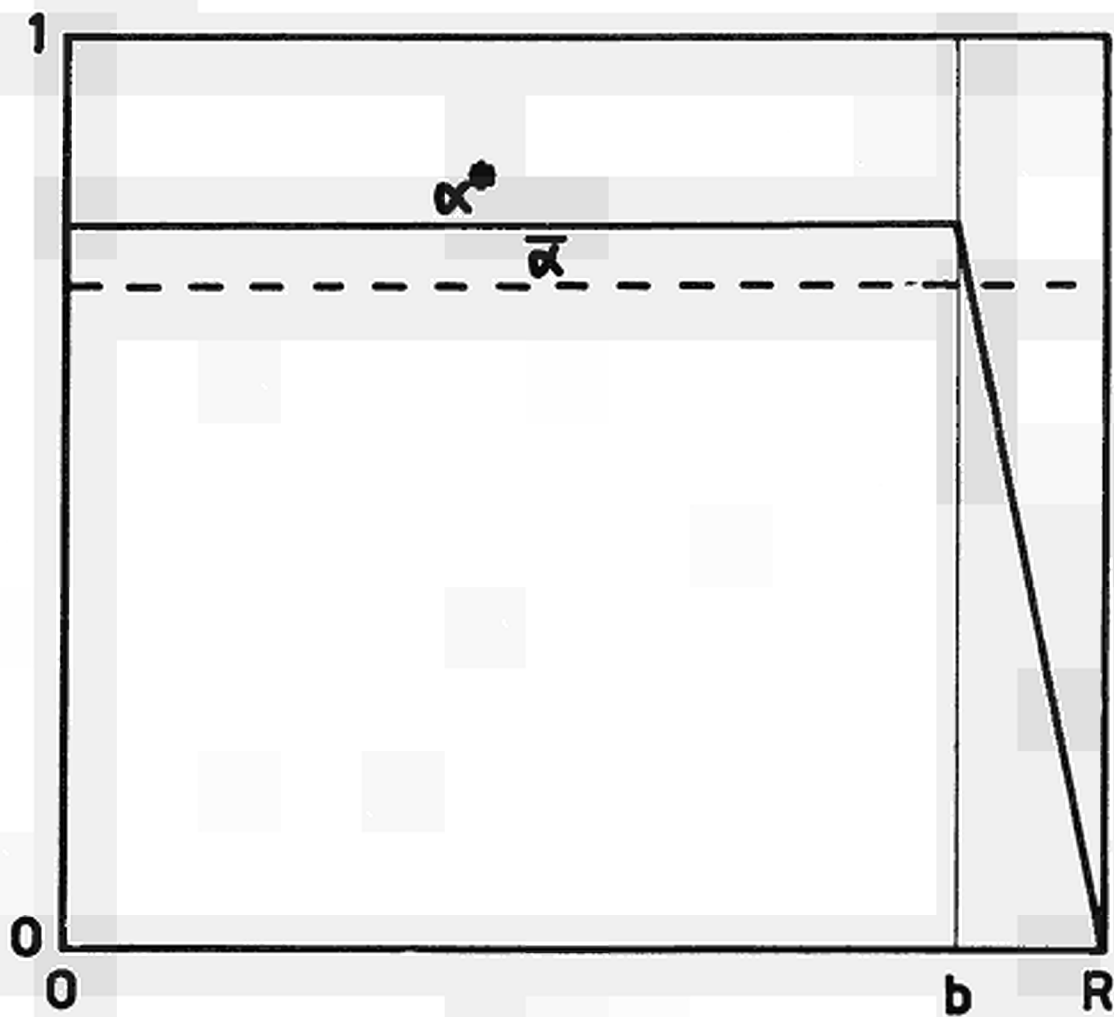


Fig. 1

3 - FILM VELOCITY DISTRIBUTION

Since the ratio between the film thickness and the duct radius is usually very small, the cylindrical geometry of fig. 2 is substituted with the plane geometry of fig. 3 in the calculation of the film velocity profile. The validity of this approximation is examined in the appendix. Assuming in the film

$$(6) \quad \tau = K_1 y + K_2$$

the constant  $K_2$ , usually equal to zero for single phase systems, is now determined by matching the shear stresses at the film-core boundary.  $\tau_0$  and  $\tau_c$  being the values of the shear stress at the wall and at  $y=b$ , they are given by

$$(7) \quad \tau_0 = \left\{ \frac{dp}{dx} - g[\rho_c \bar{\alpha} + (1-\bar{\alpha})\rho_L] \right\} \frac{R}{2}$$

$$(8) \quad \tau_c = \left\{ \frac{dp}{dx} - g\rho_c \right\} \frac{b}{2}$$

Equation (6) can be rewritten as

$$(9) \quad \tau = (\tau_0 - \tau_c) \frac{y-b}{\Delta} + \tau_c$$

where  $\frac{dp}{dx}$  is the total pressure drop per unit length and  $g$  is the gravitational constant. Following Von Karman, the shear stress  $\tau$  is connected with the velocity profile by

$$(10) \quad \tau = \rho \chi^2 \frac{(du/dy)^4}{(d^2u/dy^2)^2}$$

Circular geometry of the system.

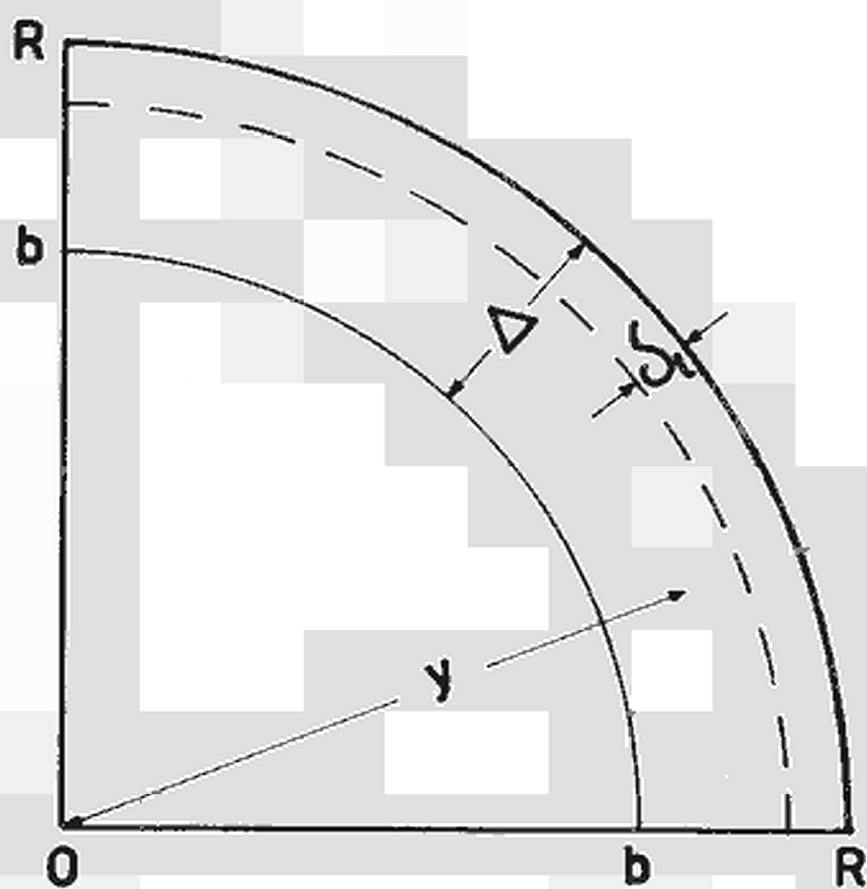


Fig. 2

Equivalent plane geometry.

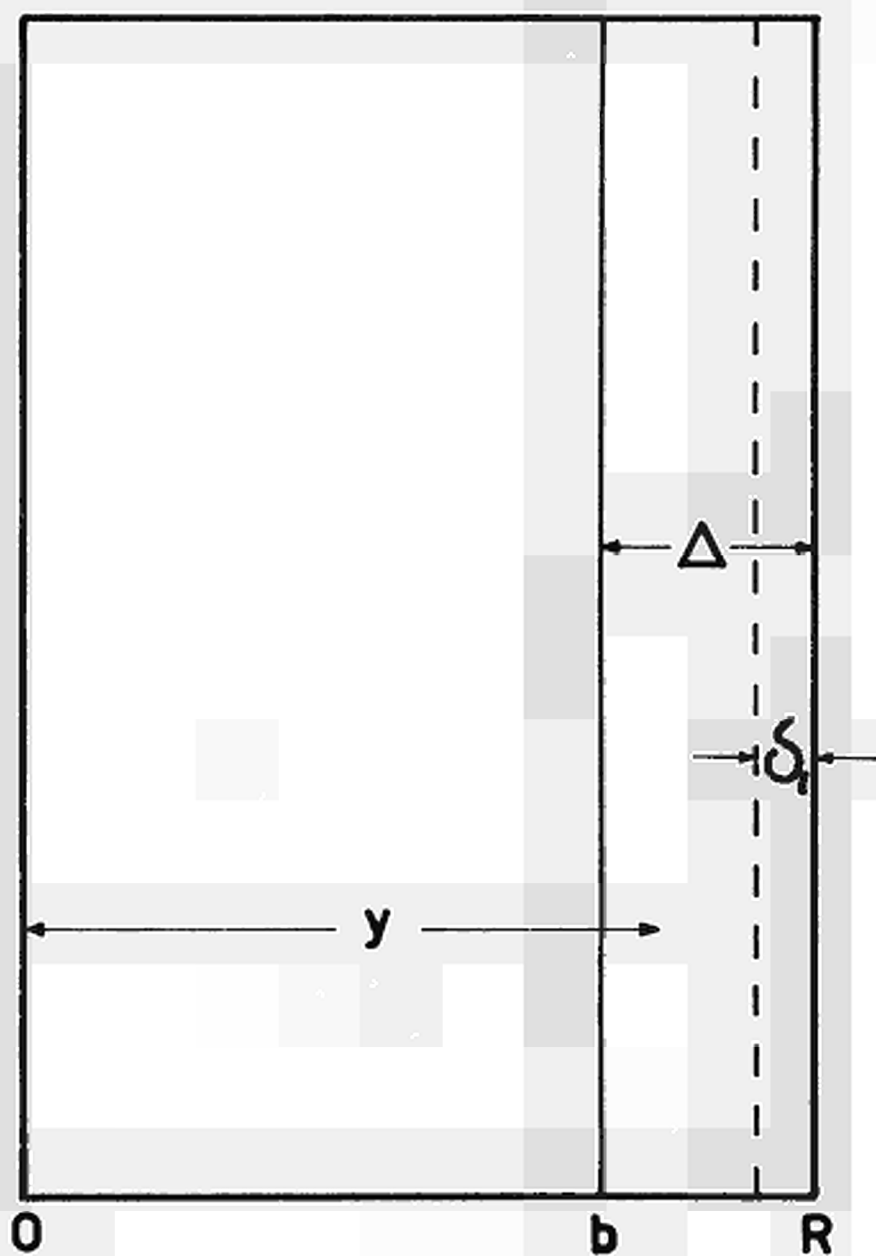


Fig. 3



By introducing the dimensionless variables

$$(11) \quad y^+ = \left(1 - \frac{\tau_c}{\tau_0}\right) \frac{y - b}{\Delta} + \frac{\tau_c}{\tau_0}$$

$$(12) \quad u^+ = \chi \sqrt{\frac{\rho}{\tau_0}} u$$

and by using eq. (9) one has

$$(13) \quad \frac{du^+}{dy^+} = - \frac{1}{\pm 2 \sqrt{y^+} + C_1}$$

The constant  $C_1$  is obtained by matching the turbulent region with the laminar sublayer of thickness  $\delta_L = h\mu / (\chi \sqrt{\tau_0 \rho}) \sim 12.1 \mu / \sqrt{\tau_0 \rho}$ . With the usual assumptions (see for instance reference 3):

$$\begin{aligned} \text{i) } \delta_L \ll R & \qquad \text{ii) } \left. \frac{du}{dy} \right|_{\delta_L^+} = \frac{1}{h} \left. \frac{du}{dy} \right|_{\delta_L^-} \\ \text{iii) } \tau(\delta_L) = \tau_0 = \rho \chi^2 \delta_L^2 \frac{d^2 u}{dy^2} & \end{aligned}$$

and the additional one

$$\text{iiii) } \frac{\delta_L}{\Delta} \left(1 - \frac{\tau_c}{\tau_0}\right) \ll 1$$

it is  $C_1 = 2$ . The sing minus of eq. (13) was taken because the velocity must decrease with  $y$ . Integrating eq. (13) and introducing the original variables, it is (for  $b \leq y \leq R - \delta_L$ )

$$(14) \quad u = \frac{1}{\chi} \sqrt{\frac{\tau_0}{\rho}} \left\{ \ln \left| 1 - \sqrt{\frac{(1-a)(y-b)/\Delta + a}{(1-a)(y-b)/\Delta + a}} \right| + \sqrt{\frac{(1-a)(y-b)/\Delta + a}{(1-a)(y-b)/\Delta + a}} \right\} + C_2$$

with  $a = \tau_c / \tau_0$ . In the laminar sublayer  $R - \delta_L \leq y \leq R$  the expression of the velocity  $u$  is:

$$(15) \quad u = \frac{\tau_c - \tau_0}{2\Delta\mu} (R - y)^2 + \frac{\tau_0}{\mu} (R - y) \sim \frac{\tau_0}{\mu} (R - y)$$

By equating eqs. (14) and (15) at  $y = R - \delta_L, c_2$  becomes:

$$(16) \quad c_2 = \frac{\tau_0 \delta_L}{\mu} + \frac{1}{\alpha} \sqrt{\frac{\tau_0}{\rho}} \left\{ \ln \left| 1 - \sqrt{1 + (a-1) \frac{\delta_L}{\Delta}} \right| + \sqrt{1 + (a-1) \frac{\delta_L}{\Delta}} \right\}$$

As it seems reasonable to think that laminar sublayer is affected only by the liquid physical properties, whilst the gas affects the film turbulent region through a density variation, it is possible to set in eqs. (10) (14) (15) and (16)  $\mu = \mu_L$ ;  $\delta_L = 42.1 \mu_L / \sqrt{\tau_0 \rho_L}$ ;  $\bar{\rho} = \bar{\rho}_f$  is the average value of the film density, obtained by averaging eq. (4):

$$(17) \quad \bar{\rho}_f = \rho_L + \alpha^2 (\rho_g - \rho_L) \frac{R - 3/2 \Delta}{2R - \Delta}$$

With these substitutions the velocity profiles in the film become:

$$(18) \quad u_f = \frac{\tau_0}{\mu_L} (R - y) \quad R - \delta_L \leq y \leq R$$

$$(19) \quad u_f = \frac{\tau_0 \delta_L}{\mu_L} + \frac{1}{\alpha} \sqrt{\frac{\tau_0}{\rho_f}} \left\{ \ln \frac{1 - \sqrt{(y-a)(y-b)/\Delta + a}}{1 - \sqrt{1 + (a-1) \delta_L/\Delta}} - \sqrt{1 + (a-1) \delta_L/\Delta} + \sqrt{(1-a)(y-b)/\Delta + a} \right\} \quad b \leq y \leq R - \delta_L$$

In the above equations the only unknown quantity is the film thickness  $\Delta$  (provided that the pressure drop and the average void fraction  $\bar{\alpha}$  are known).

4 - AVERAGE FILM VELOCITY

The average value of the film velocity is obtained by integrating eqs. (18) and (19) over the film flow section

(20)

$$\begin{aligned} \bar{U}_f &= \frac{2}{R^2 - b^2} \left\{ \int_{R-\delta}^R \frac{\tau_c (R^2 - y^2)}{\mu_c R} y dy + C_1 \int_0^{R-\delta} y dy + \right. \\ &+ \left. \frac{1}{\lambda} \sqrt{\frac{\tau_c}{\mu_c}} \int_0^{R-\delta} \left[ \ln \left| 1 - \sqrt{(t-a) \frac{y-b+a}{\Delta}} \right| + \sqrt{(t-a) \frac{y-b+a}{\Delta}} \right] y dy \right\} \\ &= \frac{2}{R^2 - b^2} \{ A_1 + A_2 + A_3 \} \end{aligned}$$

$A_1$  and  $A_2$  can be easily calculated:

$$(21) \quad A_1 = \frac{\tau_c \delta_c^2}{2\mu_c} \left( R - \delta_c + \frac{\delta_c^2}{4R} \right) \approx \frac{\tau_c \delta_c^2 R}{2\mu_c}$$

$$(22) \quad A_2 = C_1 \left\{ R(\Delta - \delta_c) - \frac{\Delta^2 - \delta_c^2}{2} \right\}$$

when  $a > 1$ , introducing the new variable  $t = \frac{y-b}{\Delta}$ ,  $A_3$  becomes:

$$\begin{aligned} (23) \quad A_3 &= \frac{1}{\lambda} \sqrt{\frac{\tau_c}{\mu_c}} \left\{ \Delta^2 \int_0^{t-\frac{\delta}{\Delta}} t \ln \left| \sqrt{(t-a)t+a} - 1 \right| dt + \Delta b \int_0^{t-\frac{\delta}{\Delta}} \ln \left| \sqrt{(t-a)t+a} - 1 \right| dt \right. \\ &+ \left. \Delta^2 \int_0^{t-\frac{\delta}{\Delta}} t \sqrt{(t-a)t+a} dt + \Delta b \int_0^{t-\frac{\delta}{\Delta}} \sqrt{(t-a)t+a} dt \right\} \\ &= \frac{1}{\lambda} \sqrt{\frac{\tau_c}{\mu_c}} \{ \Delta^2 I_1 + \Delta b I_2 + \Delta^2 I_3 + \Delta b I_4 \} \end{aligned}$$

Putting  $X = \sqrt{(1-a)t+a} - 1$  and  $Z = X + 1$ , one obtains:

$$I_1 = \frac{2}{(1-a)^2} \left\{ \left( \frac{X^4}{4} + X^3 + \frac{2-a}{2} X^2 + X - aX \right) \ln X - \left( \frac{X^4}{4} + \frac{X^3}{3} + \frac{2-a}{4} X^2 + X - aX \right) \right\} \Bigg|_{\sqrt{a}-1}^{\sqrt{1+a-0} - 1}$$

$$I_2 = \frac{2}{(1-a)} \left\{ \left( \frac{X^2}{2} + X \right) \ln X - \left( \frac{X^2}{2} + X \right) \right\} \Bigg|_{\sqrt{a}-1}^{\sqrt{1+(a-1)\frac{1}{2}} - 1}$$

$$I_3 = \frac{2}{(1-a)^2} \left\{ \frac{Z^5}{5} - \frac{aZ^3}{3} \right\} \Bigg|_{\sqrt{a}}^{\sqrt{1+(a-1)\frac{1}{2}}}$$

$$I_4 = \frac{2}{(1-a)} \left\{ \frac{Z^3}{3} \right\} \Bigg|_{\sqrt{a}}^{\sqrt{1+(a-1)\frac{1}{2}}}$$

In the case  $a < 1$ ,  $I_3$  and  $I_4$  have the same expression, whilst  $I_1$  and  $I_2$  become:

$$I_1' = -\frac{2}{(1-a)^2} \left\{ \left( -\frac{X^4}{4} + X^3 - \frac{2-a}{2} X^2 + X - aX \right) \ln X - \left( -\frac{X^4}{4} + \frac{X^3}{3} - \frac{2-a}{4} X^2 + X - aX \right) \right\} \Bigg|_{1-\sqrt{a}}^{1-\sqrt{1+(a-1)\frac{1}{2}}}$$

$$I_2' = -\frac{2}{(1-a)} \left\{ \left( X - \frac{X^2}{2} \right) \ln X + \frac{X^2}{4} - X \right\} \Bigg|_{1-\sqrt{a}}^{1-\sqrt{1+(a-1)\frac{1}{2}}}$$

where  $X = 1 - \sqrt{(1-a)t+a}$

The separation between the two cases  $a > 1$  and  $a < 1$  is due to the presence of the modulus in  $A_3$ . The case  $a=1$  is a trivial one in which  $\tau = \tau_0 = \tau_c$  and the solution can be obtained directly by eq. (9)

5 - LIQUID AND GAS FILM FLOWRATE

Neglecting the variation of the void fraction in the laminar sublayer, the liquid film-flowrate is given by

$$\begin{aligned}
 (24) \quad \dot{V}_F &= 2\pi \rho_L \left\{ \int_{\kappa \delta_L}^R \frac{\tau_o (R^2 - y^2)}{2\mu_L R} y dy + C_1 \int_b^{R-\delta_L} \left(1 - \alpha^* \frac{R-y}{\Delta}\right) y dy \right. \\
 &\quad \left. + \frac{1}{\chi} \sqrt{\frac{\tau_o}{\rho_f}} \int_b^{R-\delta_L} \left[ \ln \left| \sqrt{(b-a) \frac{y-b}{\Delta} + a} - 1 \right| + \left| \sqrt{(b-a) \frac{y-b}{\Delta} + a} \right| \right] \left(1 - \alpha^* \frac{R-y}{\Delta}\right) y dy \right\} \\
 &= 2\pi \rho_L \{ A_4 + A_5 \}
 \end{aligned}$$

where

$$(25) \quad A_4 = \left\{ R(\Delta - \delta_L) - \frac{\Delta^2 - \delta_L^2}{2} - \alpha^* \frac{\Delta R}{2} + \alpha^* \frac{\Delta^2}{3} + \alpha^* \frac{\delta_L^2 R}{2\Delta} - \alpha^* \frac{\delta_L^3}{3\Delta} \right\}$$

$$(26) \quad A_5 = (1 - \alpha^*) A_3 + \frac{\alpha^*}{\chi} \sqrt{\frac{\tau_o}{\rho_f}} \left\{ \Delta^2 (I_5 + I_6) + \Delta(R - \Delta) (I_2 + I_3) \right\}$$

In the case  $a > 1$

$$\begin{aligned}
 I_5 &= \frac{2}{(1-a)^3} \left\{ \left[ \frac{x^6}{6} + x^5 + \frac{5-a}{2} x^4 + \frac{10-6a}{3} x^3 + \frac{5-6a+a^2}{2} x^2 + (1-a)^2 x \right] \Delta x \right. \\
 &\quad \left. - \left[ \frac{x^6}{36} + \frac{x^5}{5} + \frac{5-a}{2} x^4 + \frac{10-6a}{9} x^3 + \frac{5-6a+a^2}{4} x^2 + (1-a)^2 x \right] \right\} \sqrt{\frac{1+(a-1)\frac{\delta_L}{\Delta}}{\sqrt{a}-1}}
 \end{aligned}$$

$$I_6 = \frac{2}{(1-a)^3} \left\{ \frac{x^7}{7} - \frac{2ax^5}{5} + \frac{a^2 x^3}{3} \right\} \sqrt{\frac{1+(a-1)\frac{\delta_L}{\Delta}}{\sqrt{a}}}$$

whilst in the case  $a < 1$   $I_5$  becomes

$$I_5 = -\frac{2}{(1-a)} \left\{ \left( -\frac{x^6}{6} + x^5 - \frac{a-5}{2} x^4 + \frac{10-6a}{3} x^3 - \frac{5+a^2-6a}{2} x^2 + x + a^2 x - 2ax \right) \ln x - \left( -\frac{x^6}{24} + \frac{x^5}{5} - \frac{5-a}{8} x^4 + \frac{10-6a}{9} x^3 - \frac{5+a^2-6a}{2} x^2 + (1-a^2)x \right) \right\} \Bigg|_{1-\sqrt{a}}^{1-\sqrt{(1-a)\frac{b}{a}}}$$

In the same way the gas film flowrate  $\dot{V}_G$  is given by

$$(27) \quad \dot{V}_G = 2\pi R \left\{ c_1 \kappa^* \left[ \frac{\Delta R}{2} \left( 1 - \frac{\xi^2}{R^2} \right) + \frac{\xi^3}{3R} \right] + \frac{\kappa^2}{\kappa} \sqrt{\frac{\xi}{\kappa}} \cdot \left[ \Delta^2 (I_1 + I_3 - I_2 - I_4) + \Delta b (I_5 + I_6 - I_7 - I_8) \right] \right\}$$

The integration limits have not been explicitly substituted in the above expressions since the solution requires a digital computer. The approximate expressions obtained through expansion in series are still too complex to be analytically treated owing to the presence of  $(1-\bar{a})$  and  $(1-\bar{a}^n)$  which can be of the same order as  $\Delta/R$ .

6 - CORE VELOCITY DISTRIBUTION

The shear stress in the core is obtained by eq. (6) with  $K_1 = \frac{\tau_c}{b}$  and  $K_2 = 0$ :

$$(28) \quad \tau_x = \frac{\tau_c y}{b}$$

Substituting eq.(28) in eq. (10) and integrating it twice, one has:

$$(29) \quad u = \frac{1}{\chi} \sqrt{\frac{\tau_c}{\rho}} \left\{ \ln \left( c_1' - \sqrt{\frac{y}{b}} \right) + \sqrt{\frac{y}{b}} \right\} + c_2' \quad \rho \leq y \leq b$$

with the following assumptions

- a) The core velocity distribution  $u_c$  is affected only by the gaseous phase density
- b) The presence of dispersed liquid reduces the mixing length only through a lessening in the numerical value of the constant  $\chi$

the core velocity profile becomes

$$(30) \quad u_c = \frac{1}{\chi_c} \sqrt{\frac{\tau_c}{\rho_c}} \left\{ \ln \left( c_1' - \sqrt{\frac{y}{b}} \right) + \sqrt{\frac{y}{b}} \right\} + c_2'$$

where  $\chi_c$  is the new value of the constant  $\chi$  taken equal to 0.27 according to some experimental results<sup>2/</sup>. The two constants  $c_1'$  and  $c_2'$  can be determined by matching the velocities at the film-core interface and by giving the local core slip ratio between the two phases. Since there are no information about the value of the slip ratio, the latter condition is replaced by the assumption that the ratio of the velocity derivatives at the interface is equal to a function K depending only on

the physical properties of the two phases:

$$(31) \quad \frac{du_c}{dy} \Big|_{b^-} / \frac{du_f}{dy} \Big|_{b^+} = K$$

By eq. (10) it is

$$(32) \quad \tau(b) = \tau_c = \rho_f \chi^2 \left| \frac{(du_f/dy)^4}{(d^2u_f/dy^2)^2} \right|_{b^+} = \rho_f \chi_c^2 \left| \frac{(du_c/dy)^4}{(d^2u_c/dy^2)^2} \right|_{b^-}$$

and by eq. (29) and (31)

$$(33) \quad K^2 = \frac{\rho_f \chi^2}{\rho_f \chi_c^2}$$

On the basis of these two conditions one has

$$(34) \quad C_1' = 1 + \frac{\Delta \sqrt{a}}{R \sqrt{a} + b}$$

$$(35) \quad C_2' = \frac{\tau_0 \delta_2}{\mu_c} + \frac{1}{\chi} \sqrt{\frac{\tau_0}{\rho_f}} \left[ \ln \frac{1 - \sqrt{a}}{1 - \sqrt{1 + (a-1) \frac{\delta_2}{\Delta}}} - \sqrt{1 + (a-1) \frac{\delta_2}{\Delta}} + \sqrt{a} \right] - \frac{1}{\chi_c} \sqrt{\frac{\tau_0}{\rho_f}} \left\{ \ln \frac{(C_1' - 1)}{+1} \right\}$$

Condition (31) can be replaced by stating the equality of the densities, velocities and constants  $\chi$ ,  $\chi_c$  at the film-core interface. This condition seems to be reasonable as a local one even though the film density is approximated by its average value  $\bar{\rho}_f$ . It corresponds to the physical idea that all quantities must be continuous.

The core velocity distribution was also tested with Prandtl's universal distribution:



$$(36) \quad u_c = u_m - \frac{1}{\chi_c} \sqrt{\frac{\tilde{\tau}_0}{\rho_f}} \ln \frac{R}{R-y}$$

In this case there is only a constant,  $u_m$ , which can be obtained by matching like before the velocities at the film-core interface.

$$(37) \quad u_m = \frac{1}{\chi_c} \sqrt{\frac{\tilde{\tau}_c}{\rho_G}} \ln \frac{R}{\Delta} + \frac{\tau_0 \delta_L}{\mu_L} + \frac{1}{\chi} \sqrt{\frac{\tilde{\tau}_0}{\rho_f}} \cdot$$

$$\left\{ \ln \frac{1 - \sqrt{a}}{1 - \sqrt{1 + (a-1) \frac{\delta_L}{\Delta}}} + \sqrt{a} - \sqrt{1 + (a-1) \frac{\delta_L}{\Delta}} \right\}$$

7 - LIQUID AND GAS CORE FLOWRATE

The mean value of the core velocity is obtained by integrating eq. (30) on the core section:

$$(38) \quad \bar{u}_c = \frac{2}{b^2} \int_0^b u_c y dy = c_2' + \frac{1}{\chi_c} \sqrt{\frac{\tau_c}{\rho_g}} \int_0^b \left\{ \ln \left( c_1' - \sqrt{\frac{y}{b}} \right) + \sqrt{\frac{y}{b}} \right\} y dy$$

Setting  $x = c_1' - \sqrt{\frac{y}{b}}$

$$\int_0^b y \ln \left( c_1' - \sqrt{\frac{y}{b}} \right) dy = 2b^2 \int_{c_1'}^{c_1'-1} (x^3 - 3c_1'x^2 + 3c_1'x - c_1'^3) \ln x dx =$$

$$2b^2 \left\{ \frac{c_1'^4}{4} \ln c_1' - \frac{(c_1'-1)(c_1'^3 + c_1'^2 + c_1' + 1)}{4} \ln(c_1'-1) - \frac{10c_1'^4 + 2c_1'^3 + 6c_1'^2 + 4c_1' + 3}{48} \right\}$$

and finally

$$(39) \quad \bar{u}_c = c_2' + \frac{1}{\chi_c} \sqrt{\frac{\tau_c}{\rho_g}} \left\{ \frac{4}{5} + c_1'^4 \ln c_1' + (c_1'-1)(c_1'^3 + c_1'^2 + c_1' + 1) \ln(c_1'-1) - \frac{10c_1'^4 + 2c_1'^3 + 6c_1'^2 + 4c_1' + 3}{48} \right\}$$

The gas flowrate in the core  $\dot{m}_{gc}$  can be written

$$(40) \quad \dot{m}_{gc} = A_{gc} \bar{u}_c \rho_g$$

where  $A_{gc} = \pi b^2 \alpha^*$  is the section of the core filled up with the gas. The liquid flowrate can be obtained by the balance equation on the total liquid flowrate  $\dot{m}_L$  :

$$(41) \quad \dot{m}_{Lc} = \dot{m}_L - \dot{m}_{Lf}$$

In the case of Prandtl's universal distribution eqs. (40) and (41) are still valid whilst the average core velocity becomes:

$$\begin{aligned}
 (42) \quad \bar{u}_c &= \frac{2}{b^2} \int_0^b \left\{ u_m - \frac{1}{\chi_c} \sqrt{\frac{\tau_c}{\rho_0}} \ln \frac{R}{R-y} \right\} y dy \\
 &= u_m + \frac{1}{\chi_c} \sqrt{\frac{\tau_c}{\rho_0}} \left\{ \frac{2\Delta}{R} \ln \frac{R}{\Delta} - \frac{3}{2} - \frac{\Delta}{R} \right\}
 \end{aligned}$$

8 - FILM THICKNESS CALCULATION

The film thickness can be calculated through a balance equation of the gas flowrate

$$(43) \quad \dot{M}_G = \dot{M}_{Gf} + \dot{M}_{Gc}$$

As  $\dot{M}_G$  is equal to  $\dot{M} \cdot X$ , where  $\dot{M}$  is the total mass flowrate and  $X$  the quality, by introducing in eq. (43) the expression of  $\dot{M}_{Gf}$  and  $\dot{M}_{Gc}$  given by eqs. (27) and (40), it is obtained:

$$(44) \quad \dot{M} \cdot X = 2\pi \rho_G \left\{ c_1 \alpha^* \left[ \frac{\Delta R}{2} \left( 1 - \frac{\delta_c^2}{\Delta^2} \right) + \frac{\delta_c^3}{3\Delta} \right] + \frac{\alpha^*}{\chi} \sqrt{\frac{T_0}{T_1}} \left[ \Delta^2 (I_1 + I_3 - I_5 - I_6) + b \Delta (I_2 + I_4 - I_1 - I_3) \right] \right\} + \pi b^2 \alpha^* \rho_G \left\{ c_2 + \frac{1}{\chi_c} \sqrt{\frac{T_0}{T_1}} \left[ \frac{4}{3} + c_1^4 \ln c_1 - (c_1 - 1) (c_1^3 + c_1^2 + c_1 + 1) \ln (c_1 - 1) - \frac{10c_1^4 + 2c_1^3 + 6c_1^2 + 4c_1 + 3}{12} \right] \right\}$$

The film thickness  $\Delta$  is now the only unknown of eq. (44). This equation is too complex to be analytically solved and for this reason the calculation of  $\Delta$  has been programmed on a digital computer.

## 9 - MODEL PREDICTIONS AND COMPARISON WITH EXPERIMENTAL RESULTS

The model predictions have been compared with a set of experimental results.

The data taken into account are mainly related to film thickness measurements, since only a few data about film flowrate or entrained liquid are available at present. The comparisons have been performed for water-inert gas systems and for various values of the physical and geometrical parameters. The input data required by the computer program are:

- $\sigma$  = liquid surface tension
- $\rho_L, \rho_G$  = liquid and gas density
- $\mu_L$  = liquid viscosity
- $G$  = total specific mass flowrate
- $X$  = quality
- $R$  = duct radius

As previously said, the knowledge of the total pressure drop and the void fraction is also required. The program can calculate these quantities by using available correlations or read them as input data.

10 - COMPARISON WITH CISE DATA

Several film thickness measurements 4,5/, performed at CISE laboratories in different times, have been used for testing the model predictions. The pressure drop and the average void fraction have been calculated by the following correlations 7,8/:

$$(45) \quad \frac{dp}{dz} = \frac{0.43}{D^{1.2}} \left( \frac{\gamma}{73} \right)^{0.4} \left( \frac{\mu_L}{0.01} \right)^{0.04} (G^2 \bar{v})^{0.35}$$

$$(46) \quad 1 - \bar{\alpha} = (1 - X_v) \left\{ 1 + \frac{1.35 X_v^n}{1 + 0.335 \frac{G}{\gamma} D^{1.2}} \left( \frac{1}{\rho_L} \right)^{1/4} \right\}$$

where  $n = 0.9 + 0.05\gamma$

$1 - X_v$  = liquid volume flowrate quality

$\bar{v}$  = flowrate specific volume of the mixture

Preference was given to the pressure drop calculated by means of eq.(45) rather than to the measured one in order to avoid the experimental fluctuations. However both values have been used for a set of data. As one can see in table 1° the use of the correlation (45) does not bring about remarkable differences in the calculated values of the film thickness. In the same table the result obtained by using the distributions of Von Karman eq. (39) and of Prandtl eq. (42) are also compared. In this case as well the differences are not remarkable. All the other result are summarized in tables 2° - 6°. In these tables are reported the measured and predicted film thickness and the calculated liquid film flowrate in addition to the

physical parameters describing the system. Some of the results are also shown in figs. 4 ÷ 31.

In figs. 4 ÷ 6 the film thickness values of table 1° are plotted as a function of the specific gas flowrate  $G_g$  for some values of the specific gas flowrate  $G_L$ . Here and in the following figures the full line joins the experimental points, whilst the dashed line the predicted ones.

Figs. 7 ÷ 11 show the data of table 2°, figs. 12 ÷ 15 those of table 4°, figs. 16 ÷ 18 those of table 5° and figs. 19 ÷ 20 those of table 6°. No data of table 3° are plotted since the experimental conditions are equal to those of table 5° which are more recent. As one can see by the diagrams and tables the model here presented predicts the film thickness trend as a function of  $G$ ,  $X$ ,  $P$  and  $R$  in a correct way. The agreement fails at the extreme values of  $X$  and  $G$ . This fact can be better seen in figs. 21 - 22 where some data of table 2° with the film thickness versus  $G_L$  at constant  $G_g$  are plotted.

At very low quality the substitution of the cylindrical geometry with the plane one and the matching of the laminar sublayer with the turbulent region, neglecting the buffer zone, is no longer justified. On the other hand for very high values of  $X$  the film and laminar sublayer thickness are comparable and therefore the assumption  $\frac{\delta_L}{\Delta} \left( 1 - \frac{T_c}{T_g} \right) \ll 1$  fails.

In the range of validity of the introduced assumption, also the quantitative agreement seems to be satisfactory. It can be noted that the experimental measurements define an electrical film thickness, whilst the model predicts a thickness defined by purely fluidodynamics considerations.

As for the liquid flowrate a test of the model predictions is more difficult. In figs. 23 ÷ 25 the film and entrained liquid flowrate and the ratio  $\Gamma_{Lp} / \Gamma_L$  are shown as a function of  $X$

for three values of the total flowrate ( $\Gamma = 491, 736, 982 \text{ g. / sec}$ )  
 The data are related to water-argon mixture at 22 ata, for a duct with  $R = 1.25 \text{ cm}$ . The trend with  $G$  and  $X$  seems to be reasonable and under some aspects similar to one experimentally observed at Harwell in steam-water system <sup>9/</sup>. Fig. (26) shows the velocity profile for the case  $\Gamma = 982 \text{ g./sec}$  ( $X = 0.35$ ) as a function of the radial coordinate. Some results reported by Cravarolo Hassid are also shown (dashed line) in figs. (24) (25) and (26).

Some further comparisons have been obtained by plotting the quantity  $\frac{\Gamma_{Lf}}{\pi D \mu_L}$  versus the dimensionless thickness  $\Delta^+ = \frac{\Delta}{\mu_L} \sqrt{\tau_0 \rho_L}$ . In ref.2 it is suggested that the experimental results are well correlated by the equation

$$(47) \quad \frac{\Gamma_{Lf}}{\pi D \mu_L} = 5.3 (\Delta^+)^{1.1}$$

Fig. 27 is a plot, in a log log chart, of eq. (47) together with the lines delimiting  $\pm 10\%$  variations.

The dots represent the values predicted by the model for some values of table 5°. For a fully comparison the predictions of Levy Model and those of Dukler - Hewitt analysis derived from, reference 2, are also reported.

As one can see the values predicted by these theories are overestimated (40 - 60 %) in comparison with the experimental correlation. The prediction of the present model shows a very good agreement, except for the low region, where, as previously said, the hypothesis introduced are not completely satisfied.

In the authors' opinion the model predictions are best correlated by defining  $\Delta^+ = \frac{\Delta}{\mu_L} \sqrt{\tau_0 \bar{\rho}_f}$ , since  $\bar{\rho}_f$  represent the true mean film density. Since it is always  $\bar{\rho}_f < \rho_L$ , with this definition



the predicted values are no longer in agreement with eq. (47), as shown in fig. 28 where some data of table 1° are plotted.

The relation between  $\Sigma_{L_f} / \pi D \mu_L$  and the new  $\Delta^+$  becomes:

$$(48) \quad \frac{\Sigma_{L_f}}{\pi D \mu_L} = 3.46 (\Delta^+)^{1.26} \quad \Delta^+ = \frac{\Delta}{\mu_L} \sqrt{\tau_0 \bar{\rho}_f}$$

Figs. 29 ÷ 31 show the data of tables 1°, 2°, 6° and those corresponding to  $G = 100, 150, 200, \text{ gr/cm}^2 \text{ sec}$  with the line of eq. (48).

Trend of  $\Delta$  as a function of  $G_g$  (data of table I)

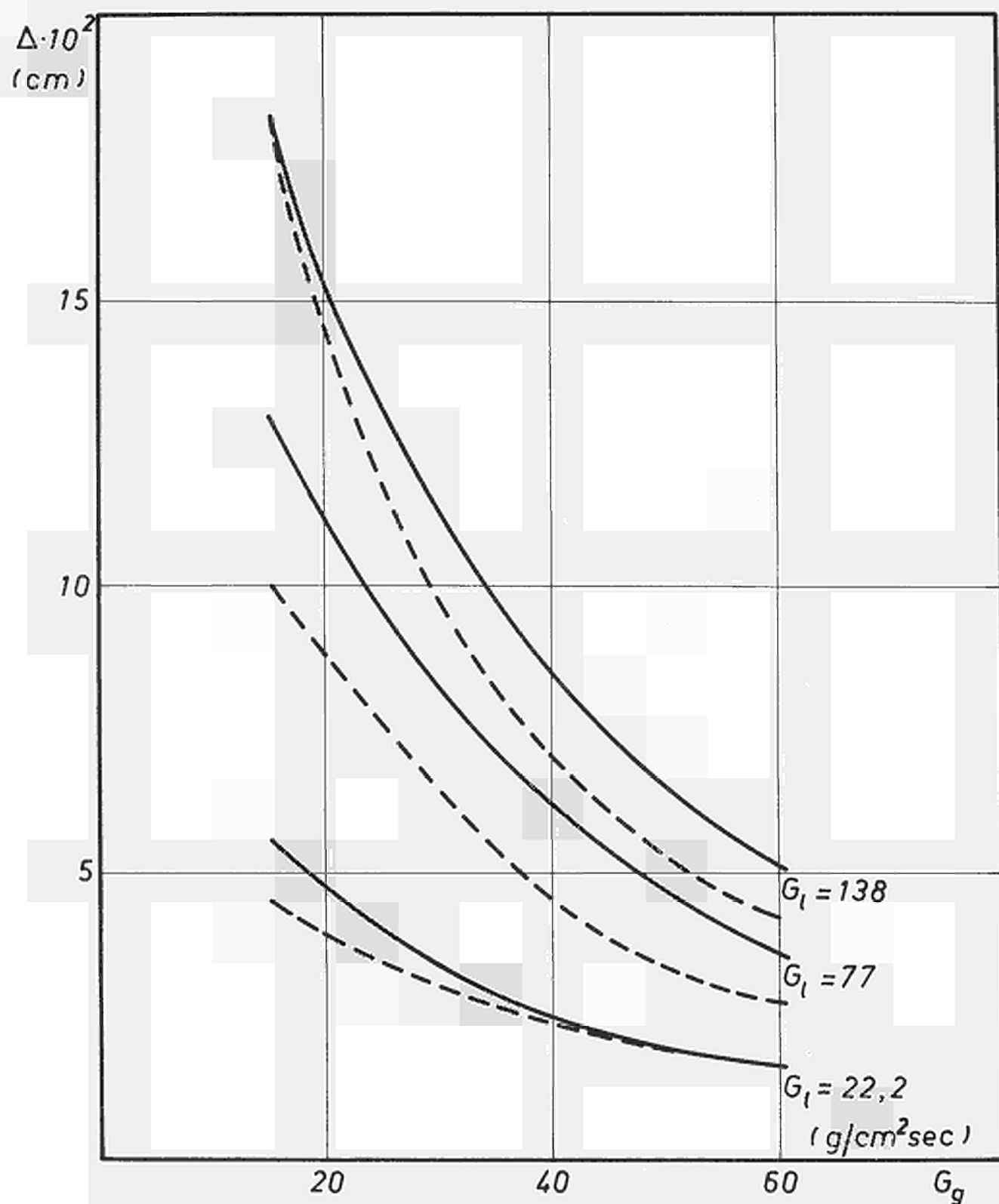


Fig. 4

Trend of  $\Delta$  as a function of  $G_g$  (data of table I)

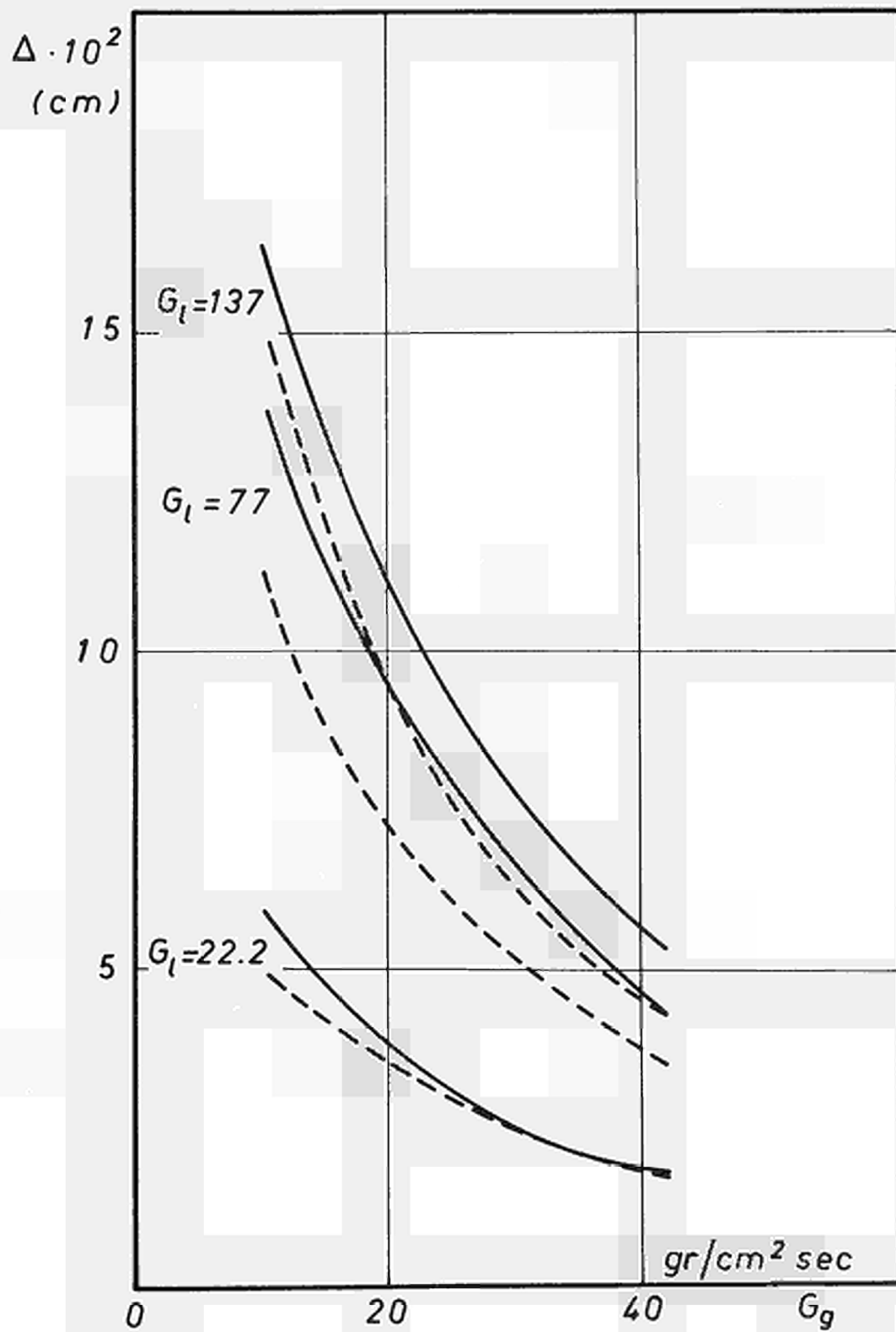


Fig. 5

Trend of  $\Delta$  as a function of  $G_g$  (data of table I)

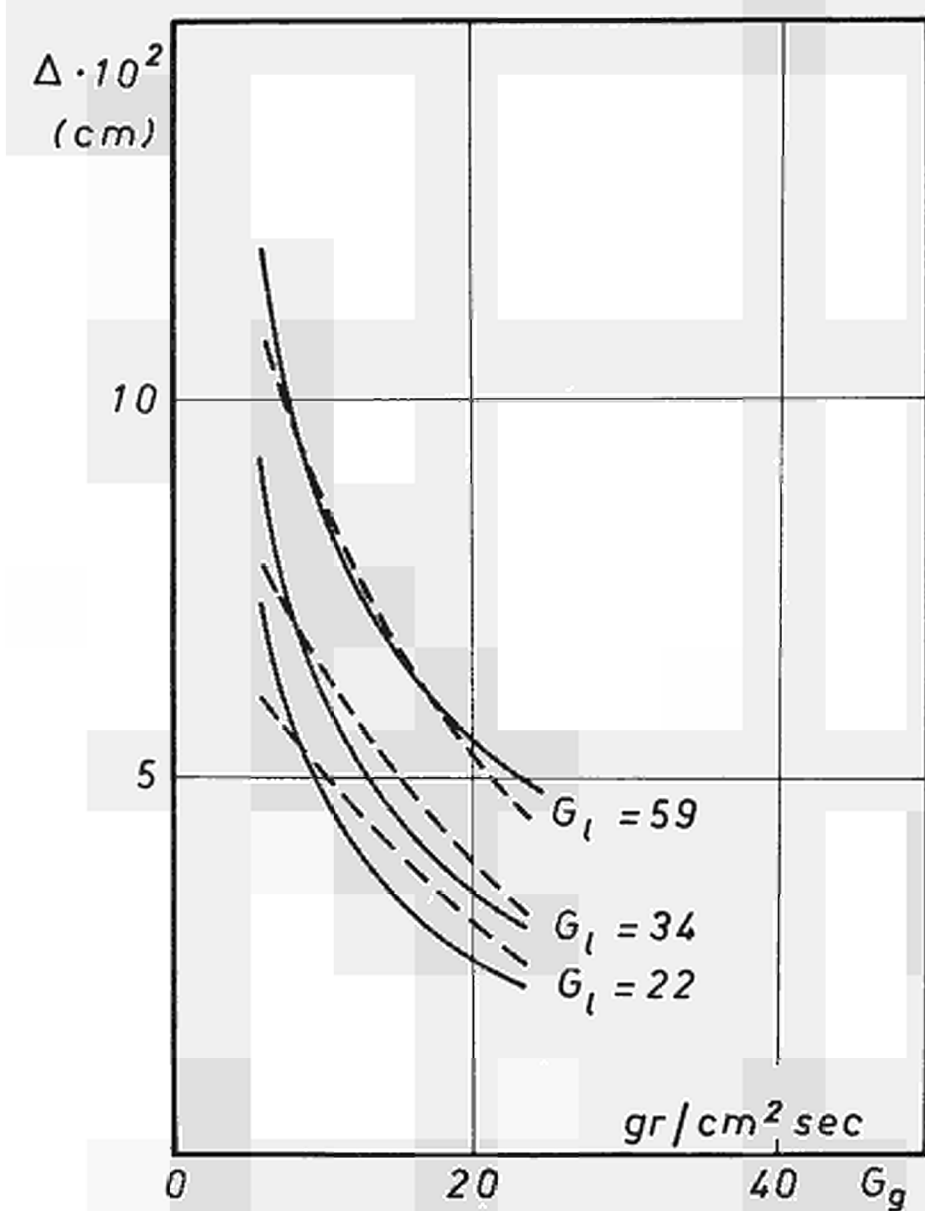


Fig. 6

Trend of  $\Delta$  as a function of  $G_g$  (data of table II)

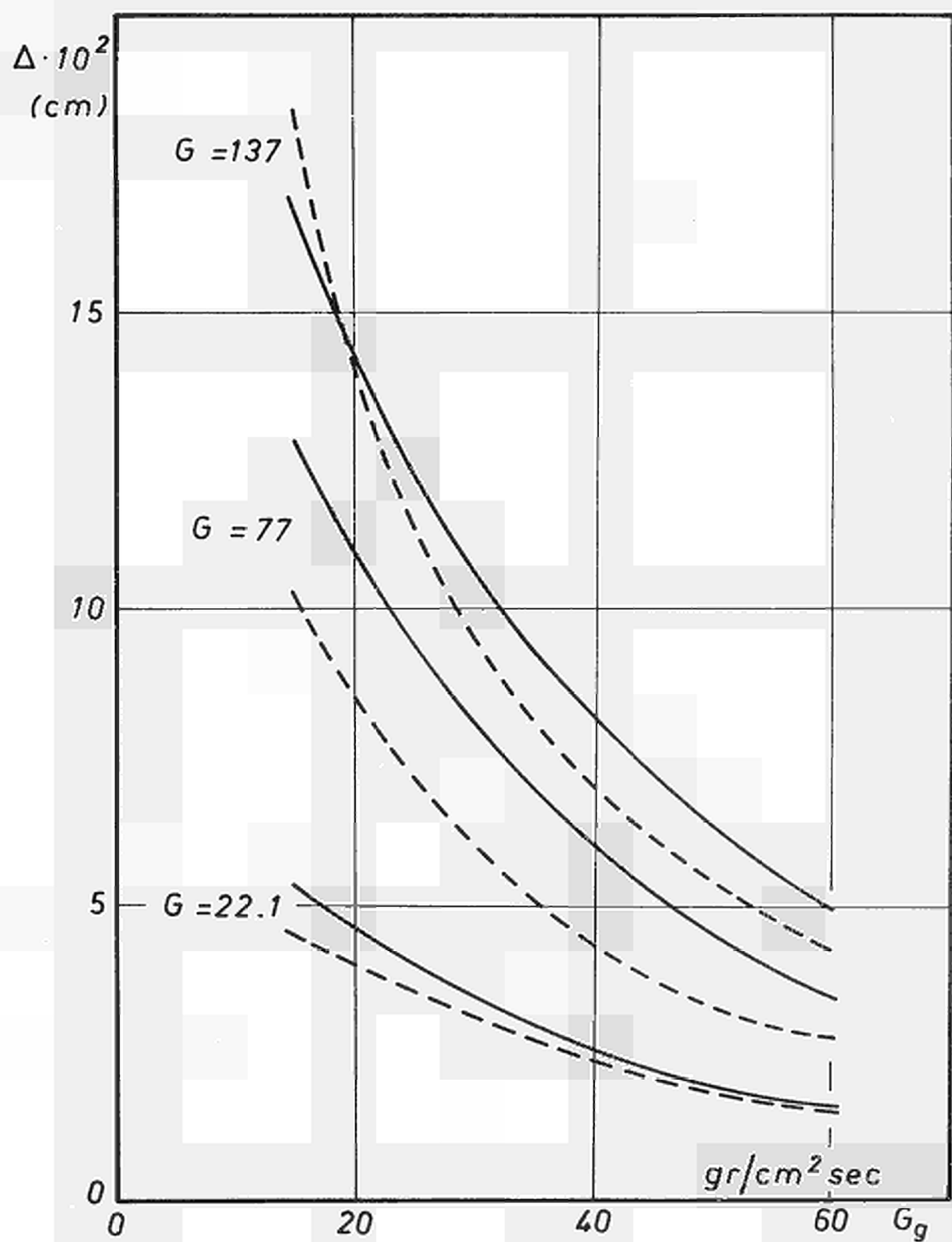


Fig. 7

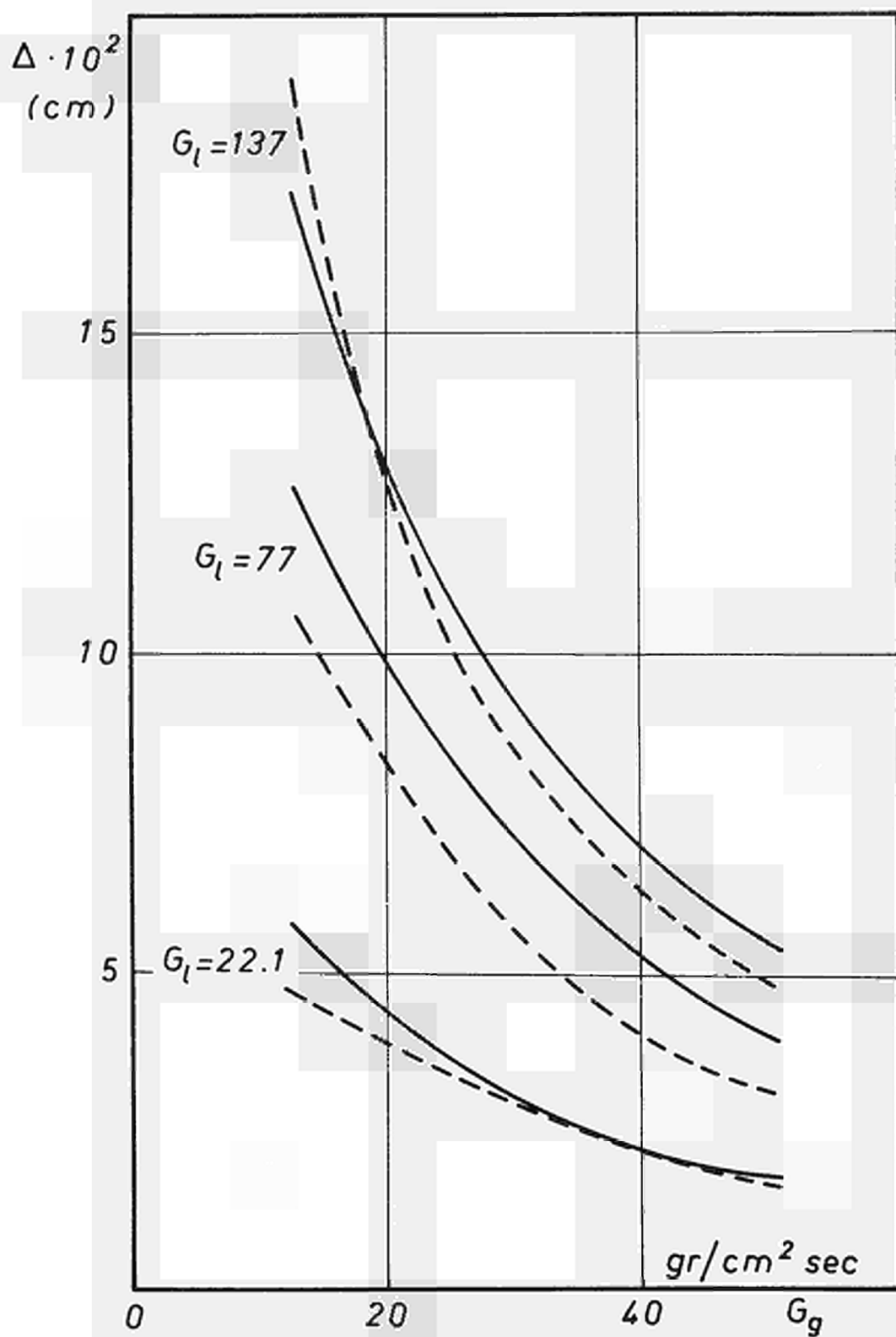
Trend of  $\Delta$  as a function of  $G_g$  (data of table II)

Fig. 8

Trend of  $\Delta$  as a function of  $G_u$  (data of table II)

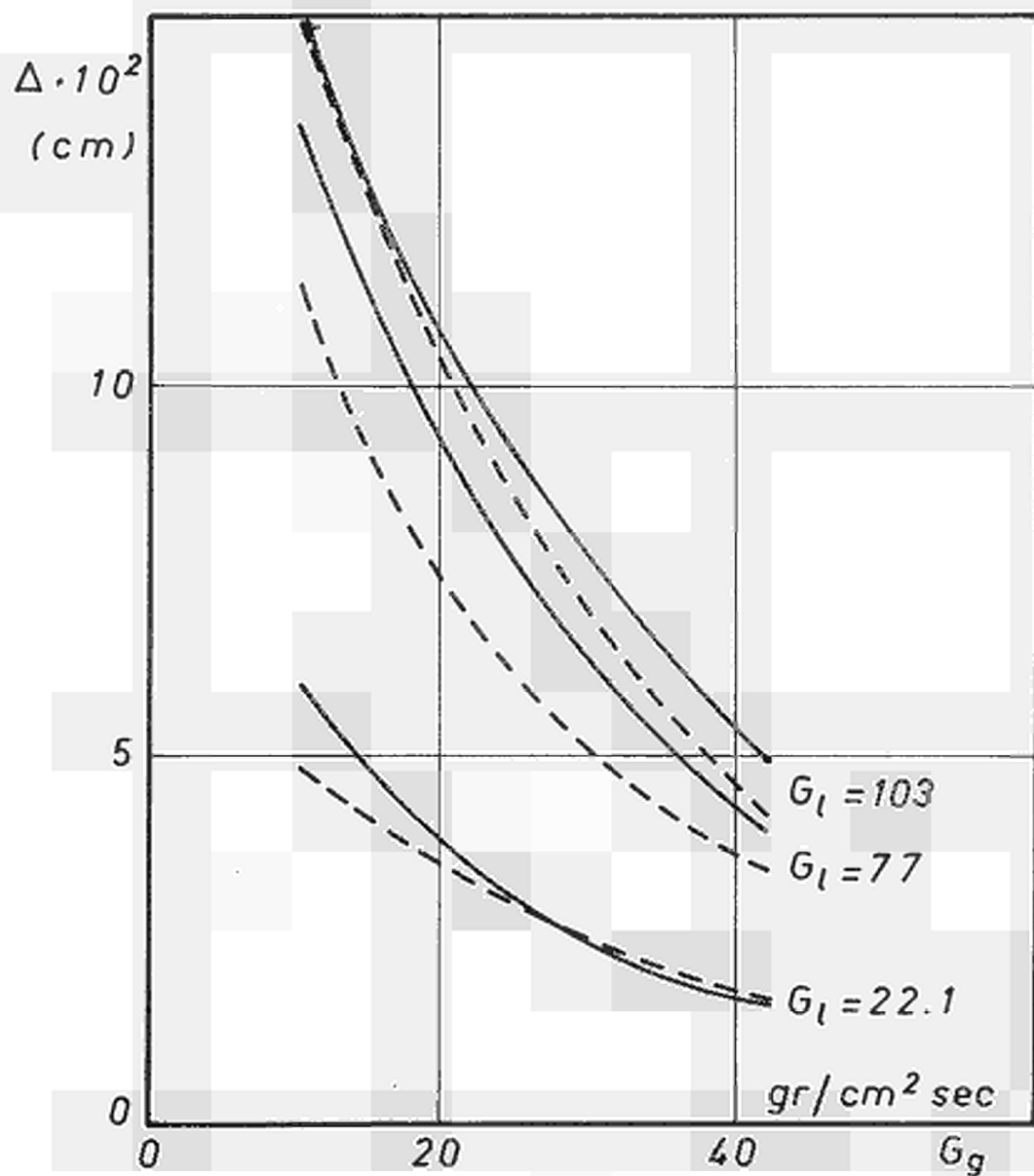


Fig. 9

Trend of  $\Delta$  as a function of  $G_g$  (data of table II)

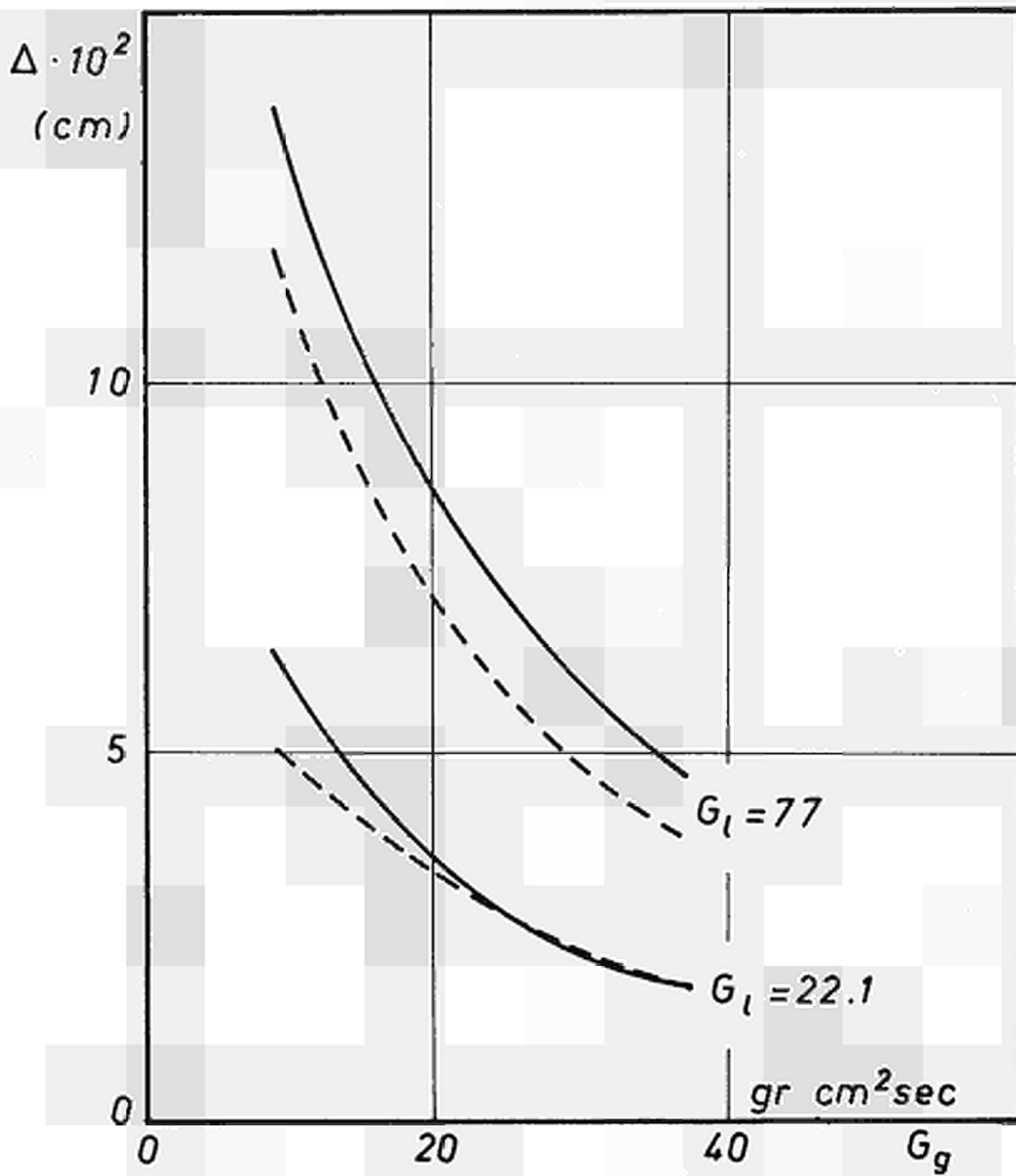


Fig. 10



Trend of  $\Delta$  as a function of  $G_g$  (data of table II)

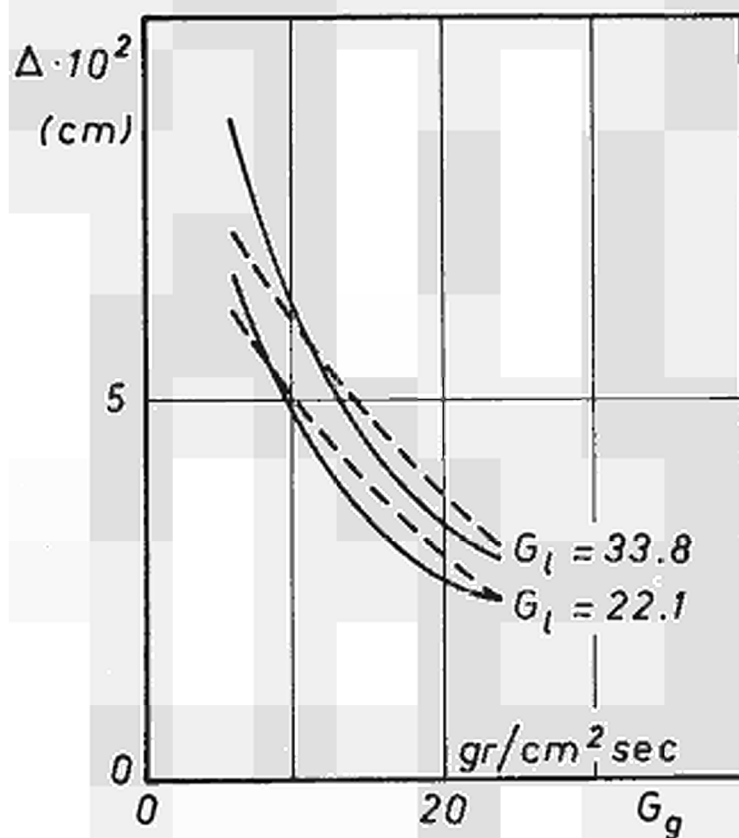


Fig. 11

Trend of  $\Delta$  as a function of  $G_g$  (data of table IV)

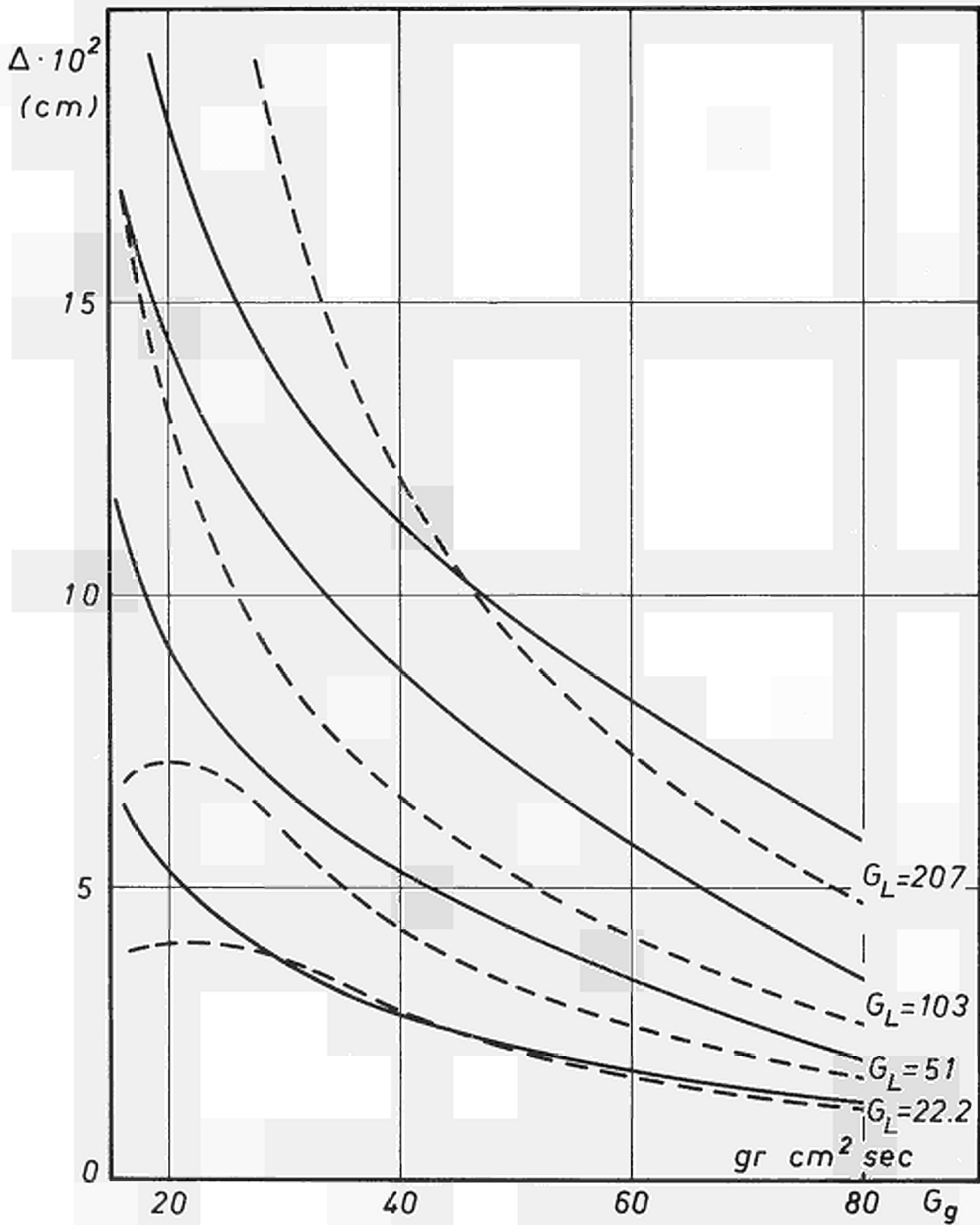


Fig. 12

Trend of  $\Delta$  as a function of  $G_g$  (data of table V)

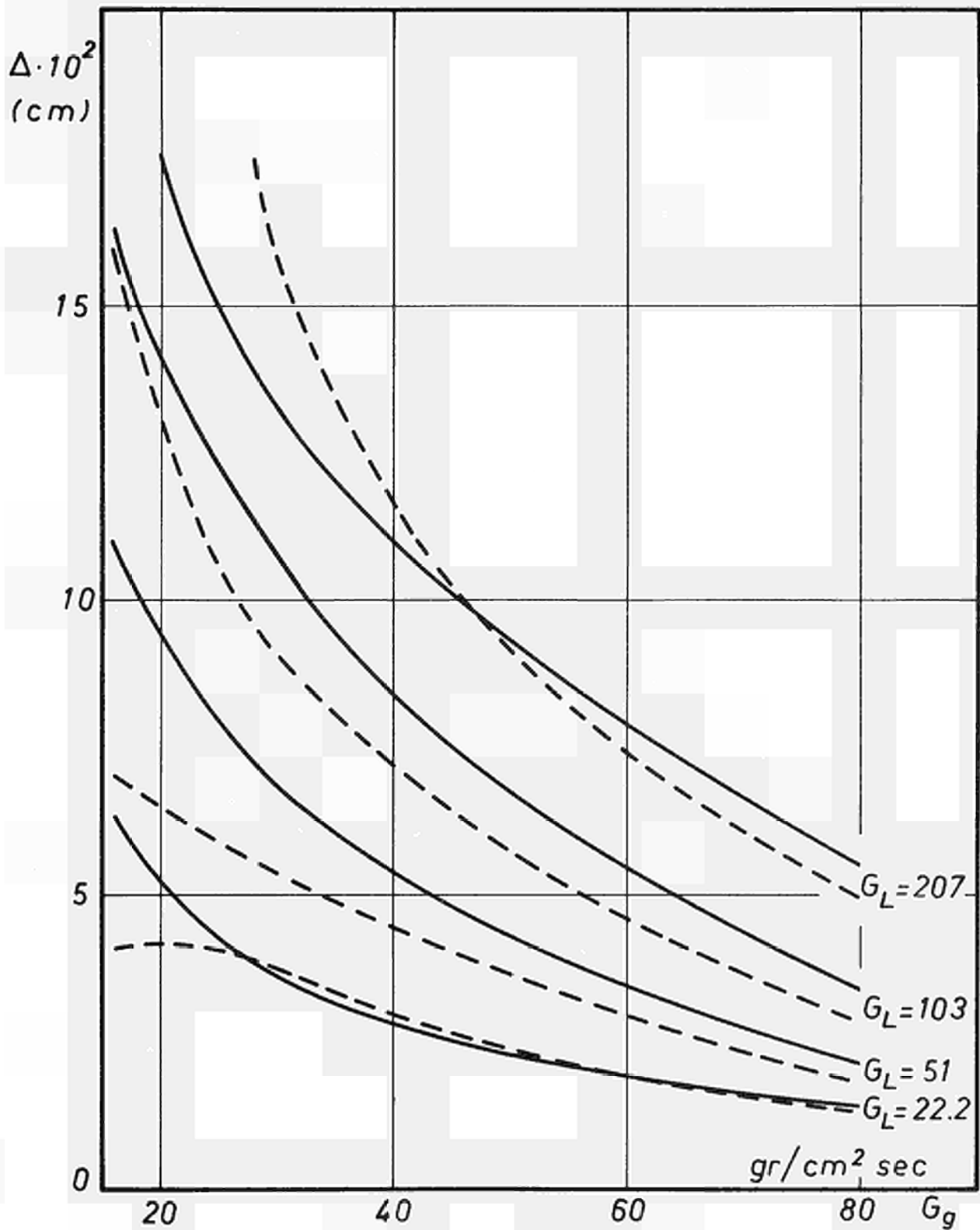


Fig. 13

Trend of  $\Delta$  as a function of  $G_g$  (data of table IV)

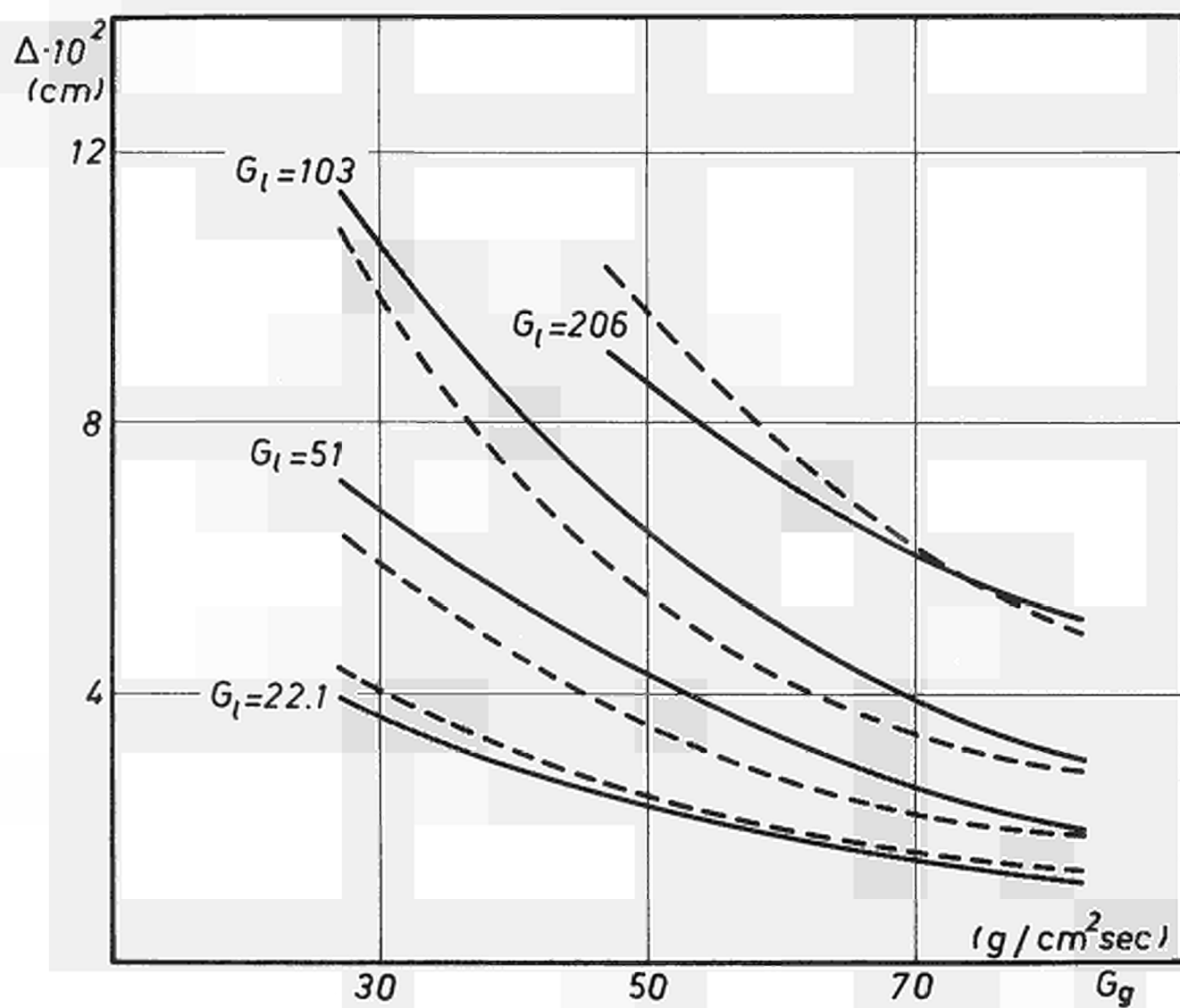


Fig. 14

Trend of  $\Delta$  as a function of  $G_g$  (data of table IV)

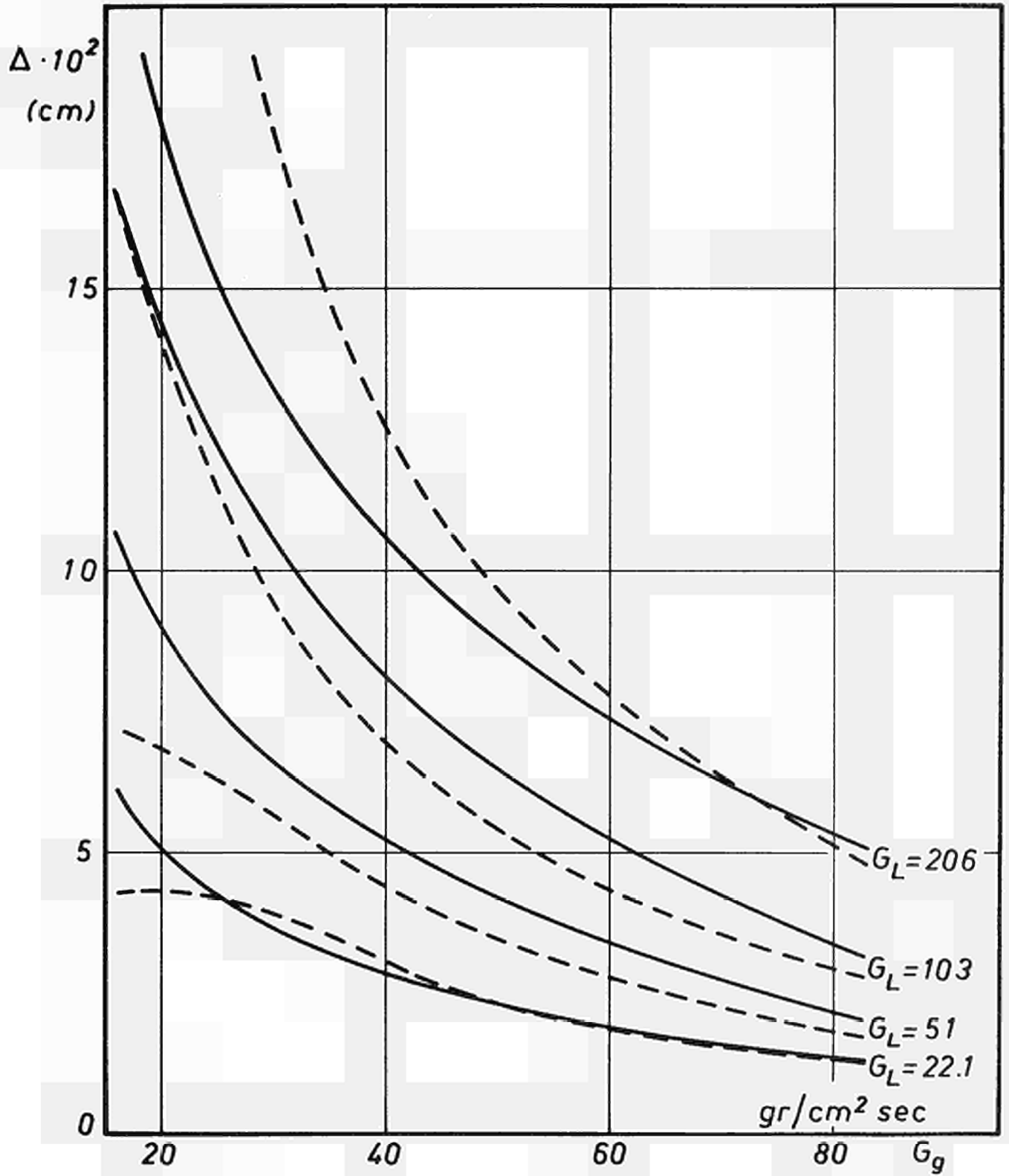


Fig. 15

Trend of  $\Delta$  as a function of  $G_g$  (data of table V)

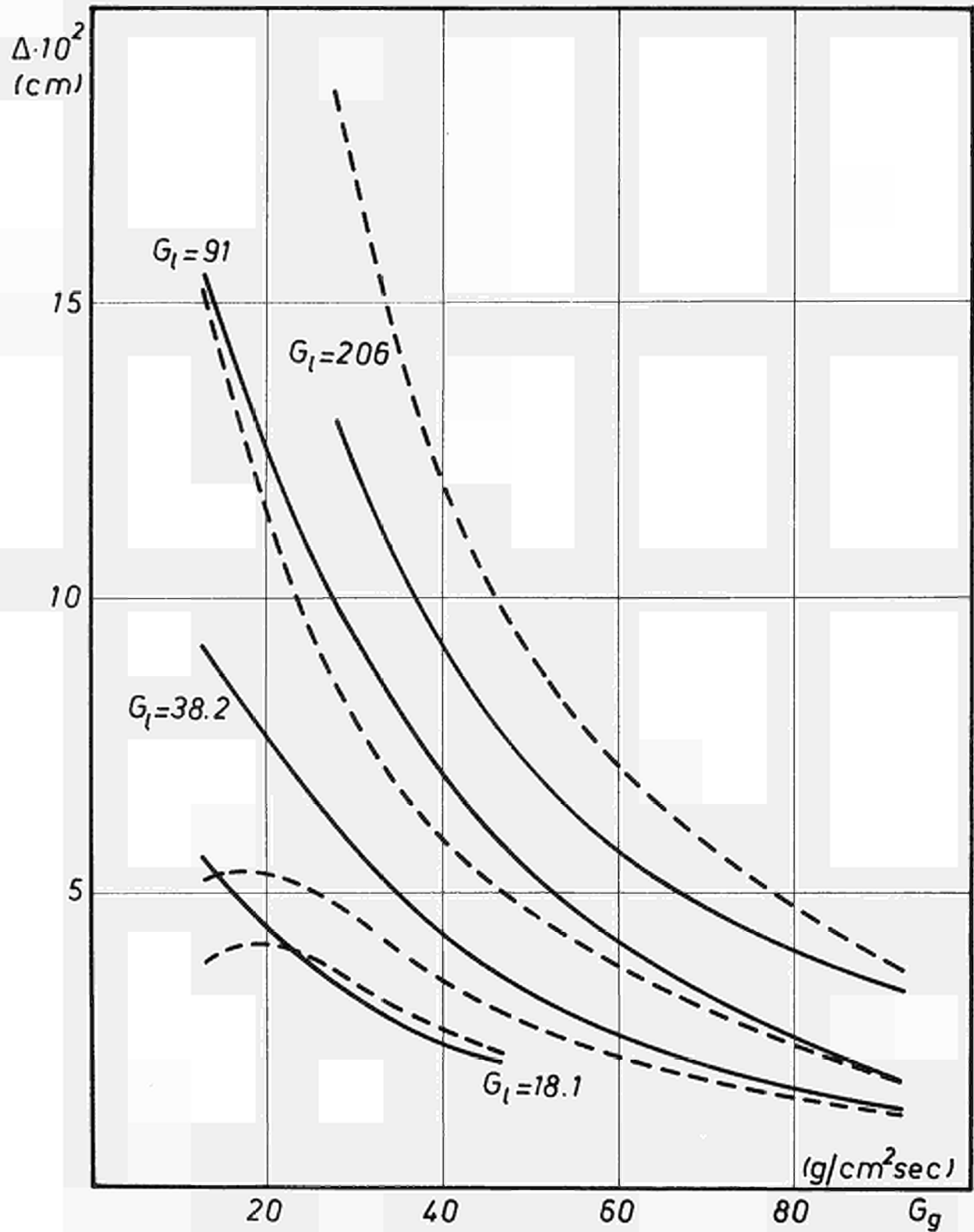


Fig. 16

Trend of  $\Delta$  as a function of  $G_g$  (data of table V)

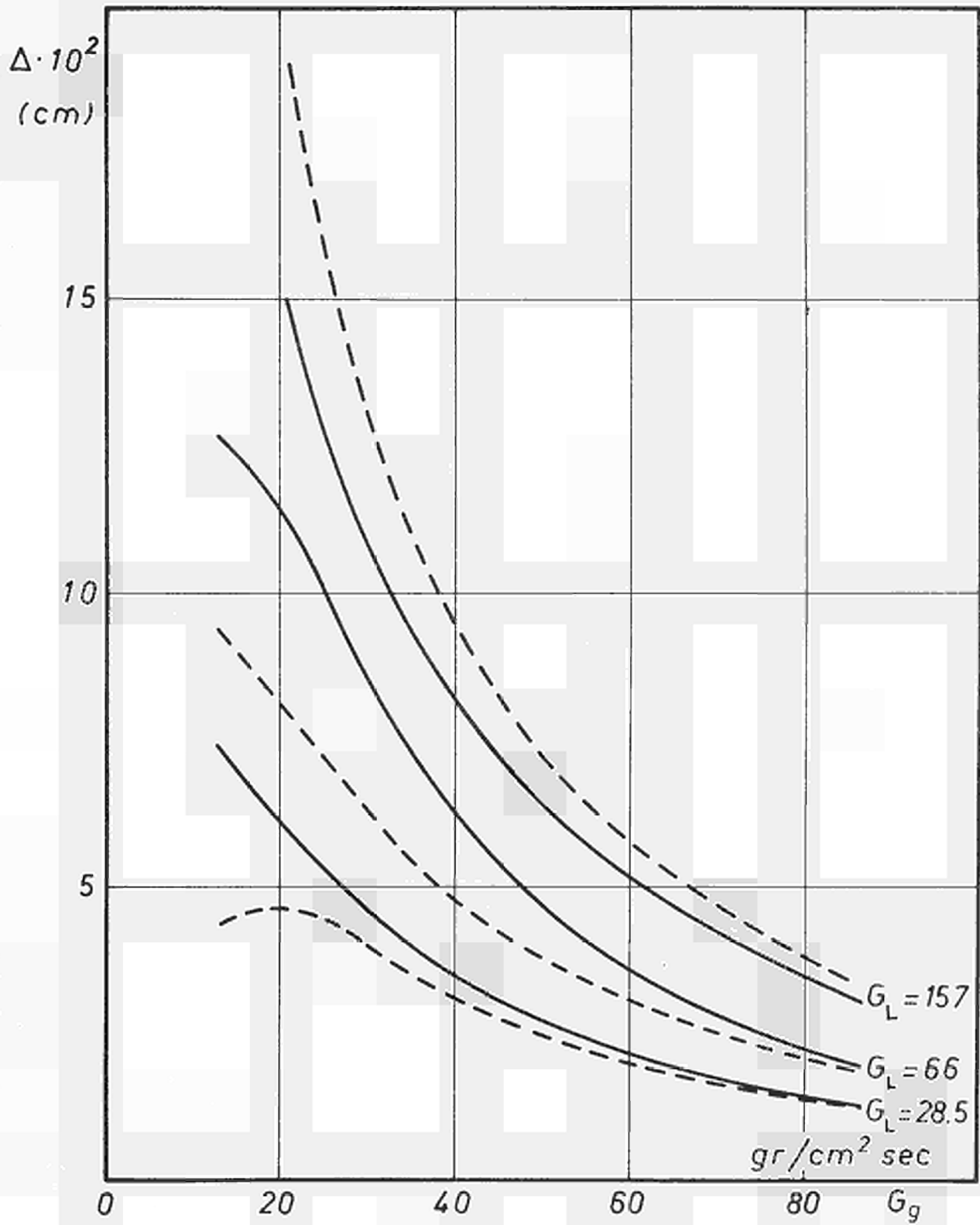


Fig. 17

Trend of  $\Delta$  as a function of  $G_g$  (data of table V)

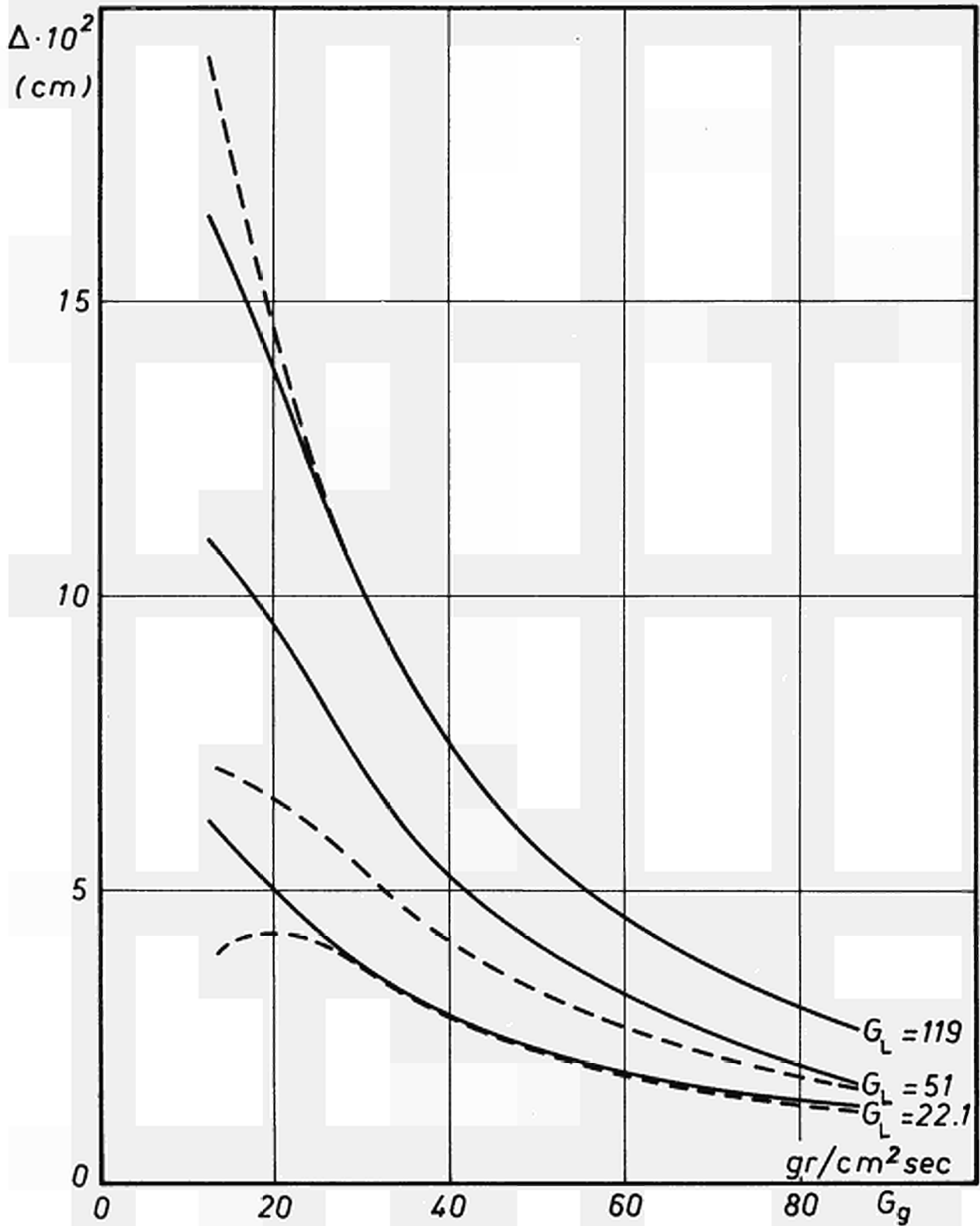


Fig. 18



Trend of  $\Delta$  as a function of  $G_g$  (data of table VI)

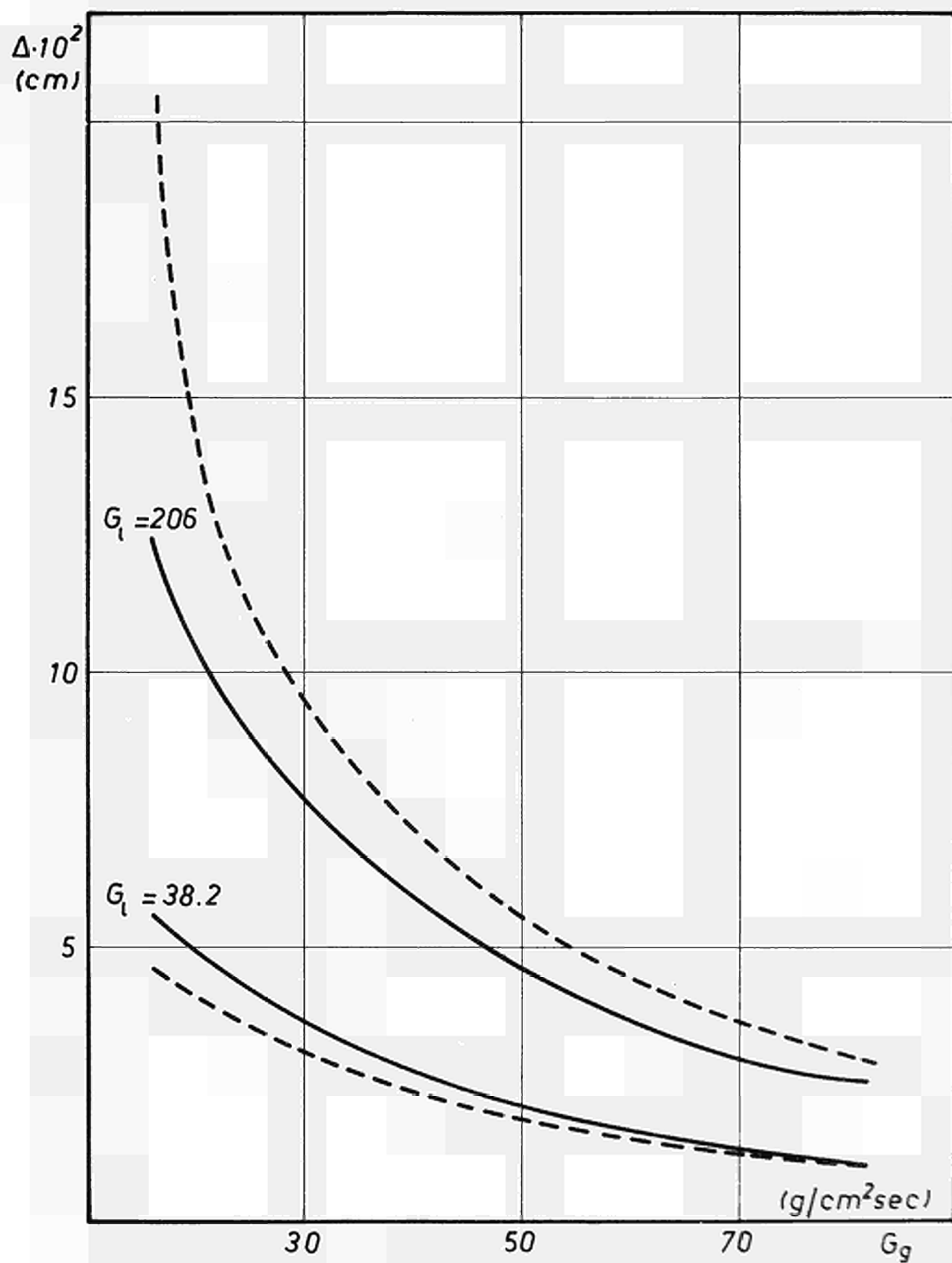


Fig. 19

Trend of  $\Delta$  as a function of  $G_g$  (data of table VI)

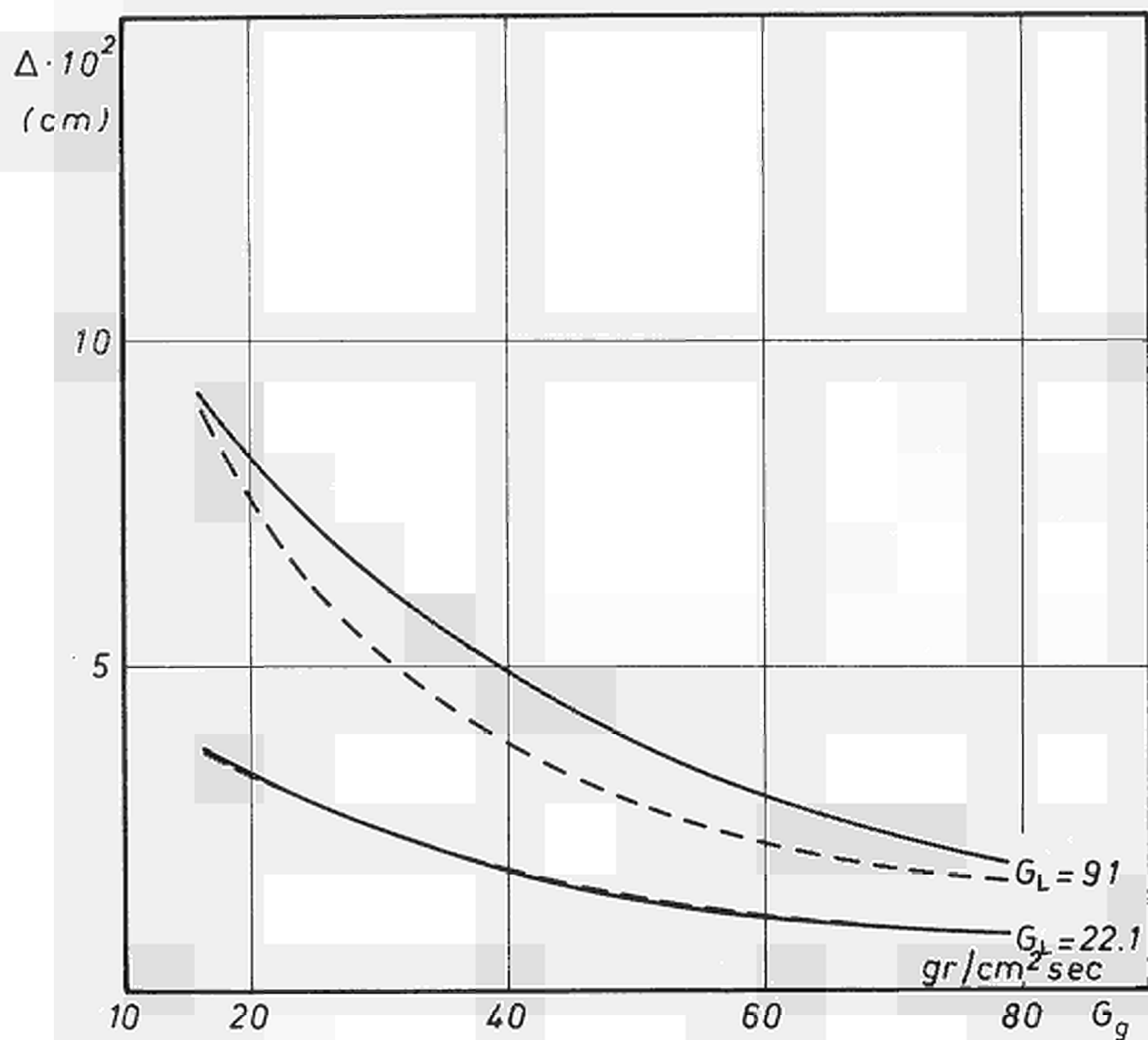


Fig. 20

Trend of  $\Delta$  as a function of  $G_t$  (some data of table II)

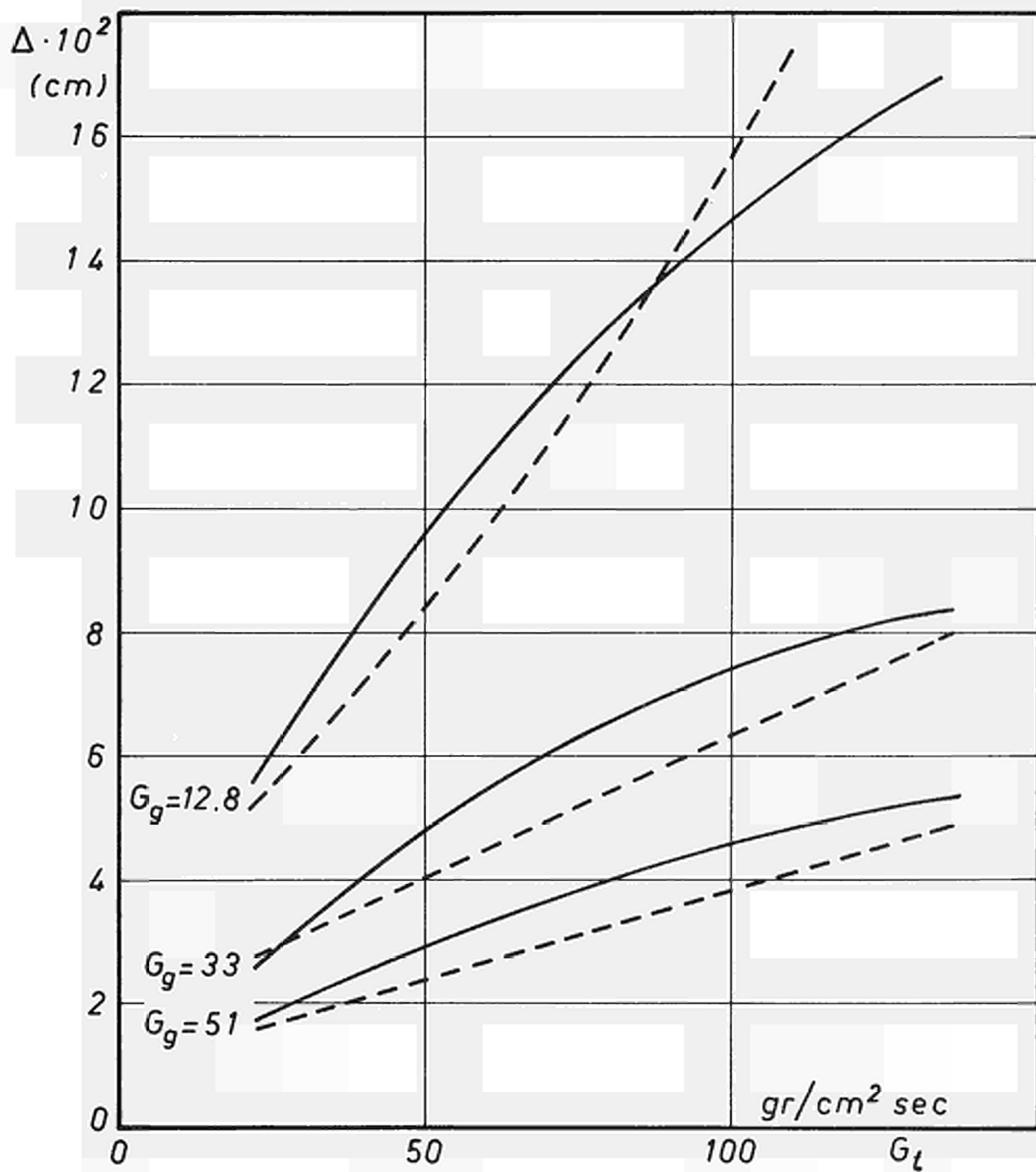


Fig. 21

Trend of  $\Delta$  as a function of  $G_L$  (some data of table II)

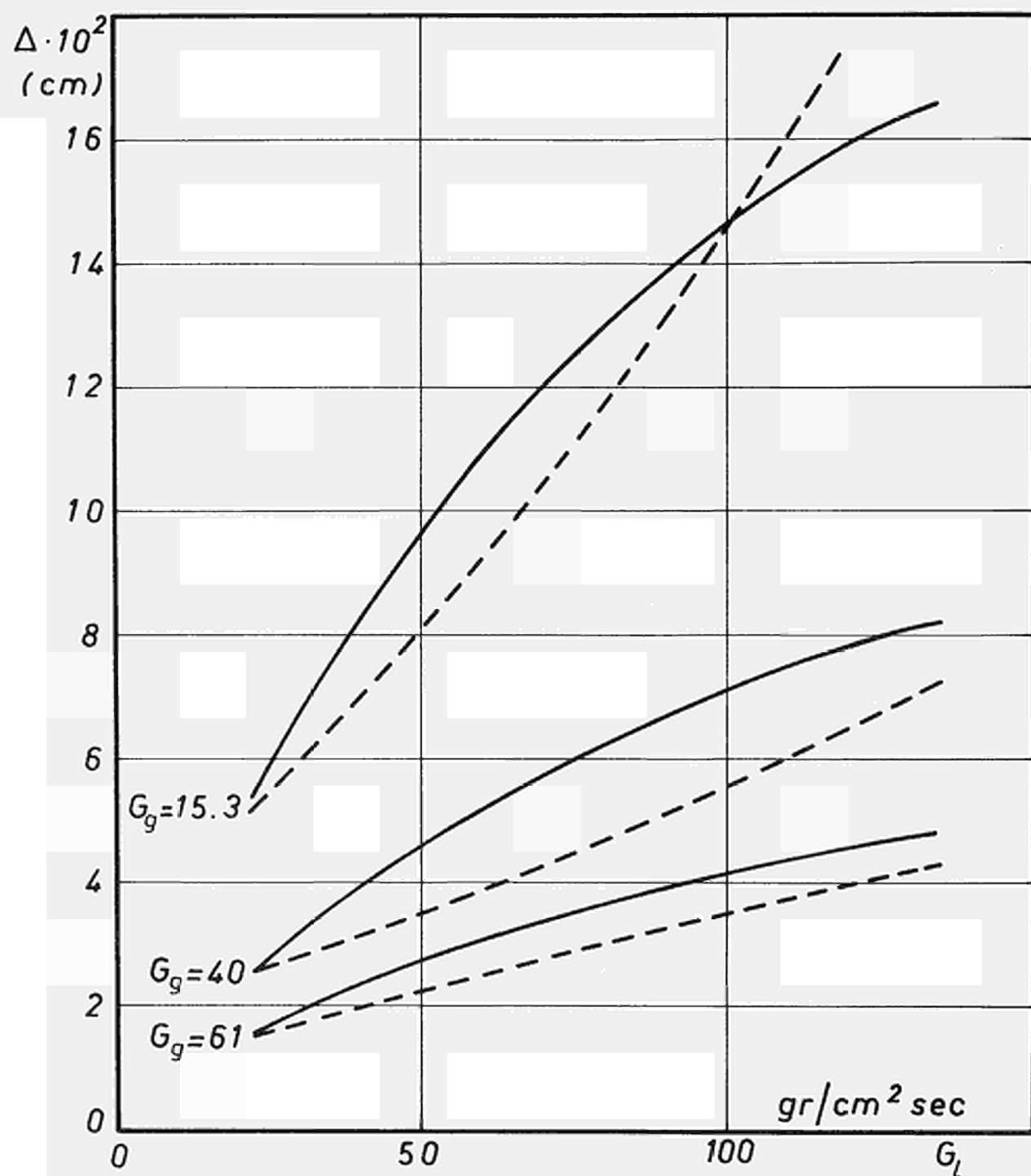


Fig. 22

Film flowrate as a function of quality X

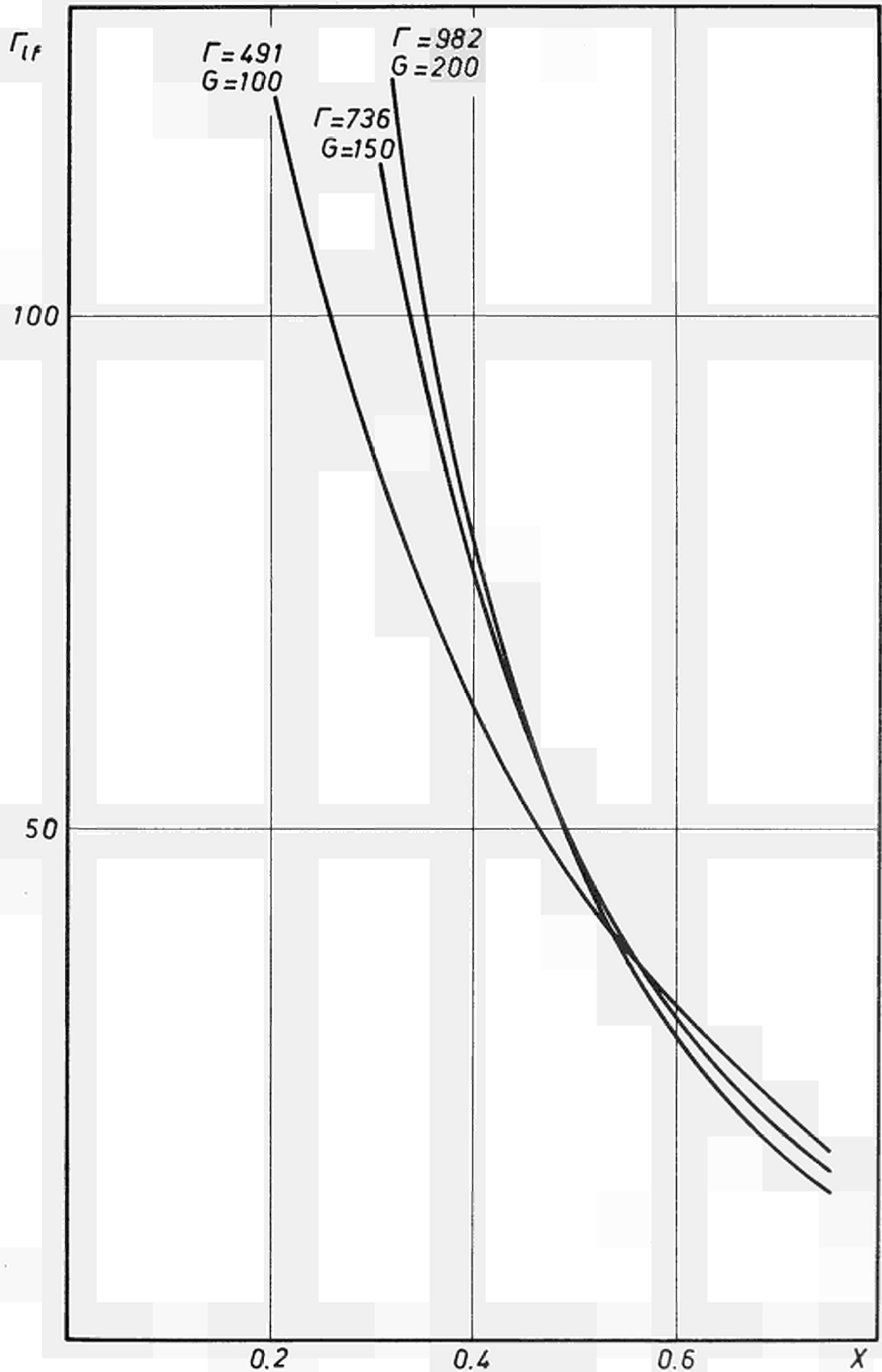


Fig. 23

Entrained liquid flowrate as a function of quality  $X$

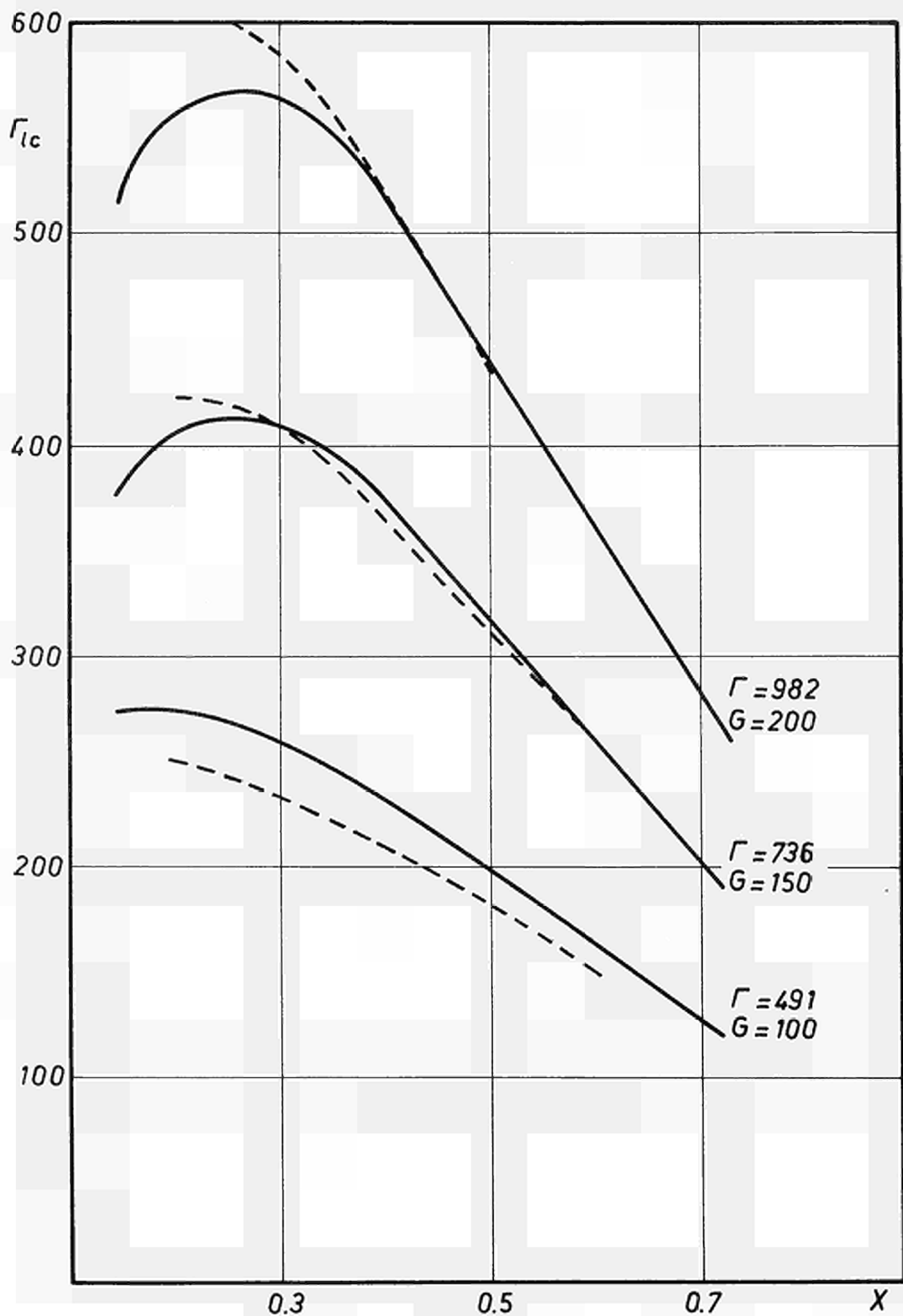


Fig. 24

Ratio  $\Gamma_{LF}/\Gamma_L$  as a function of quality  $X$

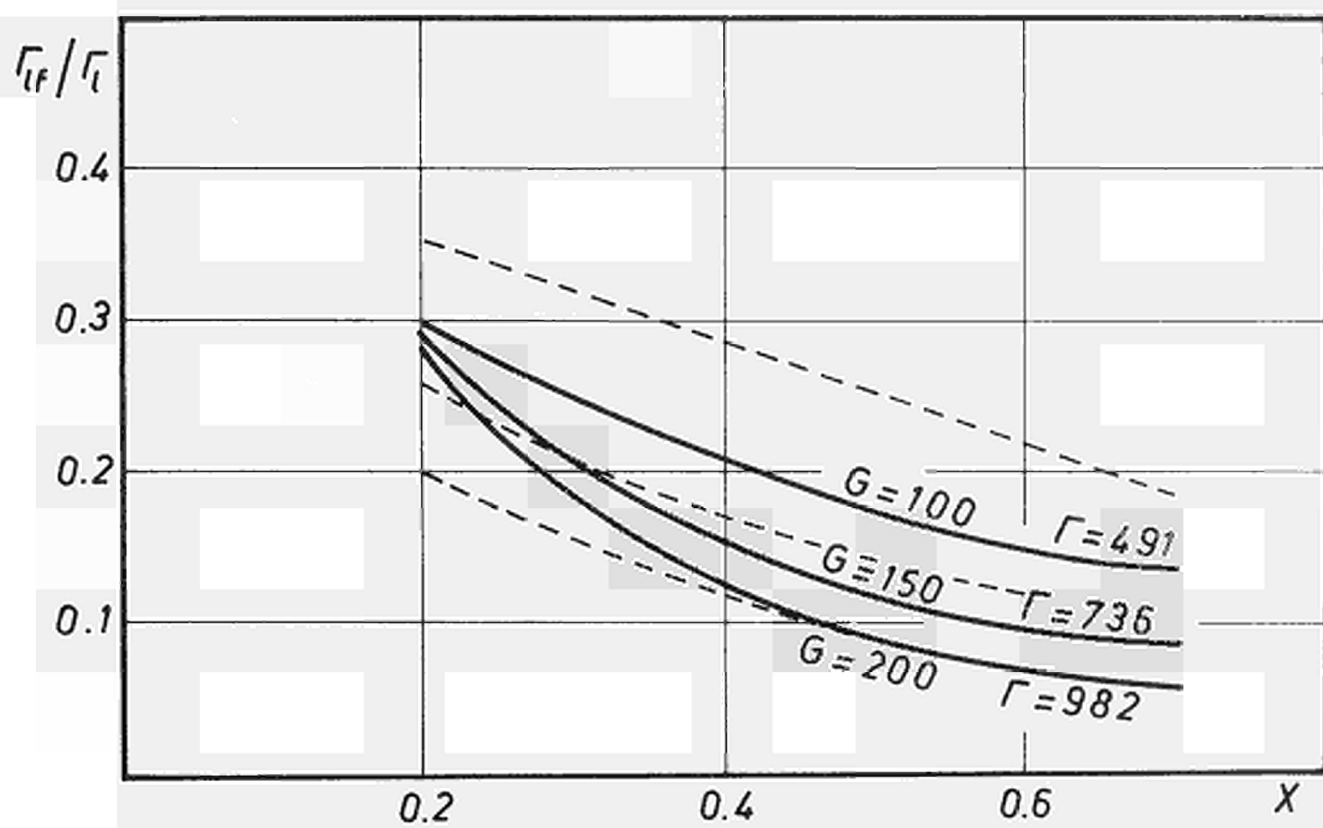


Fig. 25

Comparison between Velocity Profile of our model  
and the experimental one.

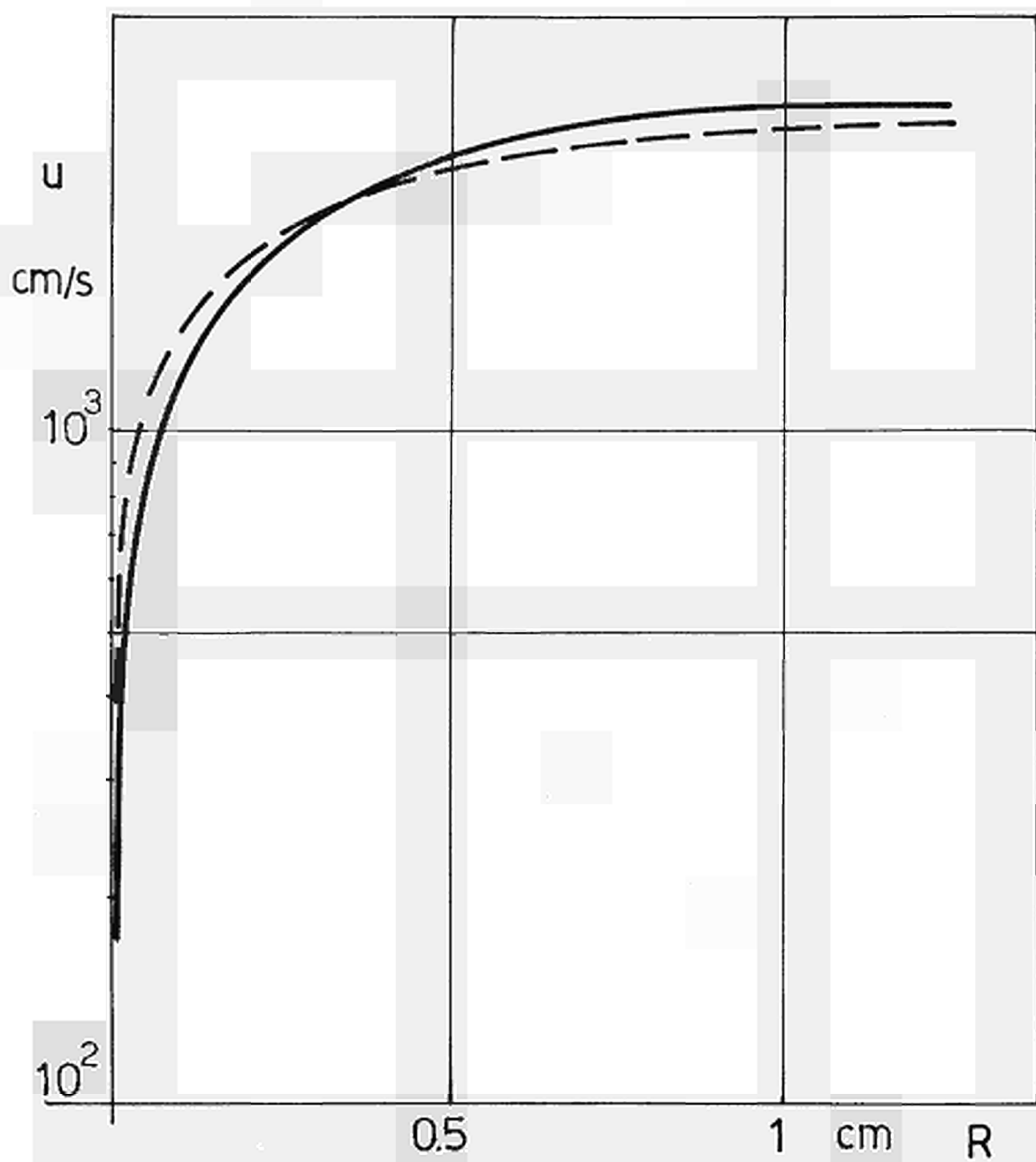


Fig. 26



Comparison amongst the predictions of Dukler - Hewitt-Levy and our model with respect to eq.47

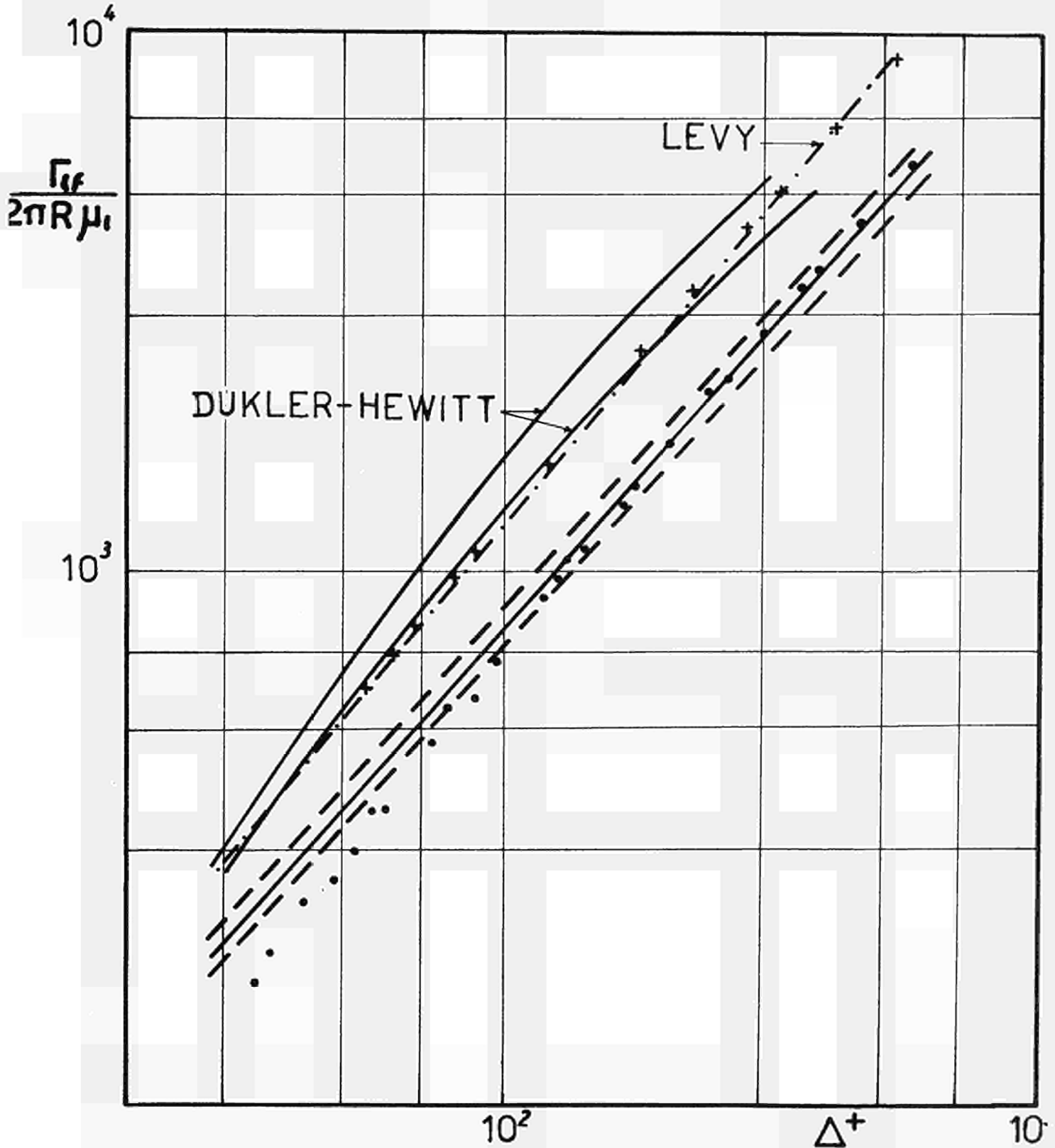


Fig. 27

Data of table I according to eq. 48

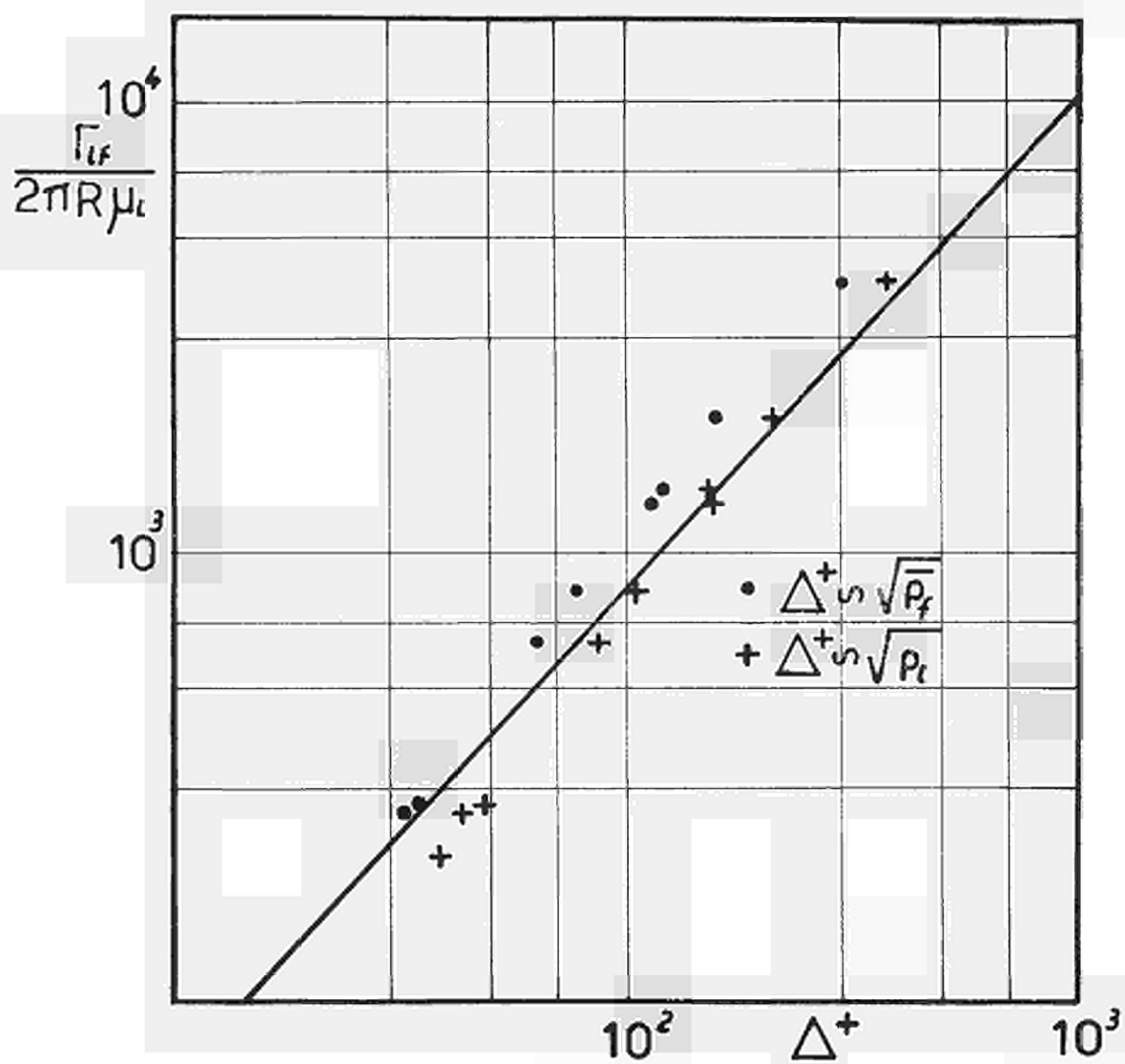


Fig. 28

Data of table II according to eq. 48

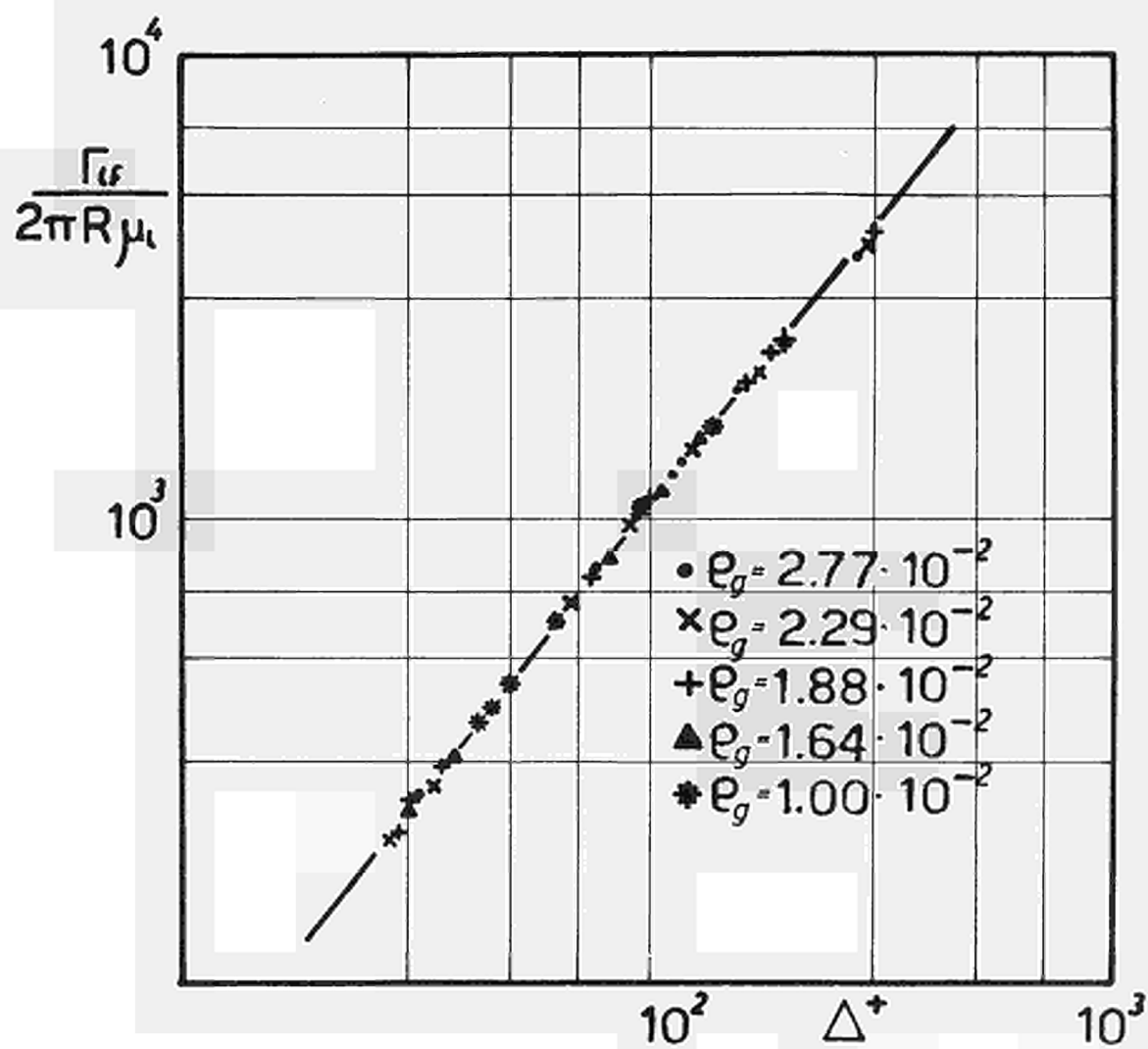


Fig. 29

Data of table VI according to eq. 48

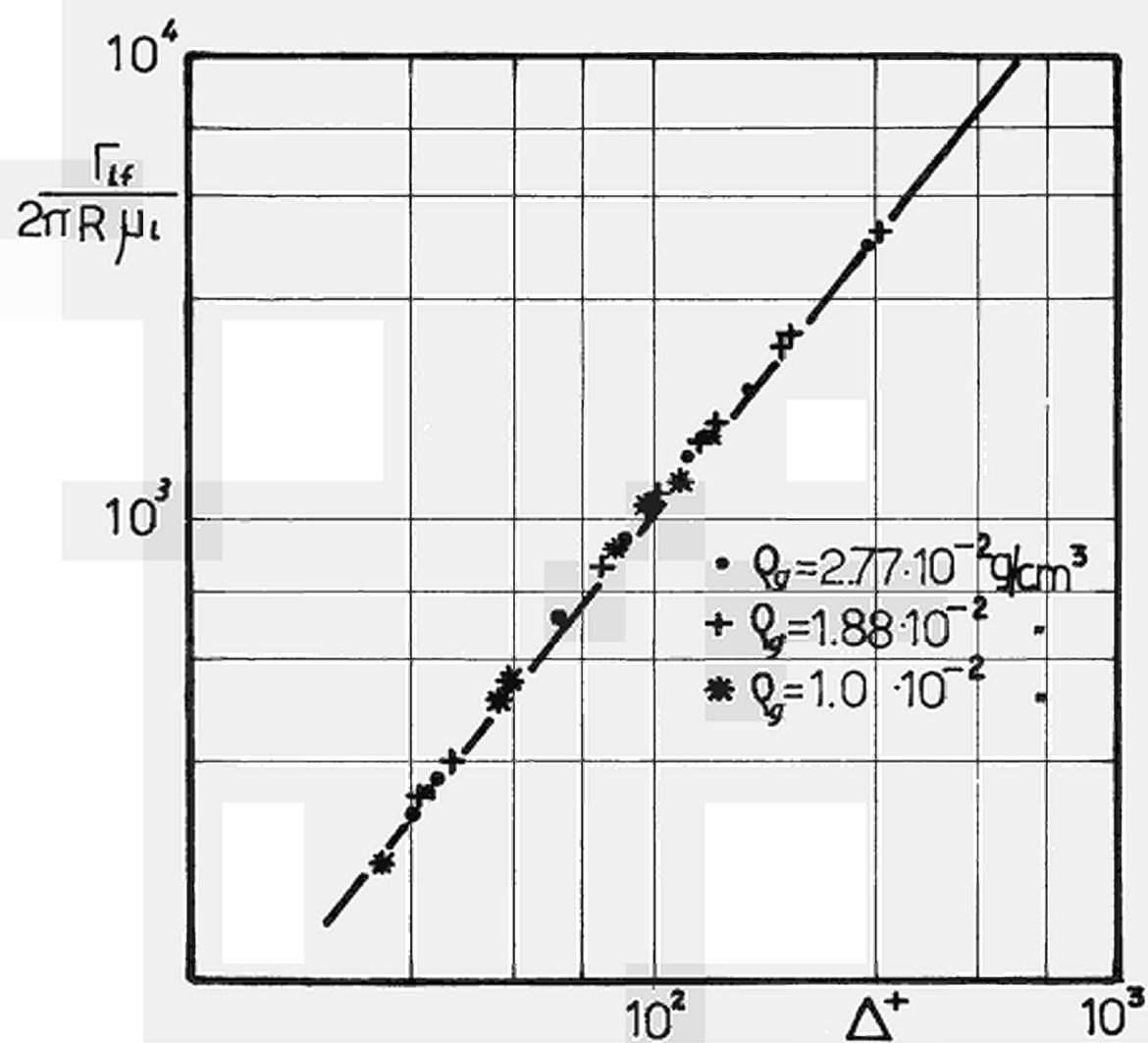


Fig. 30

Data corresponding to  $G = 100, 150, 200$  according to eq. 48

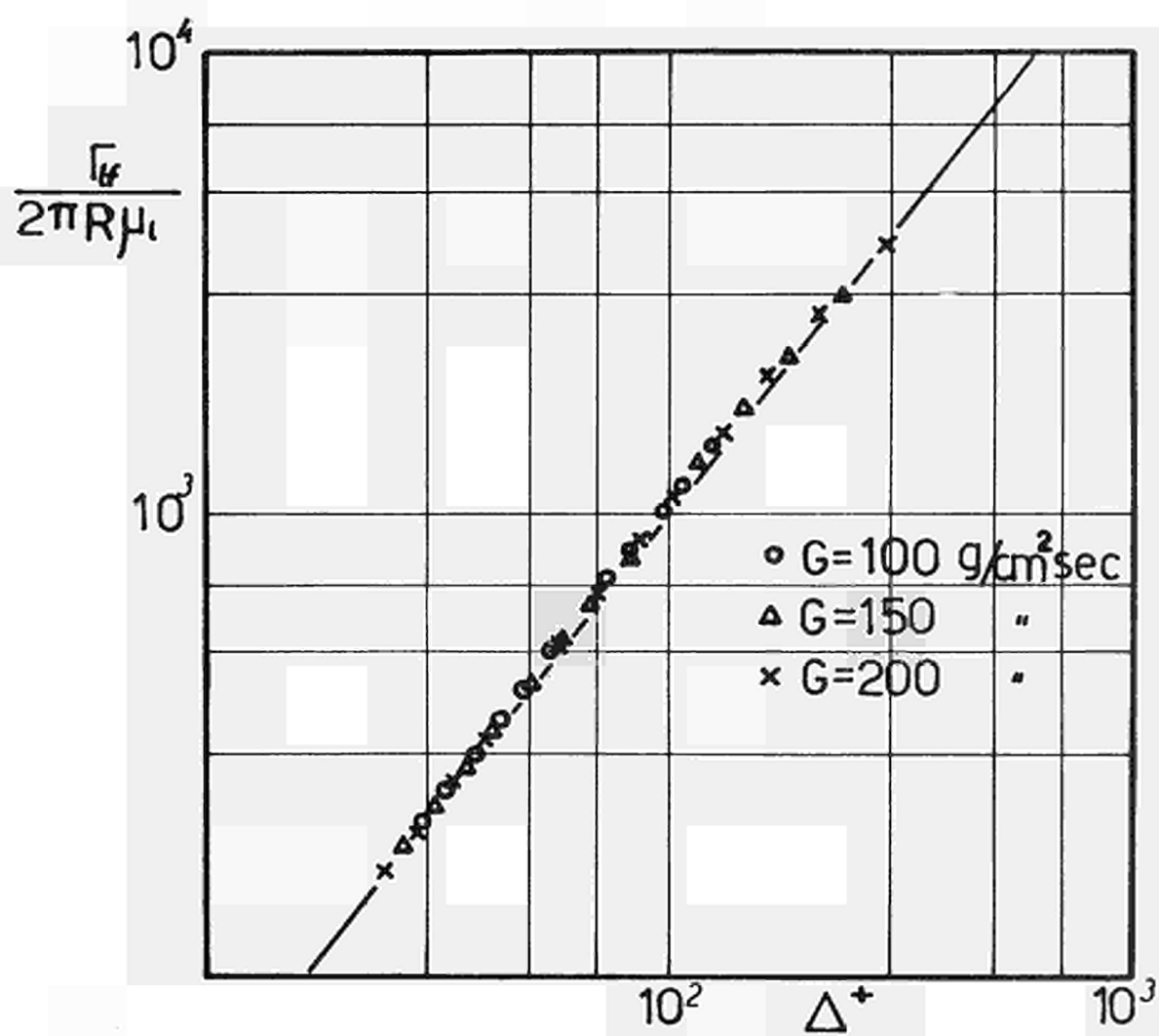


Fig. 31

11 - COMPARISON WITH HARWELL DATA

The model predictions have been compared with a set of measurements performed at Harwell <sup>10/</sup>.

Only some data have been taken into account, because many of them are external to the model validity range owing to the low mass flowrate. The values of the pressure drop and the average void fraction have been derived from experimental measurements. This leads to some fluctuations in the predicted values as it can be seen in fig. 32 where the film thickness is plotted versus  $G_L$  for  $G_G \approx 3 \div 20 \text{ g./cm}^2 \cdot \text{sec}$ . The original report gives three different film thicknesses obtained by the different measurement techniques. The first one ( $F_1$ ) was calculated from the hold up assuming that all the liquid is present in the film.

The second one ( $F_2$ ) was obtained by the CISE film conductance method and the third one ( $F_3$ ) by conductance probe method. In fig. 32 also the values corresponding to  $F_1$  and  $F_2$  are plotted. The model predictions seem to be well inside the strip defined by the values of  $F_1$  and  $F_2$ . All the examined data are reported in table 8°.

Comparison amongst Harwell predictions and our model.

● Model predictions + Holdup method ▲ Probe Conductance method

$$\rho_g = 1.5 \cdot 10^{-3} \text{ g/cm}^3$$

$$G_g = 3.2 \text{ g/cm}^2 \cdot \text{sec}$$

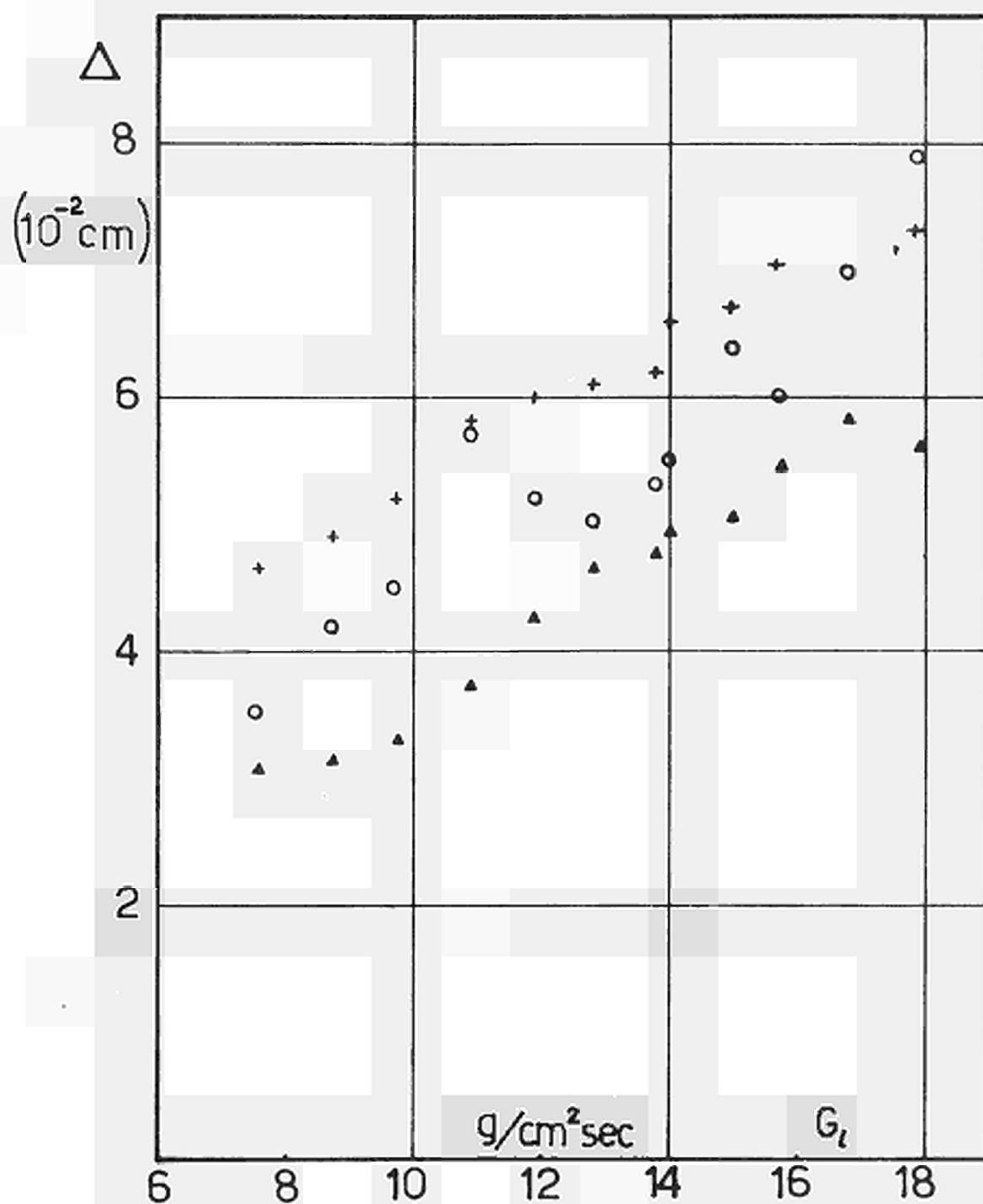


Fig. 32

12 - A SIMPLIFIED MODEL

In order to obtain some more simple analytical expressions to handle, it has also been tried to describe in another way the film and core velocity distribution. The basic assumptions of the this simplified model are the following:

a) Blasius velocity profile describes the film velocity, whilst Prandtl universal profile describes the core velocity.

b) the local void fraction exhibits a parabolic trend in the film, starting from zero at the duct wall up to a constant value  $\alpha^*$  at the film-core boundary. In the core it is assumed as constant and equal to  $\alpha^*$ .

c) The local slip ratio of the film is taken equal to 1

d) It has also been assumed in the core that the dispersed liquid travels with the gas mean velocity, except for the fraction corresponding to the one filled up with the gas in the film, which has a velocity equal to the film mean velocity.

According to this, one has in the film:

$$(49) \quad u_f = U \left( \frac{R-y}{\Delta} \right)^m \quad b \leq y \leq R$$

$$(50) \quad \alpha = \alpha^* \left( \frac{R-y}{\Delta} \right)^{1/m} \quad b \leq y \leq R$$

where  $n$  is equal to 0.5 and  $m$  is a parameter introduced so as to take into account not only linear distributions. If  $\bar{\alpha}$  is the mean value of the void fraction, obtained, as previously said, from an existing correlation,  $\alpha^*$  can be determined by



the following equation

$$(51) \quad \pi R^2 \bar{\alpha} = 2\pi \int_0^b \alpha^* y dy + 2\pi \int_b^R \alpha^* \left(\frac{R-y}{\Delta}\right)^{1/m} y dy$$

which gives

$$(52) \quad \alpha^* = \frac{R^2 (m+1)(2m+1) \bar{\alpha}}{(m+1)(2m+1)b^2 + 2\Delta \{m(2m+1)R - m(m+1)\Delta\}}$$

With this value of  $\alpha^*$ , it is now possible to define the film local density  $\rho_f$  and the mean density  $\bar{\rho}_f$

$$(53) \quad \rho_f = \rho_L \left\{ 1 - \left(\frac{R-y}{\Delta}\right)^{1/m} \alpha^* \right\} + \rho_G \left(\frac{R-y}{\Delta}\right)^{1/m} \alpha^*$$

$$(54) \quad \bar{\rho}_f = \frac{2}{R^2 - b^2} \int_b^R \rho_f y dy = \rho_L \left\{ 1 - \frac{2\alpha^*}{2R-\Delta} \left( \frac{mR}{m+1} - \frac{m\Delta}{2m+1} \right) \right\} + \rho_G \frac{2\alpha^*}{2R-\Delta} \left( \frac{mR}{m+1} - \frac{m\Delta}{2m+1} \right)$$

The core velocity profile is given by

$$(55) \quad u_c = U_m - \frac{1}{\gamma_c} \sqrt{\frac{\tau_0}{\rho_G}} \ln \frac{R}{R-y} \quad 0 \leq y \leq b$$

Eqs. (49) and (55) contain two undetermined constants,  $U$  and  $U_m$ : the former can be obtained by matching the velocities at the film-core boundary, the latter by means of the balance equation on gas flowrate  $\dot{M}_G = \dot{M}_{Gf} + \dot{M}_{Gc}$ . Thus it is

$$(56) \quad U = U_m - \frac{1}{\gamma_c} \sqrt{\frac{\tau_0}{\rho_G}} \ln \frac{R}{\Delta}$$

On the other hand,  $\dot{M}_{Gf}, \dot{M}_{Gc}$  being given by

$$(57) \quad \Gamma_{Gf} = 2\pi \rho_G \left( U_m - \frac{1}{\chi_c} \sqrt{\frac{T_0}{\rho_G}} \ln \frac{R}{\Delta} \right) \int_b^R \alpha^x \left( \frac{R-y}{\Delta} \right)^{1/m} \left( \frac{R-y}{\Delta} \right)^m y dy =$$

$$2\pi \rho_G \left( U_m - \frac{1}{\chi_c} \sqrt{\frac{T_0}{\rho_G}} \ln \frac{R}{\Delta} \right) \alpha^x \Delta^m \left( \frac{R}{1+m+m \cdot n} - \frac{\Delta}{1+2m+m \cdot n} \right)$$

$$(58) \quad \Gamma_{Gc} = 2\pi \rho_G \alpha^x \int_0^b \left( U_m - \frac{1}{\chi_c} \sqrt{\frac{T_0}{\rho_G}} \ln \frac{R}{R-y} \right) y dy = \pi \rho_G \alpha^x b^2 \bar{u}_c$$

$U_m$  becomes

$$(59) \quad U_m = \left\{ \frac{\Gamma \cdot X}{\rho_G \alpha^x} + \frac{1}{\chi_c} \sqrt{\frac{T_0}{\rho_G}} \left[ 2\Delta m \left( \frac{R}{1+m+m \cdot n} - \frac{\Delta}{1+2m+m \cdot n} \right) \ln \frac{R}{\Delta} + b^2 \left( 1 - \frac{R^2}{b^2} \right) \ln \frac{R}{\Delta} + \right. \right.$$

$$\left. \left. Rb + \frac{b^2}{2} \right] \right\} / \left\{ 2\Delta m \left( \frac{R}{1+m+m \cdot n} - \frac{\Delta}{1+2m+m \cdot n} \right) + b^2 \right\}$$

The film thickness  $\Delta$  can be calculated by the liquid flowrate balance equation:

$$(60) \quad \Gamma(1-X) = \Gamma_{Lf} + \Gamma_{Lc}$$

Now, the liquid film flowrate  $\Gamma_{Lf}$  and the core liquid flowrate  $\Gamma_{Lc}$  on the basis of the assumption d, are:

$$(61) \quad \Gamma_{Lf} = 2\pi \rho_L \int_b^R \left( U_m - \frac{1}{\chi_c} \sqrt{\frac{T_0}{\rho_G}} \ln \frac{R}{\Delta} \right) \left\{ 1 - \left( \frac{R-y}{\Delta} \right)^{1/m} \alpha^x \right\} \left( \frac{R-y}{\Delta} \right)^m y dy$$

$$= 2\pi \rho_L \left( U_m - \frac{1}{\chi_c} \sqrt{\frac{T_0}{\rho_G}} \ln \frac{R}{\Delta} \right) \Delta \left\{ \frac{b(m+1+R)}{(n+1)(m+2)} - \alpha^x \left( \frac{R}{1+m+m \cdot n} - \frac{\Delta}{1+2m+m \cdot n} \right) \right\}$$

$$(62) \quad \Gamma_{Lc} = \rho_L \left\{ \pi b^2 (1-\alpha^x) - A_{Gf} \right\} \bar{u}_c + \rho_L A_{Gf} \bar{u}_f$$

where  $\bar{u}_c$  and  $\bar{u}_f$  are the mean velocity in the core and in the film respectively,  $A_{Gf}$  is the film section filled up with the gas. Their expressions are

$$(63) \quad \bar{u}_c = U_m + \frac{1}{\chi_c} \sqrt{\frac{T_0}{\rho_G}} \left( \frac{2\Delta}{R} \ln \frac{R}{\Delta} - \frac{3}{2} - \frac{\Delta}{R} \right)$$

$$(64) \bar{u}_f = 2 \left( U_m - \frac{1}{\chi_c} \sqrt{\frac{\tau_0}{\rho_g}} \ln \frac{R}{\Delta} \right) \frac{(m+1)b + R}{(2R-\Delta)(m+1)(m+2)}$$

$$(65) A_{Gf} = 2\pi \alpha^n \left( \frac{mR}{m+1} - \frac{\mu \Delta}{2m+1} \right)$$

Thus, substituting eqs. 61 - 65 in eq. (60) one obtains

$$(66) \left\{ \gamma(1-x) - 2\pi \rho_L \left( U_m - \frac{1}{\chi_c} \sqrt{\frac{\tau_0}{\rho_g}} \ln \frac{R}{\Delta} \right) \Delta \left\{ \frac{R+b(m+1)}{(m+1)(m+2)} - \alpha^n \left( \frac{mR}{1+m+m \cdot n} - \frac{\mu \Delta}{1+2m+m \cdot n} \right) \right\} \right. \\ \left. - \rho_L \left\{ \pi b^2 (1-\alpha^n) - 2\pi \alpha^n \left( \frac{mR}{m+1} - \frac{\mu \Delta}{2m+1} \right) \Delta \right\} \cdot \left\{ U_m - \frac{1}{\chi_c} \sqrt{\frac{\tau_0}{\rho_g}} \left( 1 - \frac{R^2}{b^2} \right) \ln \frac{R}{\Delta} + \frac{R}{b} + \frac{1}{2} \right\} \right\} = 0$$

in which the only unknown is the film thickness  $\Delta$ . Also this equation is too complex to be analytically solved and therefore it has been programmed on a digital computer. The values of  $\Delta$  and of the other quantities depending on it, predicted by this simplified model, are shown in table 8<sup>o</sup> for  $m=1/2$  and  $m=1$ . As one can see from this table and from fig. 33, the qualitative and quantitative agreement between experimental data and predicted values is satisfactory for a wide range of values. The model predictions fail for high values of  $\Delta$ ; namely the trend of  $\Delta$  as a function of  $G_L$  at  $G_c$  constant shows an inversion of the dependence on  $G_L$  for  $\Delta$  values corresponding to a line in which  $X$  is  $\sim 0.2$ , whilst the trend for the other values of  $\Delta$  is correct also in the region of low  $\Delta$ .

Trend of  $\Delta$  as a function of  $G_l$  for some data of table IV.

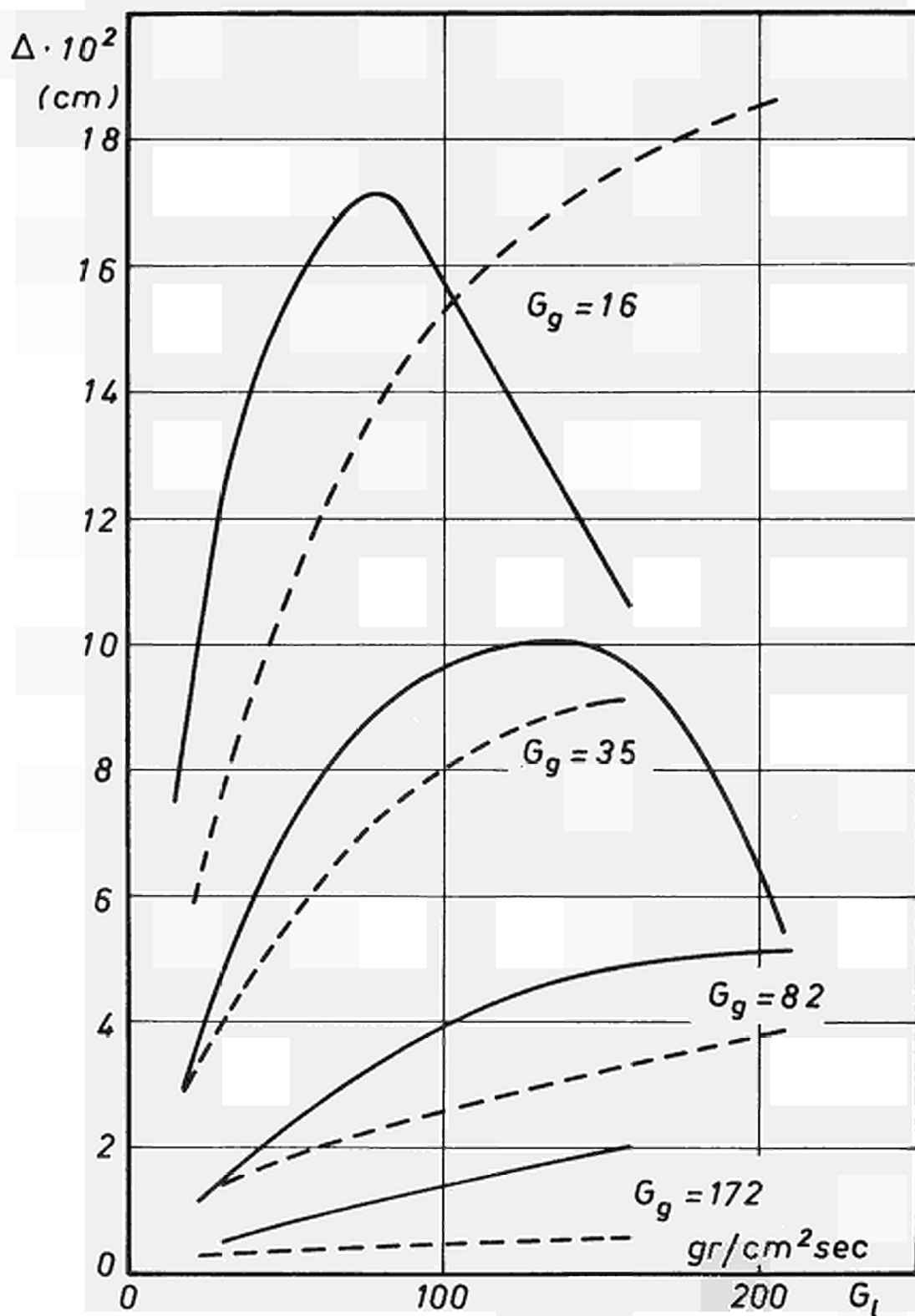


Fig. 33

APPENDIX

The shear stress  $\tau$  in cylindrical geometry is

$$(1) \quad \tau = \frac{C_1}{r} + \frac{C_2}{2} r$$

By the conditions  $\tau = \tau_c$  for  $r = b$  and  $\tau = \tau_0$  for  $r = R$  it is

$$(2) \quad C_1 = \tau_c b - \frac{b^2(\tau_0 - \tau_c \cdot b/R)}{R - b^2/R}$$

$$(3) \quad C_2 = 2 \frac{\tau_0 - \tau_c b/R}{R - b^2/R}$$

thus eq. (1) becomes

$$(4) \quad \tau_{cyl} = \frac{1}{r} \frac{bR(\tau_c R - \tau_0 b)}{R^2 - b^2} + r \frac{\tau_0 R - \tau_c b}{R^2 - b^2}$$

or also

$$(5) \quad \tau_{cyl} = \frac{R\tau_0 - b\tau_c}{R^2 - b^2} \frac{r^2 - b^2}{r} + \frac{\tau_c b}{r}$$

$\tau_{plane}$  being equal to  $(\tau_0 - \tau_c) \frac{y - b}{R - b} + \tau_c$ , eq. (5) can be rewritten

$$(6) \quad \tau_{cyl} = \tau_{plane} + \Delta\tau$$

where :

$$\Delta\tau = \frac{r - b}{r} \frac{(R - r)(\tau_0 b - \tau_c R)}{R^2 - b^2}$$

Putting now  $\Delta\tau = H(r) - \tau_{plane}$  one has

$$(7) \quad \tau_{\text{cyl}} = \tau_{\text{plane}} \{ 1 + H(r) \}$$

$$\text{where } H(r) = \frac{ab-R}{R+b} \frac{(r-b)(R-r)}{r \{ r(a-1) - (ab-R) \}}.$$

The average value of this function

$$\bar{H} = \frac{1}{R-b} \int_b^R H(r) dr = \frac{ab-R}{R^2-b^2} \left\{ \frac{\Delta}{1-a} - \frac{\ln a}{1-a} \left[ \frac{ab-R}{1-a} + R+b \right] - \frac{Rb}{ab-R} \ln \frac{ab}{R} \right\}$$

As this value is  $\approx 10^{-4}$ , for a wide range of  $\Delta$  values the substitution of  $\tau_{\text{cyl}}$  with  $\tau_{\text{plane}}$  is well justified.

TAB. I REF. 4 Water-Nitrogen R=1.25 cm

G	X	$\Delta_s \cdot 10^2$	$\Delta_c \cdot 10^2$ eq.(32)	$\Delta_c \cdot 10^2$ *eq.(32)	$\Gamma_{\xi}$
$\rho_g = 2.77 \cdot 10^{-2} \text{ g/cm}^3$					
37.6	0.408	5.65	4.87	4.48	21.8
92.4	0.166	12.9	9.74	10.1	114.33
153	0.101	18.3	13.2	18.4	325
62.3	0.643	2.5	2.35	2.39	22.58
117.2	0.342	6.3	3.22	4.54	74.95
178.2	0.225	8.5	5.61	7	16.23
83.2	0.685	1.64	1.76	1.68	19.76
138	0.442	3.56	2.31	2.70	50.81
139	0.305	5.2	2.78	4.17	108
$\rho_g = 1.88 \cdot 10^{-2} \text{ g/cm}^3$					
32.8	0.324	6.05	5.68	4.84	21.39
87.6	0.121	13.8	12.3	11.2	123.77
113.6	0.094	16.4	15.3	11.2	207.95
148.6	0.0715	18.6	18.9	19.9	346.6
49.8	0.553	2.81	2.9	2.82	25.08
104.7	0.264	7.25	4.31	5.57	91.6
130.7	0.211	8.5	5.69	6.84	133.5
165.7	0.167	9.6	7.91	8.48	197.32
64.3	0.655	1.87	1.75	1.73	18.46
119.2	0.352	4.39	2.90	3.46	64.98
145.5	0.290	5.37	2.98	4.23	93.36

$\rho_g = 1.0 \cdot 10^{-2} \text{ g/cm}^3$					
G	X	$\Delta_s \cdot 10^2$	$\Delta_c \cdot 10^2$ eq. (32)	$\Delta_c \cdot 10^2$ * eq. (32)	$\Gamma_{lf}$
28	0.208	7.3	8.22	5.9	22.78
39.8	0.146	9.2	9.3	7.6	37.27
64.8	0.0895	12	12.5	10.7	20.19
37.2	0.403	3.25	4.04	3.97	33.63
48.9	0.307	4.42	4.80	4.93	51.48
3.9	0.203	6.65	6.07	6.50	91.00
45.2	0.510	2.21	2.62	2.48	25.34
57.1	0.404	3.04	3.3	3.11	38.04
82.1	0.280	4.98	4.01	4.41	72.8

\*  $\frac{dP}{dz}$  experimental



TAB. II    REF. 2    Water-Argon     $R = 1.25 \text{ cm}$      $\rho_G = 2.77 \cdot 10^{-2} \text{ g/cm}^3$

G	X	$\Delta_S \cdot 10^2$	$\Delta_C \cdot 10^2$	$\Gamma_{lf}$
57.4	0.410	2.99	3.05	
45.7	0.515	2.41	2.42	
73.7	0.206	6.4	6.10	
48.9	0.310	4.43	4.88	51.022
37.2	0.408	3.47	3.91	33.15
64.4	0.0915	12.9	10.61	90.08
39.65	0.148	8.7	7.19	37.72
27.96	0.258	6.65	6.18	30.81
113.9	0.327	4.71	3.71	69.80
58.7	0.625	1.91	1.87	20.36
161.4	0.151	3.34	8.99	209.01
100.8	0.242	7.41	5.94	97.51
45.9	0.330	2.91	2.95	25.62
146.2	0.063	16.9	20.46	352.40
86.2	0.106	13.7	11.76	127.75
31.2	0.295	6.31	4.97	20.80

G	X	$\Delta_S \cdot 10^2$	$\Delta_C \cdot 10^2$	$\Gamma_{ff}$
145.3	0.291	5	4.21	92.85
119.2	0.354	4.24	3.43	64.38
63.8	0.663	1.74	1.70	17.86
164.8	0.169	9.08	8.37	194.23
150.6	0.185	8.49	7.70	167.26
104.5	0.267	7.01	5.50	90.40
49.3	0.555	2.68	2.82	24.87
147.6	0.072	17.0	19.7	342.41
113.6	0.0935	15.0	14.91	208.47
87.6	0.121	13.6	11.23	123.77
32.6	0.325	6.00	4.82	21.15
188	0.270	5.41	4.65	120.10
127.7	0.401	3.94	3	56.00
72.4	0.705	1.72	1.55	17.08
170.3	0.196	8.43	7.65	176.60
110.1	0.302	6.42	5.02	82.34
55.2	0.600	2.59	2.58	23.51
149.8	0.855	17.2	19.1	332.15
89.7	0.142	12.6	10.66	118.39
34.8	0.405	5.76	4.587	22.95

TAB. III REF.(4)

Water-Argon  $\rho_0 = 3.61 \cdot 10^{-2} \text{ g/cm}^3$   $R = 1.25 \text{ cm}$ 

G	X	$\Delta_S 10^2$	$\Delta_C 10^2$	$\Gamma_{if}$
185	0.508	2.31	2.02	43.72
171	0.550	2.09	1.81	36.27
160	0.585	1.92	1.67	31.30
152	0.620	1.75	1.53	27.19
145	0.650	1.62	1.44	24.25
138	0.680	1.53	1.35	21.74
132	0.710	1.42	1.28	19.58
128	0.735	1.31	1.21	17.97
122	0.770	1.18	1.13	16.04
119	0.790	1.11	1.09	15.05
116	0.810	1.01	1.06	14.19
112	0.840	0.92	1.00	13.00
288	0.285	5.53	4.64	152.11
259	0.317	4.63	4.07	122.10
239	0.343	4.28	3.70	103.46
219	0.375	3.87	3.30	85.59
200	0.407	3.33	3.00	71.66
184	0.440	3.15	2.73	60.39
172	0.472	2.88	2.49	51.73
158	0.513	2.68	2.24	42.93
147	0.550	2.52	2.05	36.65
139	0.580	2.29	1.91	32.45
132	0.615	2.08	1.77	28.32
125	0.645	1.92	1.67	25.40
119	0.680	1.80	1.55	22.43
115	0.705	1.68	1.48	20.61

G	X	$\Delta_s 10^2$	$\Delta_c 10^2$	$\Gamma_{cf}$
109	0.740	1.49	1.39	18.39
103	1.760	1.40	1.34	16.31
99.1	0.820	1.12	1.21	14.47
278	0.259	6.43	5.60	178.34
249	0.289	5.80	4.91	143.14
229	0.314	5.10	4.45	120.94
209	0.345	4.64	3.97	99.66
191	0.337	4.20	3.56	82.31
175	0.413	3.91	3.18	68.34
163	0.443	3.51	2.92	58.80
149	0.485	3.37	2.61	48.36
138	0.521	3.02	2.40	41.33
130	0.550	2.85	2.26	36.68
122	0.585	2.55	2.09	31.99
116	0.620	2.28	1.94	28.11
110	0.650	2.14	1.84	25.32
105	0.680	2.04	1.73	22.86
100	0.715	1.83	1.63	20.42
97	0.735	1.66	1.58	19.22
93.6	0.760	1.52	1.52	17.81
89.6	0.800	1.35	1.41	15.90
269	0.234	7.4	6.73	208.15
240	0.263	7.25	5.87	165.78
220	0.285	6.43	5.37	141.08
200	0.313	5.84	4.80	116.33
182	0.345	4.98	4.29	96.13
166	0.378	4.68	3.86	79.76
153	0.407	4.50	3.54	68.49
139	0.449	4.10	3.16	55.89
129	0.484	3.64	2.90	47.74
121	0.520	3.45	2.65	41.09
113	0.545	3.16	2.55	37.10

G	X	$\Delta_s \cdot 10^2$	$\Delta_c \cdot 10^2$	$\Gamma_{if}$
106	0.580	2.84	2.37	32.52
99.8	0.615	2.55	2.22	28.71
95.4	0.645	2.38	2.10	25.94
90.1	0.680	2.18	1.98	23.17
87.1	0.710	2.00	1.87	21.22
83.7	0.740	1.84	1.77	19.32
79.7	0.770	1.59	1.70	17.85
260	0.207	8.6	8.27	247.31
231	0.235	7.9	7.14	194.85
211	0.257	7.35	6.45	163.78
191	0.286	6.9	5.69	133.23
173	0.132	6.3	5.19	111.72
157	0.345	5.85	4.62	91.67
145	0.375	5.51	4.20	77.79
131	0.416	5.09	3.74	63.16
120	0.448	4.46	3.46	54.28
112	0.480	4.14	3.20	47.21
105	0.510	3.86	3.01	41.68
98.1	0.550	3.44	2.76	35.87
92.1	0.585	3.04	2.58	31.57
87.5	0.615	2.84	2.45	29.04
79.2	0.680	2.34	2.29	
75.8	0.710	2.10	2.10	
71.8	0.750	1.90	1.96	
253	0.186	9.7	9.81	285.53
224	0.213	9.31	8.40	221.21
204	0.229	8.6	7.80	190.38
184	0.254	8.5	6.94	156.10
166	0.283	8	6.14	129.96
150	0.311	7.1	5.55	105.39
138	0.339	6.7	5.04	89.14

G	X	$\Delta_s 10^2$	$\Delta_c 10^2$	$\Gamma_{if}$
113	0.413	5.5	4.08	60.67
105	0.443	5.02	3.79	53.00
97.6	0.477	4.62	3.52	45.52
90.8	0.513	4.08	3.40	
84.8	0.550	3.72	3.00	
75.1	0.620	2.96	2.96	
72.1	0.650	2.72	2.55	25.25
68.7	0.680	2.45	2.44	23.14
247	0.171	10.7	11.15	313.42
219	0.190	10.2	9.97	254.55
198	0.208	9.9	9.03	213.76
178	0.232	9.3	8.00	173.76
160	0.257	8.9	7.14	142.54
144	0.286	8.4	6.35	116.22
132	0.310	7.8	5.83	99.12
120	0.350	6.8	5.10	79.67
108	0.383	6.2	4.67	66.39
99.7	0.417	5.6	4.27	
92.2	0.447	5.11	4.00	
85.4	0.482	4.66	3.70	
79.4	0.519	4.06	3.44	37.42
74.9	0.550	3.77	3.26	33.58
69.6	0.590	3.36	3.05	29.47
66.6	0.620	3.07	2.90	26.97
63.2	0.650	2.85	2.79	24.73
59.2	0.690	2.45	2.65	22.21
241	0.140	12	14.82	395.63
212	0.165	11.7	12.22	298.31
192	0.182	11	10.94	247.56
172	0.203	10.7	9.68	200.91
154	0.226	10.4	8.60	162.99

G	X	$\Delta_s 10^2$	$\Delta_c 10^2$	$\Gamma_{if}$
138	0.250	10	7.71	133.45
126	0.277	9.2	6.83	110.46
112	0.312	8	6.05	
101	0.344	7.1	5.50	
93.2	0.372	6.4	5.10	63.10
85.7	0.405	5.8	4.69	53.93
78.9	0.440	5.4	4.33	46.37
72.9	0.476	4.67	4.04	40.28
68.5	0.506	4.32	3.82	36.15
63.2	0.550	3.77	3.55	31.35
60.2	0.580	3.46	3.40	28.71
56.8	0.610	3.21	3.27	26.33
52.7	0.660	2.76	3.06	23.17
238	0.134	13.6	15.76	413.32
209	0.153	12.7	13.56	323.43
189	0.174	12.8	11.65	258.48
169	0.188	12	10.74	217.28
151	0.211	11.5	9.43	174.21
135	0.235	10.7	8.37	140.76
123	0.258	10.1	7.57	117.68
109	0.292	8.9	6.60	
98.7	0.324	8	5.95	76.71
90.2	0.351	7.1	5.51	65.52
82.7	0.383	6.5	5.10	55.81
75.9	0.418	5.9	4.67	47.77
69.9	0.454	5.3	4.34	41.31
65.5	0.484	4.88	4.11	36.97
60.2	0.526	4.17	3.84	32.13
57.2	0.554	3.81	3.69	29.54
53.8	0.590	3.56	3.51	26.76
49.8	0.640	2.98	3.30	23.64

G	X	$\Delta_s 10^2$	$\Delta_c 10^2$	$\Gamma_{lf}$
234	0.118	14.4	18.72	472.29
205	0.135	14.1	16.04	379.94
185	0.148	13.6	14.44	306.08
165	0.168	12.8	12.44	241.65
147	0.188	12.5	10.92	193.01
130	0.211	12.0	9.57	153.49
119	0.233	11.3	8.50	123.70
105	0.264	10.00	7.47	98.98
93.8	0.293	9.1	6.70	80.59
86	0.320	8.1	6.13	68.25
78.5	0.350	7.4	5.63	57.71
71.7	0.384	6.7	5.17	48.49
65.7	0.419	6.1	4.80	42.05
61.3	0.449	5.35	4.53	37.44
56	0.491	4.76	4.23	32.40
53	0.520	4.43	4.06	29.73
49.5	0.555	3.94	3.90	26.91
45.5	0.600	3.43	3.71	24.04
230	0.105	16.0	21.85	531.75
201	0.121	15.7	18.52	410.37
181	0.133	15.4	16.5	337.72
161	0.150	14.6	14.35	268.22
143	0.169	13.8	12.43	211.13
127	0.190	13.3	13.52	
115	0.210	12.2	9.65	135.62
101	0.239	10.8	8.30	104.05
90.5	0.267	9.8	7.34	83.20
82.7	0.293	9	6.67	69.62
75.2	0.322	8.3	6.07	58.05
68.2	0.354	7.3	5.56	48.61
62.3	0.387	6.5	5.15	41.51
57.9	0.419	6	4.83	36.61



G	X	$\Delta_s \cdot 10^2$	$\Delta_c \cdot 10^2$	$\Gamma_{if}$
52.6	0.458	5.15	4.53	31.57
49.6	0.486	4.97	4.53	28.93
46.2	0.522	4.43	4.17	26.23
42.2	0.570	3.74	3.98	23.36
227	0.093	17.3	25.61	599.03
188	0.106	17.2	21.92	444.67
178	0.118	16.1	19.30	379.77
158	0.133	15.5	16.64	298.70
140	0.151	15.1	14.20	231.29
124	0.170	14.4	12.23	179.33
112	0.188	13.2	10.78	144.26
98.1	0.215	11.9	9.15	108.19
87.4	0.241	11.3	8	84.59
79.6	0.265	10	7.2	69.56
72.2	0.293	9.2	6.47	57.01
65.3	0.323	8.3	5.87	46.93
59.3	0.356	7.3	5.38	39.33
54.8	0.383	6.5	5.06	34.34
49.5	0.424	5.7	4.70	29.25
46.5	0.452	5.4	4.52	26.74
43.1	0.487	4.93	4.34	24.19
39.1	0.538	4.30	4.15	21.64
224	0.081	19.3	30.61	683.38
195	0.094	18.5	25.64	523.91
175	0.104	17.4	22.63	427.46
155	0.118	17.1	19.26	331.02
137	0.133	16.2	16.41	254.89
121	0.151	15.6	13.88	193.95
109	0.167	14.5	12.10	153.36
95.3	0.192	12.7	10.4	111.37
84.6	0.216	11.9	8.61	84.51

G	X	$\Delta_s \cdot 10^2$	$\Delta_c \cdot 10^2$	$\Gamma_{cf}$
74.5	0.238	11.2	7.50	63.96
69.3	0.264	10	6.74	53.69
62.5	0.293	8.9	6.01	43.00
56.4	0.323	8.3	5.43	34.90
52	0.350	7.7	5.05	30.00
46.7	0.390	6.7	4.66	25.09
43.7	0.416	6.1	4.47	22.74
40.3	0.452	5.31	4.30	20.57
36.3	0.502	4.88	4.14	18.50
202	0.072	21	35.4	758.03
193	0.082	20.6	30.5	595.93
173	0.092	18.9	26.4	478.92
153	0.104	18.6	22.48	371.85
135	0.118	17.9	18.9	282.04
119	0.134	16.7	15.75	210.06
107	0.149	15.6	13.48	162.19
92.9	0.171	14.7	10.97	114.00
82.1	0.192	12.7	9.18	82.90
74.3	0.213	12.1	7.91	63.69
66.8	0.237	11.0	6.80	48.25
60	0.263	10.4	5.90	36.71
54	0.293	9.2	5.19	28.63
49.6	0.319	8.4	4.74	23.81
44.3	0.357	7.4	4.3	19.22
41.3	0.383	7.0	4.1	17.22
37.9	0.417	6.2	3.91	15.40
33.9	0.474	5.57	3.86	14.47

TABLE IV Ref. 6 Water-Argon  $R=1.25$  cm  $\rho_g=3.61 \cdot 10^{-2}$  g/cm<sup>3</sup>

G	X	$\Delta_S \cdot 10^2$	$\Delta_C \cdot 10^2$	$\Gamma_{lf}$
34.1	0.47	5.6	3.85	14.45
38.1	0.42	6.2	3.96	15.91
44.5	0.36	7.4	4.34	19.82
54.2	0.296	9.2	5.23	29.31
67	0.209	11	7.03	46.46
84	0.190	12.7	9.42	87.7
107	0.133	15.5	15.2	178.6
135	0.118	16.5	18.9	282.46
173	0.0925	17.4	26.2	476.52
222	0.072	18.8	35.4	758.34
39.4	0.540	4.3	4.15	21.86
43.4	0.491	4.93	4.33	24.5
49.8	0.427	5.7	4.7	29.6
59.5	0.358	7.3	5.37	39.54
72.3	0.235	9.2	6.44	57
87.3	0.242	11.3	7.96	84.25
112.3	0.188	12.2	10.8	144.55
140.3	0.152	13.3	14.1	230
178.3	0.120	15	18.89	373.31
227.3	0.094	16.1	25.25	592.6
45.8	0.605	3.43	3.67	239.67
49.8	0.555	3.94	3.88	27.04
56.2	0.492	4.76	4.22	32.44
65.9	0.420	6.1	4.78	42.1
78.7	0.352	7.4	5.6	57.6
93.7	0.296	8.9	6.63	79.8

G	X	$\Delta_S \cdot 10^2$	$\Delta_C \cdot 10^2$	$\Gamma_{UF}$
118.7	0.233	10	8.14	118.36
146.7	0.189	10.7	10.85	192.14
184.7	0.150	11.7	14.2	301.6
233.7	0.118	13	18.7	472.47
53.1	0.660	2.76	3.05	23.24
57.1	0.614	3.21	3.23	26.14
63.5	0.550	3.77	3.55	31.42
73.2	0.478	4.67	4.00	40.17
86	0.407	5.8	4.65	53.75
101	0.346	7.35	5.44	73.40
126	0.278	8	6.85	110.30
154	0.227	8.5	8.54	162.36
192	0.181	9.3	11.02	249.43
241	0.145	11.7	14.1	379.54
65.1	0.723	2.14	2.28	20.60
69.1	0.680	2.45	2.43	23.11
75.5	0.623	2.96	2.65	27.44
85.2	0.550	3.72	2.95	45.6
98	0.480	4.47	3.47	45.6
113	0.416	5.2	4.03	60
138	0.340	5.9	5.01	89
166	0.283	6.2	6.13	127.1
204	0.230	6.95	7.74	189.47
253	0.186	7.7	9.81	283.63
84.1	0.738	1.88	1.77	19.76
100.2	0.608	2.55	2.26	29.43

G	X	$\Delta_S \cdot 10^2$	$\Delta_C \cdot 10^2$	$\Gamma_{\text{cr}}$
113	0.550	2.90	2.50	36.44
128	0.484	3.38	2.91	47.7
153	0.405	3.96	3.58	69.06
181	0.342	4.35	4.36	97.50
219	0.283	4.86	5.45	142.60
268	0.231	5.45	6.88	212.2
104.1	0.790	1.26	1.25	15.73
110.5	0.745	1.49	1.35	18.05
120.2	0.681	1.71	1.54	22.30
133	0.616	1.91	1.75	28.20
148	0.555	2.20	2	35.88
173	0.474	2.53	2.45	51.25
201	0.408	2.93	2.97	71.32
239	0.343	3.39	3.69	103.46
288	0.284	3.34	4.67	153.07
117.1	0.805	0.92	1.06	14.39
123.5	0.770	1.05	1.12	16
133.2	0.716	1.25	1.24	19.07
146	0.650	1.51	1.43	24.23
161	0.590	1.68	1.63	30.63
186	0.510	1.94	1.99	43.30
204	0.466	2.24	2.24	53.36
252	0.377	2.67	2.37	85.95
301	0.316	3.27	3.73	126

G	X	$\Delta_S \cdot 10^2$	$\Delta_C \cdot 10^2$	$\Gamma_{LF}$
149.1	0.854	0.56	0.69	10.95
155.5	0.817	0.61	0.75	12.28
165.2	0.769	0.69	0.82	14.36
178	0.714	0.78	0.95	17.46
193	0.658	0.83	1.05	21.66
218	0.582	1.00	1.27	29.85
246	0.517	1.12	1.52	40.33
284	0.447	1.35	1.88	57.77
194.1	0.887	0.360	0.45	8.55
200.1	0.86	0.377	0.48	9.2
210.2	0.82	0.395	0.51	10.37
223	0.77	0.417	0.58	12.32
238	0.723	0.450	0.65	14.66
263	0.654	0.460	0.77	19.48
291	0.59	0.57	0.92	26.05
329	0.523	0.66	1.12	36.25
222.1	0.9	0.286	0.36	76.24
228.1	0.877	0.309	0.37	80.75
238.2	0.84	0.314	0.41	89.52
251	0.797	0.325	0.45	10.26
266	0.752	0.343	0.50	12.05

TABLE V Ref. 6 Argon-Water  $R = 0.75 \text{ cm}$   $\rho_s = 3.61 \cdot 10^{-2} \text{ g/cm}^3$

G	X	$\Delta_s \cdot 10^2$	$\Delta_c \cdot 10^2$	$\Gamma_{lf}$
38.1	0.42	3.78	3.68	10.7
54.2	0.296	5.60	4.60	18.22
107	0.1495	9.20	8.95	67.32
222	0.072	12.40	20.56	264.52
49.9	0.557	2.57	2.71	11.31
66	0.422	3.79	3.31	17.9
118.8	0.236	6.60	5.44	48.44
233.8	0.119	8.10		
69.1	0.68	1.63	1.64	9.02
15.2	0.552	2.47	2.02	13.4
138	0.34	4.22	3.23	33.4
253	0.186	5.00	5.96	101.54
104.1	0.788	0.87	0.87	6.40
120.2	0.683	1.23	1.04	8.68
173	0.474	1.88	1.62	19.43
288	0.284	2.63	2.95	56.31

TABLE VI Ref. 4 Water-Argon  $R=1.25$  cm  $\rho_s = 3.61 \cdot 10^{-2}$  g/cm<sup>3</sup>

G	X	$\Delta_s \cdot 10^2$	$\Delta_c \cdot 10^2$	$\Gamma_{lf}$
<b>T = 16 °C</b>				
289	0.283	5.7	4.66	152.2
185	0.443	3.31	2.66	58.66
132	0.614	2.03	1.76	28
103.2	0.788	1.32	1.26	15.63
253.9	0.185	10.1	9.81	282.6
149.7	0.313	7.6	5.46	103
97.7	0.480	4.66	3.46	45
68.8	0.680	2.51	2.43	22.75
233.8	0.115	14.6	19.23	481
129.7	0.210	11.8	9.58	151
77.6	0.346	7.25	5.66	56.6
48.8	0.550	3.94	3.91	26.35
222.8	0.685	21.5	37.2	785.4
118.8	0.134	16.8	15.67	207.5
66.8	0.237	11.4	6.78	47.6
38.1	0.415	6.5	3.91	15.31
<b>T = 24 °C</b>				
290	0.286	5.35	4.72	160.4
184	0.450	3.19	2.67	61.47
131	0.634	2.08	1.71	28.27
103.2	0.805	1.30	1.24	16.06
264	0.216	9.8	7.92	247
234	0.092	14.2	26.8	654
130	0.209	11.8	9.96	164



<b>G</b>	<b>X</b>	<b><math>\Delta_s \cdot 10^2</math></b>	<b><math>\Delta_c \cdot 10^2</math></b>	<b><math>\Gamma_{cf}</math></b>
77.9	0.349	7.35	5.80	61.34
49.1	0.554	3.95	4.01	28.9
223.1	0.072	21.7	37.01	806
119.1	0.135	16.3	16.06	220
67	0.239	11.0	6.96	52
38.2	0.420	6.3	4.07	17.2
<b>T = 30 °C</b>				
289	0.287	5.15	4.79	167
186	0.446	3.06	2.75	66
133	0.620	2.00	1.79	31.52
104.1	0.790	1.20	1.30	17.85
253.4	0.188	9.0	10.17	309
150.1	0.317	6.95	5.65	114.6
98	0.484	4.59	3.58	50.62
69.1	0.690	2.50	2.48	25.76
233.2	0.117	13.8	20	525
130	0.209	11.4	10.2	172
77.9	0.348	7.15	5.93	64.77
49	0.565	3.92	4.01	30.16
222.1	0.0725	20.9	37.2	820
119.1	0.135	16.1	16.4	230
67	0.240	11.0	7.07	54.48
381	0.424	6.15	4.16	18.37
<b>T = 37 °C</b>				
289	0.288	5.10	4.87	174
185	0.446	3.13	2.82	69.56
132	0.629	2.03	1.79	32.32
104.1	0.790	1.31	1.32	19
253.3	0.186	9.4	10.6	328.65

<b>G</b>	<b>X</b>	<b><math>\Delta_S \cdot 10^2</math></b>	<b><math>\Delta_C \cdot 10^2</math></b>	<b><math>\Gamma_{LF}</math></b>
150.2	0.314	7.1	5.87	122.33
98	0.480	4.70	3.71	54.45
68.7	0.685	2.54	2.57	27.77
232	0.116	14.3	20.95	553
130	0.208	11.5	10.52	181
78	0.347	7.1	6.09	68.64
49.1	0.550	3.88	4.22	32.77
221.9	0.0720	21.6	39	882
118.9	0.134	16.6	16.94	242
67	0.249	10.7	7.14	57.95
38.2	0.421	6.25	4.23	19.38

TAB VII Ref. 10 Harvell - Acqua Aria  $R = 4.59 \text{ cm}$

G	X	$F_1 \cdot 10^2$	$F_2 \cdot 10^2$	$F_3 \cdot 10^2$	$\Delta_c \cdot 10^2$
$\rho_g = 1.40 \cdot 10^{-3} \text{ g/cm}^3 \quad \mu_c = 9.43 \cdot 10^{-3} \text{ g/cm} \cdot \text{sec}$					
11	0.29	4.67	3.09	3.98	3.53
12	0.27	4.90	3.17	4.11	4.23
$\rho_g = 1.50 \cdot 10^{-3} \text{ g/cm}^3 \quad \mu_c = 9.43 \cdot 10^{-3} \text{ g/cm} \cdot \text{sec}$					
13	0.25	5.18	3.32	4.24	4.53
13	0.24	5.38	3.55	4.47	5.58
14	0.22	5.81	3.73	4.62	5.78
15	0.21	5.89	4.26	4.74	5.28
16	0.20	6.09	4.64	4.95	5.05
17	0.19	6.19	4.74	5.05	5.36
17	0.18	6.65	4.95	5.15	5.54
18	0.17	6.68	5.05	5.33	6.47
19	0.17	7.03	5.43	5.43	6.03
$\rho_g = 1.60 \cdot 10^{-3} \text{ g/cm}^3 \quad \mu_c = 9.43 \cdot 10^{-3} \text{ g/cm} \cdot \text{sec}$					
20	0.16	7.03	5.58	5.56	7.19
21	0.15	7.29	5.58	5.58	7.91
$\rho_g = 1.70 \cdot 10^{-3} \text{ g/cm}^3 \quad \mu_c = 1.06 \cdot 10^{-2} \text{ g/cm} \cdot \text{sec}$					
13	0.35	3.32	2.56	3.27	4.54
14	0.33	3.42	2.71	3.35	4.61
15	0.32	3.81	2.84	3.42	3.77
16	0.3	4.47	3.10	3.68	3.89
17	0.29	4.52	3.20	3.75	3.82
17	0.27	4.52	3.35	3.83	5.09

G	X	$F_1 \cdot 10^2$	$F_2 \cdot 10^2$	$F_3 \cdot 10^2$	$\Delta_c \cdot 10^2$
$\rho_g = 1.80 \cdot 10^{-3} \text{ g/cm}^3$ $\mu_L = 9.72 \cdot 10^{-3} \text{ g/cm sec}$					
18	0.26	4.54	3.40	3.98	5.10
19	0.25	4.57	3.63	4.14	7.08
20	0.24	4.85	3.65	4.21	6.21
21	0.23	5.13	3.78	4.37	5.13
21	0.22	5.33	4.01	4.47	6.40
22	0.21	5.38	4.19	4.70	6.40
23	0.21	5.71	4.36	4.77	5.95
24	0.20	5.89	4.64	4.87	6.09
25	0.19	5.91	5.00	4.92	6.50
26	0.18	6.07	5.38	5.13	7.23
$\rho_g = 1.90 \cdot 10^{-3} \text{ g/cm}^3$ $\mu_L = 9.72 \cdot 10^{-3} \text{ g/cm sec}$					
24	0.20	5.89	4.64	4.87	6.09
25	0.19	5.91	5.00	4.92	6.50
26	0.18	6.07	5.38	5.13	7.23
27	0.18	6.85	5.53	8.23	5.74
28	0.17	6.95	5.84	5.28	7.23
29	0.17	7.13	6.19	5.36	6.86
$\rho_g = 2.10 \cdot 10^{-3} \text{ g/cm}^3$ $\mu_L = 9.28 \cdot 10^{-3} \text{ g/cm sec}$					
21	0.30	4.55	2.87	3.68	4.94
22	0.29	4.75	3.02	3.73	4.94
23	0.28	4.82	3.05	3.83	4.98
24	0.27	5.02	3.12	3.94	5.05
25	0.26	5.05	3.22	4.04	4.87
25	0.25	5.46	3.38	4.14	5.57
$\rho_g = 2.20 \cdot 10^{-3} \text{ g/cm}^3$ $\mu_L = 9.28 \cdot 10^{-3} \text{ g/cm sec}$					

G	X	$F_1 \cdot 10^2$	$F_2 \cdot 10^2$	$F_3 \cdot 10^2$	$\Delta_c \cdot 10^2$
26	0.24	5.61	3.43	4.26	5.97
27	0.24	5.36	3.32	4.36	5.58
28	0.23	5.56	3.43	4.47	5.83
29	0.22	6.04	3.53	4.52	5.65
30	0.21	6.17	3.76	4.72	6.16
$\rho_g = 2.20 \cdot 10^{-3} \text{ g/cm}^3$ $\mu_c = 1.06 \cdot 10^{-2} \text{ g/cm sec}$					
22	0.32	4.44	2.60	3.66	4.44
23	0.31	4.44	2.66	3.78	4.42
24	0.30	4.52	2.79	3.86	4.44
$\rho_g = 2.30 \cdot 10^{-3} \text{ g/cm}^3$ $\mu_c = 1.06 \cdot 10^{-2} \text{ g/cm sec}$					
25	0.29	4.64	2.92	3.96	4.80
25	0.28	4.82	2.97	4.06	5.42
26	0.27	4.92	3.04	4.14	5.38
27	0.26	4.97	3.09	4.24	5.53
28	0.26	5.23	3.22	4.34	5.02
29	0.25	5.33	3.27	4.47	4.94
29	0.24	5.38	3.40	4.54	5.64
$\rho_g = 2.40 \cdot 10^{-3} \text{ g/cm}^3$ $\mu_c = 1.06 \cdot 10^{-2} \text{ g/cm sec}$					
30	0.24	5.74	3.27	4.64	5.49
31	0.23	5.89	3.50	4.72	5.48

G	X	$\Delta_S \cdot 10^2$	$\Delta_C \cdot 10^2$	$\Gamma_{cf}$
198.1	0.308	4.88	4.12	105.91
137.7	0.442	3.61	2.71	50.80
82.6	0.730	1.58	1.48	17.10
177	0.226	8.26	6.97	160.76
109.8	0.364	6.05	4.26	66.57
61.9	0.645	2.57	2.39	22.44
152.3	0.101	16.7	18.4	322.41
92.2	0.166	12.8	10.14	113.90
37.3	0.410	5.43	4.46	21.52

TABLE VIII Some data of reference  $b$   $R=1.25$  cm  $\rho_0=3.61 \cdot 10^{-2}$  g/cm<sup>3</sup>

G	X	$\Delta_s \cdot 10^2$	$\Delta_c \cdot 10^2$	$\Gamma_{cf}$
34.1	0.470	5.6	7.80	45.17
38.1	0.420	6.2	9.36	61.62
44.5	0.360	7.4	11.52	86.99
54.2	0.236	9.2	13.97	119.8
67	0.209	11	18.21	167.5
84	0.190	12.7	16.9	167.4
107	0.133	15.5	16.57	149.1
135	0.118	16.5	13.91	117.1
173	0.093	17.4	10.64	55.26
222	0.072	18.8	7.24	=
53.1	0.660	2.76	2.81	14.87
57.1	0.614	3.21	3.43	22.41
63.5	0.550	3.77	4.40	35.67
73.2	0.478	4.67	5.64	55.37
86	0.407	5.8	6.99	79.92
101	0.346	7.35	8.25	105.2
126	0.278	8	9.36	130.2
154	0.227	8.5	9.90	142.3
192	0.181	9.3	9.64	132.3
241	0.145	11.7	8.62	100.6
104.1	0.790	1.26	1.12	9.001
110.5	0.745	1.49	1.44	15.41
120.2	0.681	1.71	1.94	26.65
133	0.616	1.31	2.49	40.89
148	0.555	2.20	3.03	56.53
173	0.474	2.53	3.79	79.67
201	0.408	2.93	4.38	98.90
239	0.343	3.39	4.88	115
288	0.284	3.34	5.17	122
194	0.887	0.360	0.38	3.855
200.5	0.860	0.377	0.49	7.25
210.5	0.820	0.395	0.66	13.29
223	0.770	0.417	0.885	22.17
238	0.723	0.450	1.105	31.97
263	0.654	0.460	1.43	47.69
291	0.590	0.57	1.75	63.81
329	0.523	0.66	2.07	80.40

BIBLIOGRAPY

- 1 -- S. Levy : "Prediction of Two-Phase Annular Flow with liquid Entrainment", Int. J. Heat Mass Transfer Vol. 9 pp. 171-188 1966.
- 2 - L. Cravarolo A. Hassid: "Phase and velocity distribution in two-phase adiabatic dispersed flow", CISE Report NO. 98
- 3 - I. P. Ginzburg: "Applied Fluid Dynamics", Israel Program for Scientific Translation - Jerusalem 1963
- 4 - "A Research program in two-phase flow", CISE - Gennaio 1963
- 5 - N. Adorni et al - "Experimental data on two-phase adiabatic flow: liquid film thickness, phase and velocity distribution, pressure drop in vertical gas-liquid flow", CISE Report NO. 35
- 6 - P. Alia - L. Cravarolo - A. Hassid - E. Pedrocchi: "Phase and velocity distribution in two-phase annular dispersed flow", CISE Report R. - 109 Dicembre 1966
- 7 - G. P. Gaspari - C. Lombardi - G. Peterlongo: "Pressure drop in steam-water mixtures. Round tubes. Vertical up flow", CISE Report - R - 83 gennaio 1964
- 8 - P. Alia - L. Cravarolo - A. Hassid - E. Pedrocchi: "Liquid volume fraction in adiabatic two-phase vertical up flow-round conduit", CISE Report R - 105 Giugno 1965
- 9 - G. F. Hewitt : Private communication at Round Table of the European two-phase Flow Group, June 1966.
- 10 - G.F. Hewitt - P.C. Lovegrove : "Comparative Film thickness and Hold up measurements in vertical Annular Flow" AERE - M 1203 - 1963



ACKNOWLEDGMENTS

We gratefully acknowledge the many useful discussions with Professor M. Silvestri, who gave his time generously, during the development of the research. We want also to thank Mr. Gaspari and Mr. Hassid **who** allowed us to utilize their more recent experimental data.



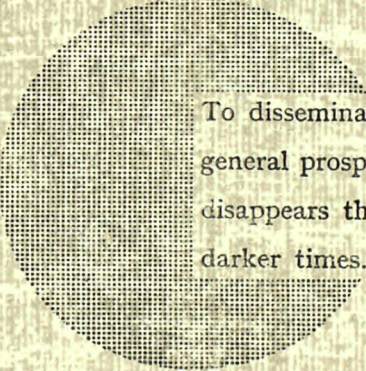
## NOTICE TO THE READER

All Euratom reports are announced, as and when they are issued, in the monthly periodical **EURATOM INFORMATION**, edited by the Centre for Information and Documentation (CID). For subscription (1 year: US\$ 15, £ 5.7) or free specimen copies please write to:

**Handelsblatt GmbH**  
**"Euratom Information"**  
**Postfach 1102**  
**D-4 Düsseldorf (Germany)**

or

**Office central de vente des publications**  
**des Communautés européennes**  
**2, Place de Metz**  
**Luxembourg**



To disseminate knowledge is to disseminate prosperity — I mean general prosperity and not individual riches — and with prosperity disappears the greater part of the evil which is our heritage from darker times.

**Alfred Nobel**

## SALES OFFICES

All Euratom reports are on sale at the offices listed below, at the prices given on the back of the front cover (when ordering, specify clearly the EUR number and the title of the report, which are shown on the front cover).

### OFFICE CENTRAL DE VENTE DES PUBLICATIONS DES COMMUNAUTES EUROPEENNES

2, place de Metz, Luxembourg (Compte chèque postal N° 191-90)

#### BELGIQUE — BELGIË

MONITEUR BELGE  
40-42, rue de Louvain - Bruxelles  
BELGISCH STAATSBLAD  
Leuvenseweg 40-42, - Brussel

#### LUXEMBOURG

OFFICE CENTRAL DE VENTE  
DES PUBLICATIONS DES  
COMMUNAUTES EUROPEENNES  
9, rue Goethe - Luxembourg

#### DEUTSCHLAND

BUNDESANZEIGER  
Postfach - Köln 1

#### NEDERLAND

STAATSDRUKKERIJ  
Christoffel Plantijnstraat - Den Haag

#### FRANCE

SERVICE DE VENTE EN FRANCE  
DES PUBLICATIONS DES  
COMMUNAUTES EUROPEENNES  
26, rue Desaix - Paris 15<sup>e</sup>

#### ITALIA

LIBRERIA DELLO STATO  
Piazza G. Verdi, 10 - Roma

#### UNITED KINGDOM

H. M. STATIONERY OFFICE  
P. O. Box 569 - London S.E.1

EURATOM — C.I.D.  
51-53, rue Belliard  
Bruxelles (Belgique)

CDNA03765ENC